

Accepted Manuscript

Carbon and hydrogen isotopes of methane, ethane, and propane:
A review of genetic identification of natural gas

Quanyou Liu, Xiaoqi Wu, Xiaofeng Wang, Zhijun Jin, Dongya
Zhu, Qingqiang Meng, Shipeng Huang, Jiayi Liu, Qi Fu



PII: S0012-8252(18)30388-X

DOI: <https://doi.org/10.1016/j.earscirev.2018.11.017>

Reference: EARTH 2740

To appear in: *Earth-Science Reviews*

Received date: 6 July 2018

Revised date: 27 October 2018

Accepted date: 24 November 2018

Please cite this article as: Quanyou Liu, Xiaoqi Wu, Xiaofeng Wang, Zhijun Jin, Dongya Zhu, Qingqiang Meng, Shipeng Huang, Jiayi Liu, Qi Fu , Carbon and hydrogen isotopes of methane, ethane, and propane: A review of genetic identification of natural gas. *Earth* (2018), <https://doi.org/10.1016/j.earscirev.2018.11.017>

This is a PDF file of an unedited manuscript that has been accepted for publication. As a service to our customers we are providing this early version of the manuscript. The manuscript will undergo copyediting, typesetting, and review of the resulting proof before it is published in its final form. Please note that during the production process errors may be discovered which could affect the content, and all legal disclaimers that apply to the journal pertain.

**Carbon and hydrogen isotopes of methane, ethane, and propane: A review of
genetic identification of natural gas**

Quanyou Liu^{a,b*}, Xiaoqi Wu^{a,b}, Xiaofeng Wang^c, Zhijun Jin^{a,b}, Dongya Zhu^{a,b},
Qingqiang Meng^{a,b}, Shipeng Huang^d, Jiayi Liu^{a,b}, Qi Fu^e

^a*State Key Laboratory of Shale Oil and Gas Enrichment Mechanisms and Effective
Development, SINOPEC, Beijing 100083, China*

^b*Petroleum Exploration and Production Research Institute, SINOPEC, Beijing
100083, China*

^c*Lanzhou Institute of Geology, Chinese Academy of Sciences, Lanzhou 730000, China*

^d*Research Institute of Petroleum Exploration and Development, PetroChina, Beijing
100083, China*

^e*Department of Earth and Atmospheric Sciences, University of Houston, Houston, TX
77204, USA*

* Corresponding author: liuqy.syky@sinopec.com or qyouliu@sohu.com

Abstract

The genetic identification of different types of natural gas is notably important for assessment of its sources and exploration potential. However, the chemical and isotopic (C and H, in particular) compositions of natural gas vary significantly due to the complexity of its generation, migration, and accumulation processes. Notwithstanding organic precursors and sedimentary environments, both isotope compositions of alkanes tend to be heavier with prograde thermal evolution. Therefore, in addition to thermal maturity, source material is the major controlling factor of carbon isotope compositions, whereas sedimentary environment is predominant in governing hydrogen isotopes. Secondary processes, including thermochemical sulfate reduction (TSR) and diffusion, increase carbon and hydrogen isotope values following mass-dependent kinetic isotope effect. Microbe-prompted degradation causes a decrease in content and an increase in carbon and hydrogen isotopes for propane. The abiogenic gases may include deep mantle-derived methane and high molecular weight hydrocarbons through Fischer-Tropsch type (FTT) synthesis. Mantle-derived methane possesses a narrow range of isotope compositions, although it is still a tall task to determine the exact values. In contrast, isotopes of alkane gases synthesized from FTT processes are in a wide range. In sedimentary basins, the mixing of gases from multiple sources and/or through different secondary processes may pose a challenge to identification of their origins. The detailed assessment is provided here with case studies from major oil and gas basins in China. This review clarifies misconceptions in identifying genetic types of natural gas using

carbon and hydrogen isotopes of alkanes, and sheds insights into using isotope geochemistry as an important diagnostic tool for energy exploration as well.

Key words: natural gas, alkane, carbon isotope, hydrogen isotope, genetic identification, secondary process

1. Introduction

Owing to the complexity of formation processes of natural gas, the classification scheme varies with different criteria, including original source and thermal maturity. On the basis of sources, there are two broad categories: biogenic and abiogenic gas. Biogenic gas mainly refers to the natural gas formed by organic matter, while abiogenic gas includes gas both directly from mantle (mantle-derived gas) and from abiogenic formation (Fischer-Tropsch type synthesis) in the crust (Galimov, 1988; Schoell, 1980; Stahl, 1973; Jenden et al., 1993; Sherwood Lollar et al., 2002). Based on the type of organic matter, biogenic gas can be further divided into “coal-type” gas and “oil-type” gas (Dai et al., 1985, 1992; Xu, 1994). Coal-type gas, also called coal-formed gas, is formed by thermal decomposition of humic organic matter (type III kerogen), and coal seams are included in the source rocks of this type. Oil-type gas is generated from decomposition of sapropelic organic matter (type I and II kerogen), including gases from direct decomposition of sapropelic rocks and secondary cracking of crude oil. On the basis of thermal maturity, natural gas can be classified into microbial gas, low-mature or immature gas, bio-thermocatalytic transitional zone gas (Liu et al., 1997), and thermal cracking gas (Xu, 1994). Among them, thermal cracking gas includes natural gas (also known as kerogen-cracking gas) formed by primary cracking of humic (coal-bearing) and sapropelic source rocks, and secondary cracking gas through thermal decomposition of crude oil (Liu et al., 2007). The latter can be further divided into three different gases, depending on burial and thermal history in the basin. They are: 1) oil-cracking gas, which is generated from secondary

cracking of oil; 2) oil-and-gas-cracking gas, generated from secondary cracking of both oil and gas; and 3) gas-cracking gas, which is from secondary cracking of previously formed gas.

Water plays an important role in hydrocarbon generation and evolution, and participates in chemical reactions as source of hydrogen (Lewan, 1993, 1997; Schimmelmann et al., 2001; Wang et al., 2015; Yoshinaga and Morita, 1997). Hydrogen atoms in water can undergo reversible isotope exchanges with hydrogen in kerogen, most of which are linked to heteroatoms (for example, N-H, S-H, and O-H) (Hoering, 1984; Seewald et al., 1998). After alkane gases are generated, however, their hydrogen atoms barely participate exchange reactions with hydrogen in water (Schimmelmann et al., 2001, 2004).

For oil-type gas from sapropelic organic materials, sedimentary environment could be marine or lacustrine, which leads to distinct chemical and isotope compositions. In addition, secondary processes during migration and accumulation may also contribute to this change. For example, with increasing thermal maturity, liquid hydrocarbons generated earlier may be subject to molecular breakdown and thermochemical sulfate reduction (TSR) to form natural gas. The involvement of H₂S in TSR alteration processes causes changes in geochemical characteristics that are different than typical oil-type gas (Cai et al., 2005; Hao et al., 2008; Liu et al., 2013; Machel, 2001; Worden and Smalley, 1996). Similarly, with participation of deep fluids, methane becomes not only enriched in heavy carbon forming a reversed isotope pattern with other alkanes (Dai et al., 2005b), but also depleted in deuterium

(Liu et al., 2016; Sherwood Lollar et al., 2002, 2006). The alkane gas generated in Hakuba Happo hot spring through water-rock interaction, however, shares similar carbon isotope values with biogenic gases (Suda et al., 2014).

Thus, the key scientific question for assessing natural gas resource potential and finding favorable areas for exploration is: How can the genetic types and sources of natural gas be effectively identified in different geological backgrounds and secondary alteration processes, including TSR and water-rock interactions? The alkane gas is composed of carbon and hydrogen elements. Therefore, the correlation between chemical compositions and carbon and hydrogen isotopes is the key approach to identify the origin of natural gas under different geological conditions. Many scholars have already established numerous geochemical parameters and classic diagrams. However, due to the limitation of analytical data, in particular, hydrogen isotope compositions of heavy hydrocarbon gases, effective genetic identification has been hindered in cases that involve complex geological history and secondary alteration processes.

In recent years, a number of large- and medium-sized natural gas fields have been discovered in China, which vary significantly in sedimentary environment and gas formation processes. For example, a series of gas reservoirs are found in Sichuan and Ordos basins, and kerogen is of type II and III in marine, terrigenous and transitional source rocks. In the eastern Sichuan Basin, natural gas is predominantly from marine reservoirs (Puguang and Wolonghe gas fields), and contains various amounts of H₂S (Cai et al., 2003; Hao et al., 2008; Li et al., 2005b). Natural gas in the

Jingbian gas field in Ordos Basin is in marine reservoirs and derived from marine and transitional source rocks (Liu et al., 2009), while natural gas in the Upper Paleozoic strata in Daniudi gas field is from typical coal measures, with heavy carbon enrichment (Liu et al., 2015). In other petroliferous basins, including Liaohe depression and Huanghua depression in Bohai Bay Basin, Turpan-Hami Basin, Santanghu Basin, and Pearl River Mouth Basin, natural gas belongs to low-mature oil-type gas in lacustrine environment (Dai, 2014; Huang et al., 2015, 2017; Wang et al., 2015). The Tertiary gas in Luliang-Baoshan (Xu et al., 2006) and Quaternary gas in Qaidam Basin (Ni et al., 2013) are generated from microbial activities. The gas in the Xujiaweizi depression in Songliao Basin is a combination of deep-sourced abiogenic gas and lacustrine oil-type gas (Li et al., 2005a; Liu et al., 2016).

This paper collects the chemical composition, carbon and hydrogen isotope compositions (methane, ethane and propane) of 431 gas samples from commercial gas reservoirs in China and northern Appalachian basin in U.S., in combination with data from water-rock reaction experiments (Fu et al., 2007) and Hakuba Happo hot spring in Japan (Suda et al., 2014). By assessing isotope compositions of alkane gases from different sources, the authors intend to overview the current knowledge on the impact of different geologic backgrounds (sedimentary environment and source rocks) on isotope compositions of alkane gases, and re-examine this relationship with newly collected data. Building on this knowledge base, a new approach for identifying alkanes of different origins is established, taking all potential environmental factors into consideration. It would shed insights into deciphering the formation of natural

gas with isotope geochemistry as a diagnostic tool and facilitate future energy exploration.

2. Geochemical characteristics of source rocks and natural gas

2.1. Source rocks

At present, natural gas discovered with potential for commercial exploration is mainly formed by biodegradation or thermal cracking. Although abiogenic natural gas has been observed, commercial abiogenic gas field has yet to be found. Therefore, natural gas in major gas reservoirs was generated from source rocks with different sedimentary environments, organic matter, and thermal maturities. The geological characteristics of source rocks, carbon and hydrogen isotope values of alkane gases (C_{1-3}) from 15 large-scale natural gas reservoirs in China and northern Appalachian basin in U.S. have been summarized in Table 1. Their source rocks are made up of a variety of sedimentary facies, including marine, lacustrine, lagoon, and transitional facies. The lithology includes carbonate rocks, mudstone or carbonaceous mudstone, and coal seams. The organic matter displays all types of kerogen (I, II, and III), and thermal maturity (R_o) ranges from 0.2% (Quaternary gas in Qaidam Basin) to 3.5% (Upper Carboniferous Huanglong Formation (C_2h) – Upper Permian Changxing Formation (P_2ch) - Lower Triassic Feixianguan Formation (T_1f) gas in Sichuan Basin) (Table 1).

Overall, geological conditions before, during, and after natural gas formation are in a wide range, which may control and/or contribute to different geochemical characteristics of natural gas. Delineation of this complex relationship is important,

not only in evaluating current resources, but aiding in future exploration as well.

ACCEPTED MANUSCRIPT

Table 1 Characteristics of source rocks and carbon and hydrogen isotope values of C₁ to C₃ alkanes from 16 major natural gas reservoirs in China and U.S.

Basin	Basin/ Area	Prod uctio n layer	So urc e roc k str ata	Sedimen tary facies of source rocks	Salinit y of sedime ntary waterb ody	Lithology and kerogen types	Ther mal matu rity Ro%	$\delta^{13}\text{C}_1$	$\delta^{13}\text{C}_2$	$\delta^{13}\text{C}_3$	$\delta^2\text{H}-$ C_1	$\delta^2\text{H}-\text{C}_2$	$\delta^2\text{H}-\text{C}_3$	Sources
Qaidam	Qaidam	Q	Q	Lacustrin e facies	freshto slightly saline water	Grey and dark grey mudstone, type III kerogen	0.2-0. 47	-69.6~ -66.3	-47.8~ -36.3	n.d	-234~ -210	n.d	n.d	Li et al., 2008; Ni et al., 2013

Lulian g-Baos han	Luliang -Baosh an	N ₂	N ₂ c	Semi-dee p and deep lacustrin e facies	Freshw ater	Carbonaceou s mudstone, coal, II-III kerogen	0.31-0 .44	-73.3~ -62.5	-66~~ 46.1	n.d	-260~ -234	n.d	n.d	Xu et al., 2005
Turpan -Hami	Tupan- Hami Basin	J	J ₁₊₂ sh	Terrestri al swamp	Freshw ater	Dark mudstone,coa l series, type III kerogen	0.4-0. 9	-44~~ 36.9	-31~~ 24.2	-28.7~ -13.9	-265~ -220	-249~~ 179	-224~~ 166	Wang et al., 2015
Santan ghu	Santang hu Basin	C	C	Marine/t errestrial transition -facies	Freshw ater	Dark mudstone and coal, type II ₂ -III kerogen	0.5-1. 6	-38.7~ -33.8	-28.2~ -23.6	-28~~ 23.3	-234~ -207	-216~~ 144	-214~~ 146	Wang et al., 2015

Tarim foreland d	Foreland d area of Tarim Basin	T-J	T-J	Terrestrial swamp	Freshwater	Coal series, type III kerogen	1.0-2.2	-35.4~ -27.3	-25.8~ -18	-25.1~ -19	-191~ -154	-137~- 112	-114~- 75	
Tarim Platform Basin Area	Platform area of Tarim Basin	O	ε, O	Marine facies	Saline water	Carbonate rock, type I-II kerogen	1.0-3.0	-42.6~ -32	-40.5~ -31.4	-34.6~ -23.8	-224~ -125	-191~- 114	-149~- 91	
Sichuan Basin	Sichuan Basin	C ₂ h, P ₂ ch, T ₁ f	S ₁ , P ₂ l	Marine facies	Saline water	Black shale, type II kerogen	2.5-3.5	-37~- 27	-35.2~ -29.4	-38.2~ -24	-131~ -107	-167~- 88	n.d	

Table 1 (continued)

Basin	Basin/Area	Prod uctio n layer	Sour ce rock strat a	Sediment ary facies of source rocks	Salinit y of sedime ntary rocks	Lithology and kerogen types	The rma l mat urit y Ro %	$\delta^{13}\text{C}_1$	$\delta^{13}\text{C}_2$	$\delta^{13}\text{C}_3$	$\delta^2\text{H}-\text{C}_1$	$\delta^2\text{H}-\text{C}_2$	$\delta^2\text{H}-\text{C}_3$	Sourc es
Sichuan Basin	Sichuan Basin	T ₃ X, J	T ₃ X	Marine/terrestrial transition facies	Saline water	Coal series, type III kerogen	0.8-2.6	-43.2~ -30	-28.7~ -21.1	-26.5~ -19.8	-198~ -148	-161~ -115	-139~ -102	
Ordos	Upper	C-P	C-P	Marine/ter	Freshw	Coal and	0.7-	-40.1~	-26.7~	-26.4~	-209~	-169~	-227~	

Basin Upper Paleoz oic	Paleozoic of Ordos Basin			restrial transition- facies	ater	dark mudstone, type II ₂ –III kerogen	2.0	-32.5	-23.7	-22.8	-107	-133	-130	
Ordos Basin Lower Paleoz oic	Lower Paleozoic of Ordos Basin	O ₁	O?	Marine facies	Saline water	Carbonate rock, type II kerogen	1.0- 3.0	-40.3~ -31	-33.8~ -27.7	-30~- 27.1	-197~ -160	-181~ -127	-193~ -147	
Huang hua Depres sion	Huanghua Depressio n	Es	Es3	Lacustrine facies	Semi-sa line water	Dark mudstone, mainly type I-II kerogen	0.5- 2.5	-47.3~ -36.8	-31.3~ -21.5	-29.8~ -17.2	-258~ -170	-212~ -137	-237~ -111	Wang et al., 2015
Liaohe	Eastern	E ₂ s ³	E ₂ s ³	Deep or	Freshw	Mudstone,	0.7-	-53.5~	30.4~-	27.5~-	-261~	-246~	-203~	Huang

East	part of Liaohe Depressio n			semi-deep lacustrine facies	ater	shale, and coal seams, Humic, type II-III kerogen	1.3	-34.5	22.3	18.7	-188	-154	-106	et al., 2017
Liaohe West	Western part of Liaohe Depressio n	E _{2s} ³	E _{2s} ³	Deep or semi-deep lacustrine facies	Freshw ater	Sapropelic, type I-II kerogen	0.5- 1.3	-54.8~ -31	-38.3~ -24.8	-29.8~ -16.1	-267~ -173	-269~ -130	-232~ -123	Huang et al., 2017
Liaohe West	Western part of Liaohe Depressio	E _{2s} ⁴	E _{2s} ⁴	Deep or semi-deep lacustrine facies	Semi-sa line water	E2s4, type I-II kerogen,	0.5- 2.0							Huang et al., 2017

	n												
--	---	--	--	--	--	--	--	--	--	--	--	--	--

ACCEPTED MANUSCRIPT

Table 1 (continued)

Basin	Basin/ Area	Prod uctio n layer	Sourc e rock strata	Sedimen tary facies of source rocks	Salinit y of sedime ntary waterb ody	Lithol ogy and kerog en types	Ther mal matu rity Ro%	$\delta^{13}\text{C}_1$	$\delta^{13}\text{C}_2$	$\delta^{13}\text{C}_3$	$\delta^2\text{H}-\text{C}_1$	$\delta^2\text{H}-\text{C}_2$	$\delta^2\text{H}-\text{C}_3$	Sources
Songlia o	Songlia o Basin	J-K	K	Shore-shallow and semi-deep lacustrine facies, swamp	Freshwater	Dark mudstone, mainly type II kerogen	0.5-2. 1	-32.7~- 17.4	-33.2~ -22.2	-34.3~ -23.1	-205~ -181	-247~-1 60	-237~ -126	Yang, 2009

					facies											
Pearl River Mouth Basin	Baiyun Depression	N	E	Shallow lacustrine and swamp facies	Saline water	Coal series, type II-III kerogen	0.5-2.2	-38~-36.6	-29.6~ -28.4	-29.1~ -26.6	-176~ -142	-165~-129	-160~ -116	Dai et al., 2016		
northern Appalachia basin	northern Appala chian basin		O ₂ (Utica Formation)	Marine facies	Shale, type II kerogen	0.5-2.3	-44.8~-26	-41.1~ -31.5	-42.9~ -28.3	-207~ -133	-192~-137	-135~ -128	Burruss and Laughrey, 2010			

2.2. Different types of natural gas

Natural gas in sedimentary basins is generated from microbial activities or thermal cracking of organic matter. The microbial gas is mainly composed of alkane gases, and formed by biochemical CO₂ reduction and acetate fermentation under the actions of anaerobic bacteria at low temperatures. The typical characteristics of microbial gases include methane-dominated chemical composition and its carbon isotope value of less than -60‰ or -55‰ (Rice and Claypool, 1981; Schoell, 1980). The thermal maturity (R_o) of source rock is less than 0.5%, and kerogen can be either type II or type III. The formation of microbial gas is unrelated to the type of organic matter, and controlled by temperature and environment of anaerobic bacteria. In thermal cracking processes, however, chemical compositions and stable isotopes of natural gas generated from different organic precursors vary significantly.

Bernard et al. (1978) established the relationship between chemical compositions of natural gas and methane carbon isotope values ($C_1/(C_2+C_3)$ vs $\delta^{13}C_1$) for different types of kerogen (Fig. 1). Following this classification, natural gas from Luliang-Baoshan and Qaidam Basin is of microbial origin. The burial depth of gas zone in the Luliang-Baoshan gas field is 638m on average, and source rocks are coal seams of kerogen type II-III, with R_o between 0.31% and 0.45%. The methane content in natural gas is more than 99.8%, with the heavy hydrocarbon content being less than 0.12% and the C_1/C_{2+3} ratio higher than 300. The $\delta^{13}C_1$ and δ^2H-C_1 values range from -73‰ to -62‰ and -260‰ to -234‰, respectively. The carbon isotope

value of alkane gases becomes less negative with increasing burial depth, a typical feature observed for thermogenic gas (Schoell, 1983; Xu et al., 2006). In Qaidam Basin, the burial depth of gas field is less than 2100 m, and the Quaternary argillaceous source rock contains type III kerogen with R_o of 0.20-0.47%. The methane content in natural gas is more than 98%, with heavy hydrocarbon gases less than 1.2%. The $\delta^{13}\text{C}_1$ and $\delta^{13}\text{C}_2$ values range from -69.6‰ to -66.3‰ and -47.8‰ to -36.3‰, respectively, while the $\delta^2\text{H-C}_1$ value varies from -234‰ to -210‰. With increasing burial depth, no tendency of becoming heavier in carbon isotope is present in alkanes. The overall chemical components and carbon isotopic compositions indicate typical microbial origin (Ni et al., 2013).

When the thermal maturity of the source rock is relatively low ($R_o=0.5\text{-}1.0\%$), the abundance and carbon isotope composition of methane show a transition from microbial gas to thermogenic gas. The carbon isotope composition of methane is low ($\delta^{13}\text{C}_1 < -35\text{\textperthousand}$), and natural gas is relatively wet ($\text{C}_1/\text{C}_{2+3} < 100$). The examples are natural gas in Liaohe depression (in Tertiary Es₃ coal seams and Es₄ lacustrine mudstone), Huanghua depression (in lacustrine mudstone), Turpan-Hami Basin (in coal seams) and Santanghu Basin (in transitional facies of coal seams). The natural gas in Liaohe and Huanghua depressions mainly comes from lacustrine source rocks with type I-II organic matter. Due to low thermal maturity, most data suggest the mixing between thermogenic and microbial gases (Liu et al., 1997). The microbial-thermocatalytic transitional gas is mainly formed when biochemical processes come to end while gas generation from thermal cracking has yet to

develop in large scale. The generated alkanes are predominantly small molecules that are formed through decarboxylation, de-condensation and poly-condensation, under low temperatures, low pressures, and thermodynamic drive from catalysis of clay minerals and tectonic stress as well. The R_o value is between 0.5% and 0.6% in general, with $\delta^{13}C_1$ value from -55‰ to -45‰ (Liu et al., 1997). Although natural gas in Turpan-Hami and Santanghu basins is formed from coal seams of terrigenous or transitional facies, it still shows light carbon isotope compositions ($\delta^{13}C_1 < -35\text{‰}$) and wet components ($C_1/C_{2+3} < 100$). Therefore, for natural gas with low maturity ($R_o=0.5\text{-}1.0\%$), the type of organic matter has a minor effect on gas compositions and carbon isotope values of methane.

As thermal maturity increases ($R_o > 1.0\%$), the influence of organic matter on natural gas becomes prominent. As seen in Fig. 1, natural gas from the foreland in Tarim Basin, the Upper Paleozoic rocks in Ordos Basin, the Xujiahe Formation in Sichuan Basin, and lacustrine mudstone in Songliao Basin are apparently related to type II₂-III kerogen. The gas is mainly from terrigenous or transitional facies in coal-seams. The natural gas in the Ordovician stratum in Tarim Basin, C₂h-P₂ch-T₁f in Sichuan Basin, O₁m in Ordos Basin, and Northern Appalachian Basin in United States originates from marine sapropelic kerogen.

In terms of natural gas from marine strata in Tarim, Sichuan and Ordos basins, the $C_1/(C_2+C_3)$ ratio varies in a wide range along with limited methane carbon isotope compositions. This relationship can be attributed to the increase of methane content and carbon isotopic ratio caused by TSR alteration (Hao et al., 2008).

Therefore, with the effect of thermal evolution, the chemical composition and carbon isotopes of natural gas formed by organic matter in different types vary significantly. For natural gas with similar thermal maturity of source rocks, the carbon isotope of gas from type II₂-III kerogen is heavier than that from type I-II₁ kerogen.

The abiogenic and abiogenic-thermogenic mixed gas (e.g., deep mantle-derived or from water-rock reaction), however, cannot be identified effectively in Fig. 1. For instance, natural gas in Kidd Creek Mine is proposed to be of abiogenic origin (Sherwood Lollar et al., 2002), while its data fall into the range of thermogenic gas derived from type III kerogen (Fig. 1). A similar observation has also been obtained in the Qingshen gas field, Songliao Basin (data of Songliao-mixing in Fig. 1), where methane is derived from both deep mantle and Fischer-Tropsch type (FTT) reactions (Liu et al., 2016). The gas shows the characteristics of thermal cracking of type III kerogen (Fig. 1). Therefore, the relationship between $C_1/(C_2+C_3)$ and $\delta^{13}C_1$ may be misleading for identifying abiogenic gas.

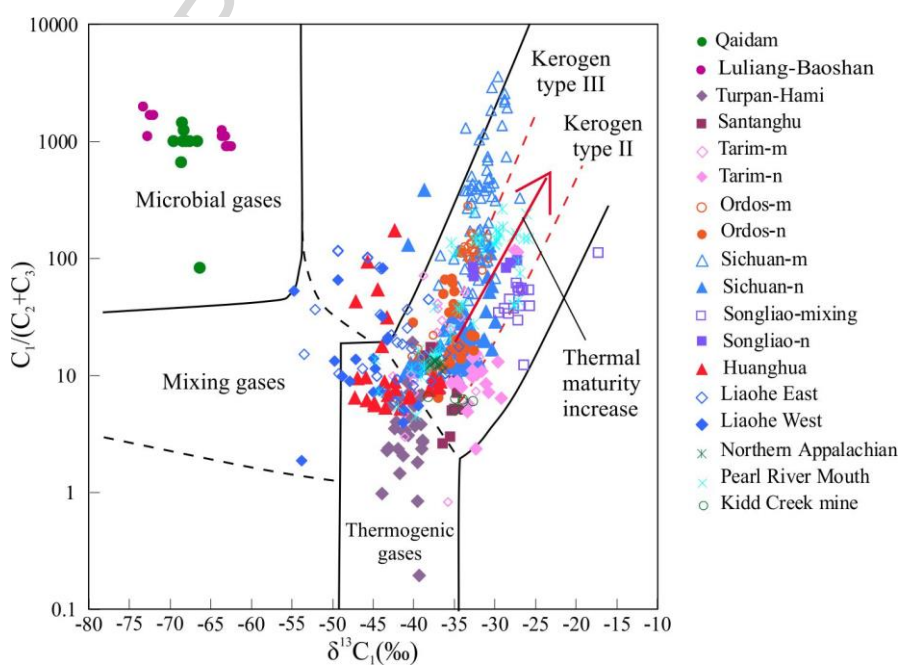


Fig. 1 The correlation diagram between $\delta^{13}\text{C}_1$ and $\text{C}_1/(\text{C}_2+\text{C}_3)$ (modified Bernard diagram) for different types of natural gas

¹ –m: natural gas derived from marine source rock

² –n: natural gas derived from non-marine source rock

³ –mixing: mixture of non-marine gas and abiogenic gas

In summary, the $\text{C}_1/(\text{C}_2+\text{C}_3)$ - $\delta^{13}\text{C}_1$ pattern (modified Bernard diagram) is of significance in identifying microbial gas and natural gas from different types of kerogen. In some cases, however, the complexity of organic source and secondary processes, both of which may result in variations in chemical and isotopic compositions, causes uncertainty in genetic classification.

3. Carbon and hydrogen isotopes of alkane gases and genetic identification

3.1. Carbon isotopes of alkanes and genetic types of natural gas

Since the isotope composition of heavy hydrocarbon gases is relatively stable, it provides important information for identifying genetic types of natural gas. The carbon isotope composition of natural gas reflects the type of organic source materials and the extent of thermal evolution (Galimov, 1988; Schoell, 1980; Stahl, 1973; Stahl and Carey, 1975). It has been successfully applied to classify natural gas into “coal-type” gas and “oil-type” gas (Dai et al., 1985; Xu, 1994). In general, natural gas with $\delta^{13}\text{C}_2$ value higher than -28‰ and $\delta^{13}\text{C}_3$ higher than -25‰ is classified as coal-type gas, while the one with lower values is referred as oil-type gas (Clayton, 1991; Dai et al., 2005a). For example, the carbon isotopes of methane and

ethane in Luliang-Baoshan and Qaidam Basin are lighter than other basins, with the $\delta^{13}\text{C}_1$ and $\delta^{13}\text{C}_2$ values less than -55‰ and -35‰, respectively (Fig. 2), suggesting a different origin of gases in both basins than others. The microbial gas is characterized by $\delta^{13}\text{C}_1$ values significantly less than -55‰ (Schoell, 1988), although there is a certain overlap in carbon isotope compositions between microbial ethane and thermogenic ethane from marine type II organic matter.

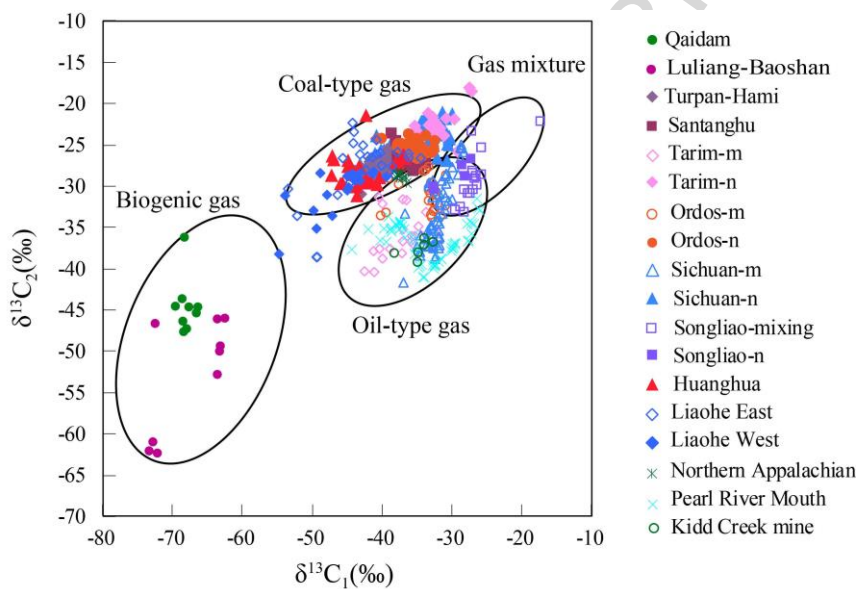


Fig. 2 The diagram of $\delta^{13}\text{C}_1$ versus $\delta^{13}\text{C}_2$ for identifying genetic types of natural gas

${}^1\text{-m}$, ${}^1\text{-n}$, and ${}^1\text{-mixing}$: see Fig. 1

The thermogenic gas also shows a wide range of carbon isotopes of methane and ethane (Fig.2). The oil-type gas from marine type II organic matter distributes below gas formed by type II-III kerogen from terrigenous (lacustrine) or transitional facies in Fig. 2. It suggests, under similar thermal maturity conditions, carbon isotope compositions of methane and ethane in oil-type gas from marine type II organic matter are lighter than in terrigenous (lacustrine) or transitional facies. Based on the linear correlation between carbon isotope compositions of methane and ethane,

natural gas from marine organic matter has a higher slope than that from type II-III organic matter in terrigenous (lacustrine) or transitional facies (Fig. 2). Although alkanes from Qingshen gas field in Songliao Basin are from lacustrine organic matter (II-III) (Fig. 1), their carbon isotope compositions overlap with natural gas derived from marine type II organic matter, suggesting the complex sources of organic materials. Liu et al. (2016) suggested that heavy hydrocarbon gases in this gas field are mainly formed by thermal cracking of organic matter, while methane is derived from the combination of thermal cracking of organic matter, deep mantle source, and FTT, with mantle-derived methane having less negative carbon isotopic compositions. Suda et al. (2014) analyzed the gas associated with Hakuba Happo hot spring, and suggested that water-rock interaction can generate methane at temperatures lower than 150 °C. The carbon isotope value of methane in Hakuba Happo varies between -38.1‰ and -33.2‰. The distribution of carbon isotope composition of methane formed by low-temperature water-rock interaction overlaps, to some extent, with that of thermogenic methane in sedimentary basins. If methane formed by water-rock reactions does exist, its carbon isotope composition will become more negative when it mixes with thermogenic oil-type gases. In intracontinental serpentinized peridotites, reactions between H₂ formed by serpentinization and CO₂ with mineral catalysts can generate CH₄ through FTT at temperatures below 100 °C (Etiope, 2017).

Natural gas formed from lacustrine and transitional organic matter, which is not typical coal-type or oil-type gas, displays similar variations between carbon isotopes

of methane and ethane. It mainly results from heterogeneity of organic matter formed in lacustrine or transitional environment, which contains interbedded sapropelic mudstone (type II kerogen), humic coal, or carbonaceous mudstone (type III kerogen). The natural gas formed from sapropelic mudstone is predominantly oil-type gas, whereas that formed from humic coal or carbonaceous mudstone is coal-type gas. The extent of mixing between those two types of natural gas depends on the contribution from two different kerogens. When coal or carbonaceous mudstone is dominant, natural gas is mostly composed of coal-type gas. For example, the carbon isotope compositions of methane and ethane in eastern and western Liaohe Depression are different (Fig. 3). The mudstone and coal seams (coal and carbonaceous mudstone) in the third member of Tertiary Shahejie Formation (Es_3) in eastern Liaohe Basin are interbedded. The kerogen in mudstone is type II, while the coal and carbonaceous mudstone is of type III. The natural gas derived from Es_3 is characterized by mixing between oil-type and coal-type gas, with coal-type being predominant (Huang et al., 2017). However, the third and fourth members of Tertiary Shahejie Formation in western Liaohe Basin are mainly composed of deep-water and semi-deep lacustrine facies, forming sapropelic organic matter with type I-II kerogen. Although in some areas, the developed coal seams may contribute to the formation of coal-type gas in limited amount, the generated natural gas is mainly oil-type gas (Huang et al., 2017). Therefore, the genetic types of natural gas generated from source rocks in lacustrine or transitional facies are controlled by the distribution of sapropelic and humic organic matter within those source rocks.

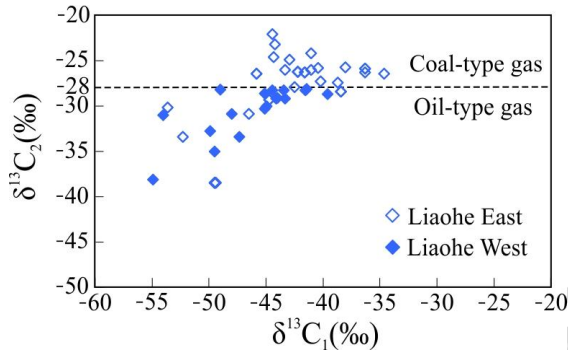


Fig. 3 The diagram of $\delta^{13}\text{C}_1$ versus $\delta^{13}\text{C}_2$ for natural gas in eastern and western Liaohe Basin. They are mainly attributed to different kerogen types: type II-III in eastern and type I-II in western.

In the diagram that shows carbon isotope compositions of ethane and propane, there is a good linear relationship for both coal-type and oil-type gases (Fig. 4). Carbon isotopes of ethane and propane become heavier with increasing thermal maturity. Moreover, the coal-type gas displays less negative carbon isotope compositions than oil-type gas. The values of $\delta^{13}\text{C}_2$ (-28‰) and $\delta^{13}\text{C}_3$ (-25‰) can be used to distinguish them. It is noteworthy that those two values may change and be influenced by the degree of thermal evolution and isotope compositions of organic precursors (Dai et al., 2005a, 2007a; Liu et al., 2007; Schoell, 1988; Stahl, 1973). For Luliang area, the propane content in microbial gas is below the detection limit. Therefore, the gas samples from Luliang area cannot be displayed in Fig. 4. For Turpan-Hami Basin, the carbon isotopes of propane become enriched in ^{13}C with carbon isotopes of ethane, i.e., the $\delta^{13}\text{C}_2$ and $\delta^{13}\text{C}_3$ values are positively correlated. The lowest $\delta^{13}\text{C}_2$ and $\delta^{13}\text{C}_3$ values are -31‰ and -28.7‰, respectively, and the

highest $\delta^{13}\text{C}_2$ and $\delta^{13}\text{C}_3$ values are -24.2‰ and -13.9‰, respectively. Following the presumption that $\delta^{13}\text{C}_2 > -28\text{\textperthousand}$ and $\delta^{13}\text{C}_3 > -25\text{\textperthousand}$ are for coal-type gas and $\delta^{13}\text{C}_2 < -28\text{\textperthousand}$ and $\delta^{13}\text{C}_3 < -25\text{\textperthousand}$ for oil-type gas, natural gas in Turpan-Hami Basin is classified as both coal-type and oil-type gas. Considered as the source rocks in Turpan-Hami Basin, coal measures and dark mudstone have thermal maturity of 0.4%-0.9% (Wang et al., 2015). Therefore, natural gas in the basin was mainly derived from low-mature humic organic matter with kerogen type III. Several gas samples are most likely related to low-mature oil-type gas derived from sapropelic-prone organic matter interbedded with coal-measure source rocks. The extremely heavy carbon isotopes of propane, for example, $\delta^{13}\text{C}_3$ value of -13.9‰ from Ba18 well, might be linked to biodegradation. The effect of biodegradation on the carbon isotopic composition of alkanes is discussed in section 5.2.

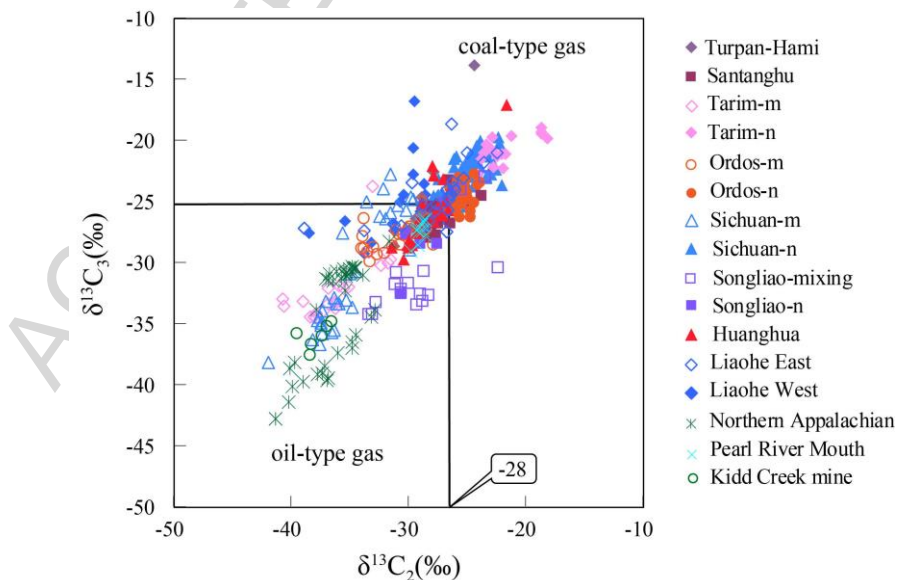


Fig. 4 The diagram of $\delta^{13}\text{C}_2$ versus $\delta^{13}\text{C}_3$ for natural gas of different genetic types

¹-m, -n, and -mixing: see Fig. 1

Chung et al. (1988) performed theoretical simulation on decomposition of crude oils from Monterey and Statfjord in a closed system at 300°C. The results suggested that the carbon isotope composition of alkane gases becomes heavier with the carbon number. A linear relationship was proposed between the carbon isotope value of alkane gases and the reciprocal of carbon number, i.e., $\delta^{13}\text{C}_n$ and $1/n$. The premise of this relationship is that the carbon isotope composition of organic matter in source rocks is homogeneous, and organic matter has only experienced a single thermal cracking reaction. Because the organic sources of natural gas are rarely homogeneous, this "ideal" linear relationship is not observed in most cases. For sapropelic organic matter, which is mainly composed of long-chain aliphatics, its carbon isotope composition may be relatively constant. Fig. 5 shows the carbon isotope values of alkanes in different types of natural gas. The coal-type gas and oil-type gas at low maturity stages demonstrate more or less linear characteristics of carbon isotope values between alkanes, including coal-type gas with low maturity in eastern Liaohe (Fig. 5a), Turpan-Hami (Fig. 5b) and Santanghu basins (Fig. 5c), as well as oil-type gas in western Liaohe (Fig. 5d) and Pearl River Mouth Basins (Fig. 5e). At mature to highly-mature stages, the carbon isotopes of coal-type gas and oil-type gas show different trends with maturity. The distribution of carbon isotope values for coal-type gas gradually evolves from a nearly straight line to an upward convex curve. For oil-type gas, however, the distribution becomes a concave curve. For example, mature to highly-mature coal-type gas in Ordos (Fig. 5f), Sichuan (Fig. 5g), Tarim (Fig. 5h) and Songliao (Fig. 5i) basins shows a linear to convex curve.

The highly- to over-mature oil-type gas in Ordos (Fig. 5f), Sichuan (Fig. 5g) and Tarim (Fig. 5h) basins shows a concave curve, which resembles partially reversed carbon isotope trend between methane and ethane due to high carbon isotope values of methane.

Zou et al. (2007) provided a variety of factors that may lead to the deviation from linear function, including cracking of heavy hydrocarbon gas, TSR alteration, and mixing between gases from different sources. The upward convex curve with heavier ethane and propane indicates thermal cracking of coal-type gas and TSR alteration, while the concave with large differences in isotopic values of ethane and propane suggests secondary cracking of oil-type gas. The over-mature oil-type gas and coal-type gas display concave and convex curves, respectively. The migration and diffusion of methane will increase the carbon isotope value of residual methane, leading to a concave curve. If there is a mixing with microbial gas which contains methane with significantly low carbon isotope values, the overall carbon isotope value of methane will decrease, showing a convex curve. Depending on the extent of reaction, TSR can be divided into heavy hydrocarbon-dominated TSR and methane-dominated TSR. Considering ^{12}C is preferentially involved in reactions, the carbon isotope composition of residual hydrocarbon gas becomes heavier following TSR. There is a positive correlation between gas souring index (GSI, $\text{H}_2\text{S}/(\text{H}_2\text{S}+\sum\text{C}_{1-3})$) and $\delta^{13}\text{C}_2$ values in marine strata of Sichuan Basin. However, no significant correlation between GSI and $\delta^{13}\text{C}_1$ values is present, suggesting marine natural gas has experienced heavy hydrocarbon-dominated TSR, but not reached the

stage dominated by methane (Hao et al., 2008; Li et al., 2015; Liu et al., 2011, 2013, 2017). The role of TSR at the heavy hydrocarbon-dominated stage may not be the cause of carbon isotope reversal between methane and ethane. Instead, it is the reason that transforms the reversal trend into normal trend (Hao et al., 2008).

Galimov (2006) and Sherwood Lollar et al. (2008) suggested that the kinetic isotope effect of C-C bond breaking and formation controls the carbon isotope trend of hydrocarbon gases in sedimentary and magmatic rocks. The C₁-C₄ gases in sedimentary rocks are generated from kerogen degradation which involves breakage of C-C bonds, while the C₁-C₄ gases in magmatic rocks are generated by continuous polymerization of small molecules, with exceptions of gases that are accumulated in magmatic rocks but of organic origin. Therefore, the former shows the normal carbon isotope trend, i.e., the carbon isotope value increases with carbon number. The latter shows the reversed trend of carbon isotopes, i.e., the carbon isotope value decreases with carbon number. Natural gas mixed with abiogenic alkanes in the Songliao Basin shows a reversed trend (Fig. 5i), which is consistent with theoretical prediction (Galimov, 2006). It has been reported that natural gas in the Qingshen gas field of Songliao Basin exhibits carbon isotope reversal (Liu et al., 2016). Combined with the values of CH₄/³He and R/Ra ratios, it suggested that mantle-derived abiogenic gas may contribute 30%-40% of the total mixed gas (Liu et al., 2016).

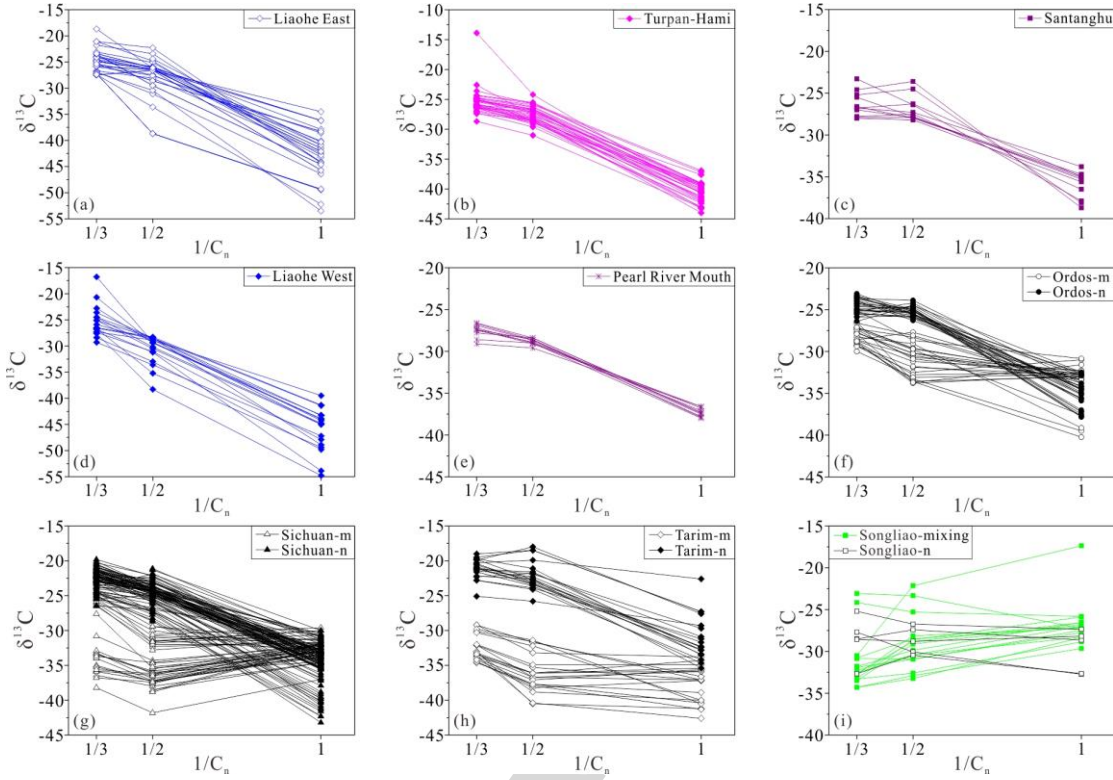


Fig. 5 Diagrams of $1/C_n$ versus $\delta^{13}\text{C}$ for coal-type gas and oil-type gas in major petroliferous basins in China (see text).

$^1\text{-m}$, $-\text{n}$, and $-\text{mixing}$: see Fig. 1

3.2. Hydrogen isotopes of alkanes

Although hydrogen isotopes of alkane gases are not used as widely as carbon, they can provide important information on sedimentary environment (Liu et al., 2008; Schoell, 1980; Shen et al., 1988; Shen and Xu, 1986; Sherwood Lollar et al., 2002; Wang, 1996). The hydrogen isotope composition of methane in different sedimentary environments is varied due to high hydrogen content in freshwater environment and high deuterium in saline water (Schoell, 1980). The hydrogen isotope composition of methane derived from source rocks in terrigenous freshwater is less than $-190\text{\textperthousand}$, and that in brackish-water environment generally varies between

-190‰ and -180‰, while that in marine saltwater possesses $\delta^2\text{H}$ values above -180‰ (Schoell, 2011; Shen and Xu, 1986). The value of -190‰ ($\delta^2\text{H-C}_1$) is assigned to distinguish marine from terrigenous facies. The hydrogen isotope composition of microbial methane from Qaidam Basin and Luliang-Baoshan area is less than -190‰, and the source rocks are formed in fresh-brackish water environments. Hydrogen isotopic compositions of heavy hydrocarbon gases cannot be obtained due to the fact that their contents (including ethane) are below the detection limit.

Although gases were derived from different depositional environments and different types of organic matter, hydrogen isotope compositions of methane and ethane may display a certain linear relationship (Fig. 6). In particular, coal-type methane and ethane are distributed left to oil-type gas, i.e., the hydrogen isotope compositions of coal-type methane and ethane are less than those in oil-type gas, respectively. Within coal-type gas, there are variations in hydrogen isotope composition of methane and ethane due to different salinities of environment where source rocks were deposited and buried. For example, natural gas in the Upper Triassic Xujiahe Formation (T_3X) and Jurassic (J) gas reservoirs in Sichuan Basin mainly was formed from source rocks in saltwater depositional environment, and hydrogen isotope compositions of methane and ethane are significantly heavier than those source rocks from freshwater-brackish water in the foreland of Tarim Basin, the Upper Paleozoic strata of Ordos Basin, Songliao Basin, Huanghua Depression in Bohai Bay Basin and Liaohe Basin (Fig. 7). The T_3X -J reservoirs are mainly

composed of the Xujiahe Formation in Upper Triassic in transitional and lacustrine facies. Although organic matter contains type III kerogen, sediments that are characterized by brackish water environment have been observed due to transgression. The fresh to brackish water depositional environments had also been developed in the foreland of Tarim Basin, the Upper Paleozoic strata in Ordos Basin, Songliao Basin, Huanghua Depression in Bohai Bay Basin, and Liaohe Basin.

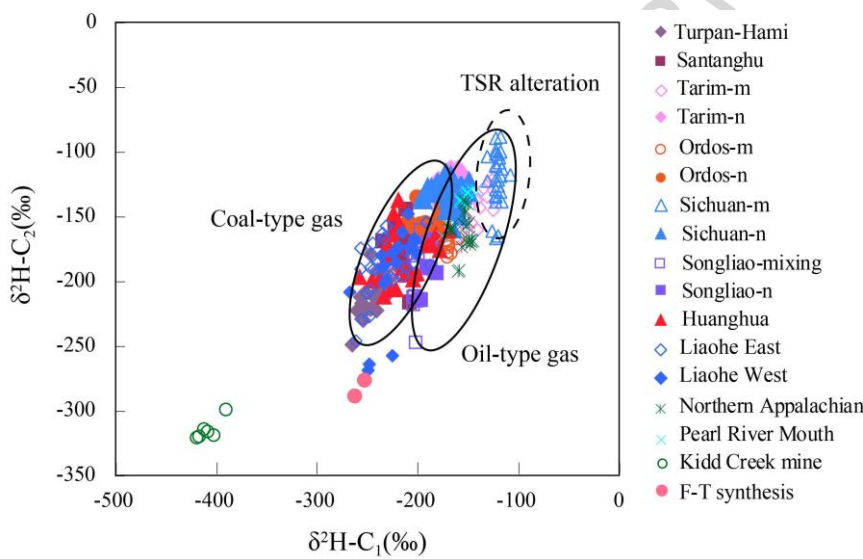


Fig. 6 Diagram of $\delta^2\text{H-C}_1$ versus $\delta^2\text{H-C}_2$ for natural gas with different genetic types

${}^1-\text{m}$, $-\text{n}$, and $-\text{mixing}$: see Fig. 1

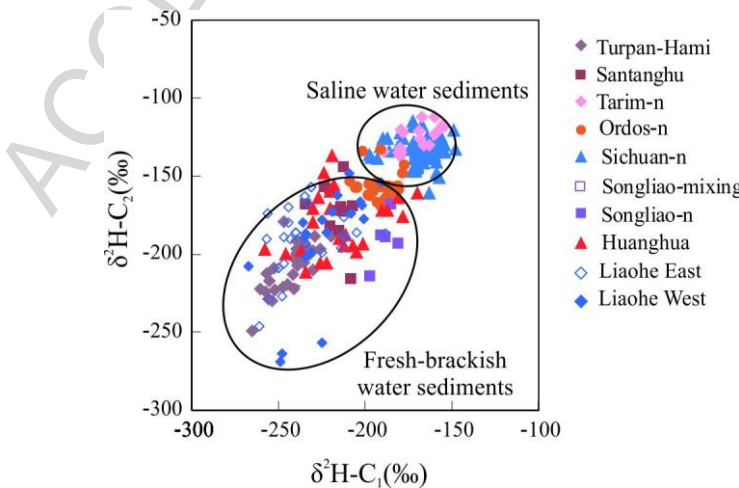


Fig. 7 Diagram of $\delta^2\text{H-C}_1$ versus $\delta^2\text{H-C}_2$ for coal-type gas under different

sedimentary environments (saline water, and fresh-brackish water)

¹-m, -n, and –mixing: see Fig. 1

A variety of terrigenous sedimentary facies, including transitional facies, lacustrine facies, and swamp facies, have been observed (Dai et al., 2005a; Huang et al., 2017; Liang et al., 2003; Liu et al., 2015; Yang et al., 1985). There are discrepancies of hydrogen isotope compositions of methane and ethane in different sedimentary environments (Fig. 7). Natural gas from the T₃x-J gas reservoir in Sichuan Basin has shown different hydrogen isotope values than other areas, including marine sapropelic organic matter in the Ordovician stratum in Tarim Basin, C₂h-P₂ch-T₁f in Sichuan Basin, O₁ in Ordos Basin, Neogene stratum in Pearl River Mouth Basin, and Northern Appalachian. Although T₃x-J is formed in saltwater depositional environment, organic matter is mainly consisted of type III kerogen that generates coal-type gas. Other rock formations, deposited in marine saltwater environments, contain type II kerogen and generate oil-type gas. The hydrogen isotope composition of methane in T₃x-J in Sichuan Basin is lighter, and ethane is heavier. Therefore, depositional environment of parent materials plays a major role in hydrogen isotope compositions of methane. The values from salt water environments are heavier than brackish water and fresh water environments.

Hydrogen isotope values of methane from O₁m in Ordos Basin partially fall into the range of coal-type gas (Fig. 7). It may be attributed to the incorporation of coal-type gas from Paleozoic source rocks (Liu et al., 2009). As for the Ordovician

gas reservoirs in Tarim Basin and C₂h-P₂ch-T₁f in Sichuan Basin, hydrogen isotope composition of methane remains nearly constant with the gradual increase of hydrogen isotope composition of ethane. The oxidative alteration of hydrocarbons during TSR may be the reason, and also causes a narrow fluctuation of hydrogen isotope compositions of methane (Liu et al., 2014b).

The main factors controlling hydrogen isotope compositions are the participation of external hydrogen sources during hydrocarbon formation (Lewan, 1997; Yoneyama et al., 2002), and hydrogen exchange between organic matter and water (Schimmelmann et al., 2001, 2004; Wang et al., 2011). Water plays an important role in hydrocarbon generation, and it also participates in chemical reactions forming hydrogen (Lewan, 1993; Wang et al., 2011; Yoneyama et al., 2002). The hydrogen atoms in water can interact with hydrogen in kerogen through reversible isotope exchange reactions, in which hydrogen is predominantly linked to heteroatoms (N-H, S-H, and O-H) (Hoering, 1984; Seewald et al., 1998). However, after alkane gas is generated, its hydrogen atoms barely undergo isotope exchange reactions with hydrogens from other sources (Schimmelmann et al., 2001, 2004). Laboratory experiments have confirmed that methane generation rate is the dominant factor controlling hydrogen isotope compositions of methane (Wang et al., 2011). The extent of thermal evolution is one of the important factors that constrain the yield of methane. Moreover, hydrogen isotope value of methane varies slightly compared to ethane in Northern Appalachian reservoirs (Fig. 6). It might be caused by seepage diffusion leading to the preferential loss of ¹H-enriched methane and

accumulation of ^2H -enriched methane in reservoirs (Burruss and Laughrey, 2010; Xiao, 2012).

In Qingshen gas field of Songliao Basin, hydrogen isotope composition of methane has shown little variation (-205~ -181‰), while hydrogen isotope composition of ethane varies significantly (-247~ -160‰) (Fig. 6) (Liu et al., 2016). The main reason for the nearly constant hydrogen isotope values of methane is that besides thermal cracking of organic matter, mantle-derived source or FTT synthesis may be another contribution owing to relatively constant hydrogen isotope compositions of methane in mantle (Liu et al., 2016).

Natural gas from Kidd Creek Mine (Ontario, Canada) is proposed as abiogenic gas (Sherwood Lollar et al., 2002, 2006). Hydrogen isotope compositions of methane and ethane are completely different than those of oil-type and coal-type gases in sedimentary basins (Fig. 6). The hydrogen isotopes are lighter than microbial gas and thermogenic gas, with values of methane, ethane and propane ranging from -419‰ to -390‰, -321‰ to -299‰, and -270‰ to -262‰, respectively. In contrast, methane from the CO₂ well in Salton Sea area (California, USA), another example of abiogenic gas, has much higher $\delta^2\text{H}$ values (-16‰) (Welhan, 1988). In Hakuba Happo Hot Springs, the carbon isotope value of methane is between -38.1‰ and -33.2‰, and hydrogen isotope is between -300‰ and -210‰ (Suda et al., 2014). This range for methane formed through low temperature water-rock reactions, is overlapped with microbial methane. The hydrogen isotope composition of methane in FTT synthesis experiments ranges from -262‰ to -253‰,

and ethane from -288‰ to -276‰, with the values of methane and ethane being reversed, i.e., $\delta^2\text{H-C}_1 > \delta^2\text{H-C}_2$, although it depends on the value of H₂ source and possibly H₂O (Fu et al., 2007).

A positive correlation between hydrogen isotope compositions of ethane and propane may exist for natural gas regardless of origin (Fig. 8). There is no clear boundary between coal-type gas and oil-type gas. As the extent of thermal evolution increases, hydrogen isotope composition of ethane and propane becomes heavier. The hydrogen isotopes of abiogenic ethane and propane are significantly lighter than those of microbial origin. Therefore, hydrogen isotopes of ethane and propane are not as effective as carbon isotopes in distinguishing coal-type gas from oil-type gas, but it can serve as an essential means to identify abiogenic gas. However, there still is a debate on hydrogen isotope compositions of abiogenic methane, which vary in a wide range under different geological conditions and present challenges to source identification.

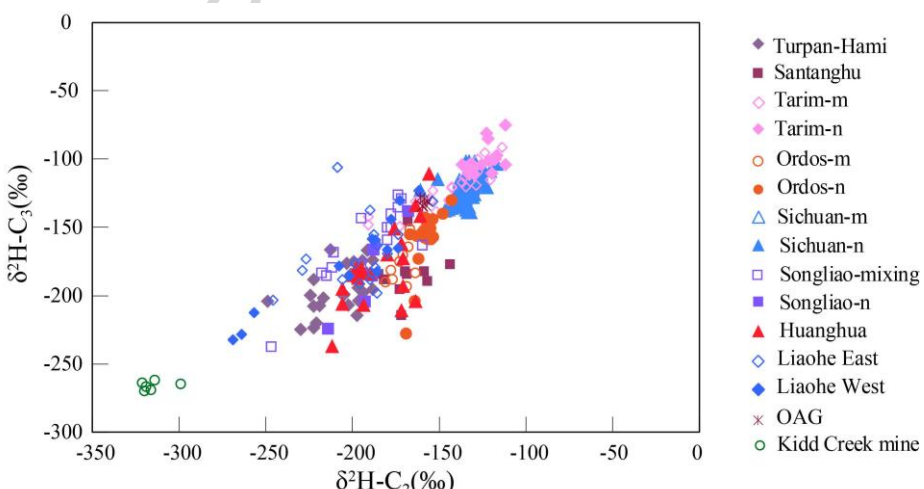


Fig. 8 Diagram of $\delta^2\text{H-C}_2$ versus $\delta^2\text{H-C}_3$ for different types of natural gas

¹-m, -n, and -mixing: see Fig. 1

The hydrogen isotope pattern of alkanes in coal-type gas and oil-type gas at low maturity stages shows a linear feature, for example, coal-type gas in eastern Liaohe Basin (Fig. 9a) and Turpan-Hami Basin (Fig. 9b), as well as oil-type gas from western Liaohe Basin (Fig. 9c) and Pearl River Mouth Basin (Fig. 9d). However, hydrogen isotopes of coal samples with low maturity in Santanghu Basin are different, showing a convex pattern (Fig. 9e). This is due to higher values of ethane ($> -190\text{\textperthousand}$) in Santanghu Basin and lower values in Turpan-Hami ($< -190\text{\textperthousand}$). At mature to highly mature stages, hydrogen isotope values of coal-type gas show nearly linear characteristics, as observed in Ordos (Fig. 9f), Sichuan (Fig. 9g) and Tarim (Fig. 9h) basins. Due to high values of methane, oil-type gas at highly-mature to over-mature stages shows a partial reversed trend between methane and ethane. For example, oil-type gas in Tarim Basin illustrates a concave curve (Fig. 9h). The alkane gases in Ordos Basin (Fig. 9f) and Songliao Basin (Fig. 9i) even exhibit a continuously reversal trend.

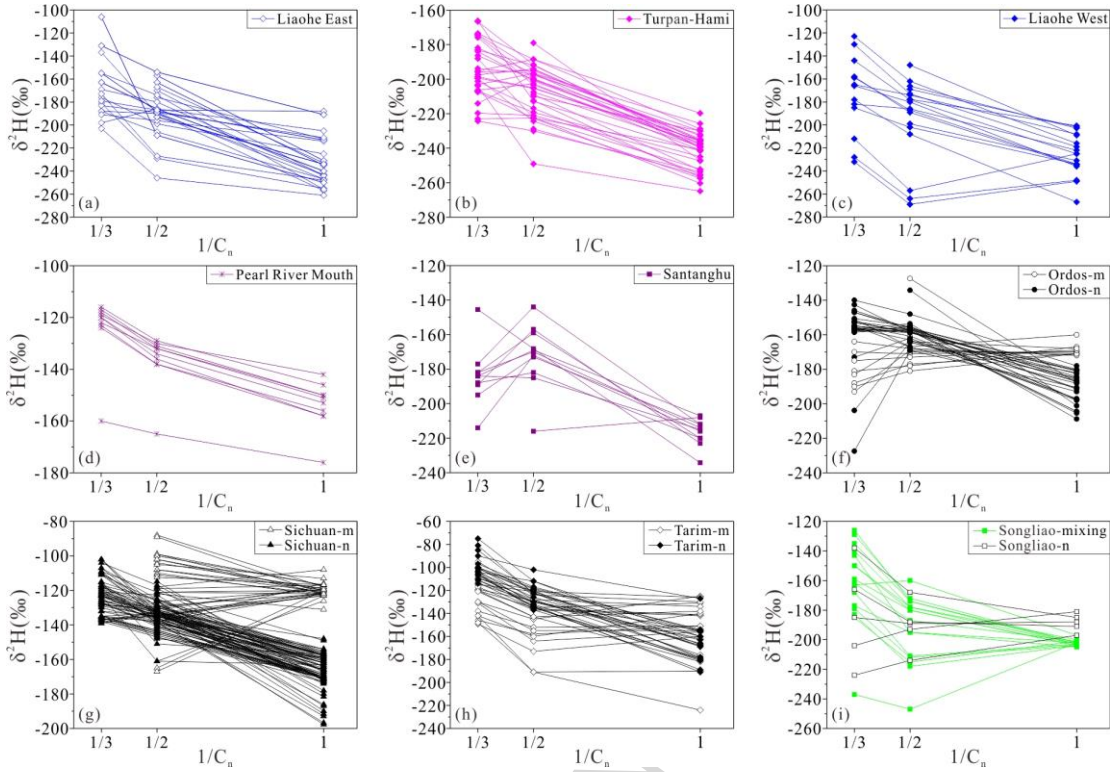


Fig. 9 Diagrams of $1/C_n$ versus $\delta^2\text{H}$ for coal-type gas and oil-type gas from major petroliferous basins in China (see text).

${}^1\text{-m}$, ${}^1\text{-n}$, and ${}^1\text{-mixing}$: see Fig. 1

During TSR reactions, hydrogen isotope compositions of alkanes are also affected. Natural gas from marine strata in Sichuan Basin are dominated by heavy hydrocarbon compounds with a wide range of hydrogen isotopic compositions of ethane, some of which are higher than $-100\text{\textperthousand}$ (Fig. 9g). There is a positive correlation between GSI and hydrogen isotopes of ethane ($\delta^2\text{H-C}_2$), but such correlation is not observed between GSI and methane (Liu et al., 2014b). It is most likely due to preferential participation of ${}^1\text{H}$ in TSR, making hydrogen isotope compositions of residual alkanes (ethane in particular) heavier. TSR alteration can increase hydrogen isotope values, even significantly higher than oil-type gas in Ordos and Tarim basins (Liu et al., 2014b).

In addition to carbon isotope compositions of natural gas, the information obtained from hydrogen isotope compositions may be of specific significance to oil and gas exploration. However, compared to organic carbon precursors, the source of hydrogen is rather complicated. Hydrogen can be derived from kerogen and aquifer media (Lewan, 1997; Seewald, 2003). The contribution from inorganic sources (for example, natural gas in Qingshen gas field), is another possibility (Coveney et al., 1987; Jin et al., 2004; Liu et al., 2016).

Wang et al. (2011) conducted three series of laboratory experiments on thermogenic hydrocarbon generation in closed systems under different aqueous conditions: no water (anhydrous), deionized water ($\delta^2\text{H-H}_2\text{O}=-58\text{\textperthousand}$), and seawater ($\delta^2\text{H-H}_2\text{O}=-4.8\text{\textperthousand}$). The experimental results have shown that addition of water not only increases the amount of generated hydrogen and CO₂ significantly, but also the yield of methane at high-maturity stages (Fig. 10). There is a positive relationship between the hydrogen isotope value of methane and its yield. The results suggest that the aqueous medium is involved in chemical reactions during hydrocarbon generation and evolution, and affects the hydrogen isotope composition of gaseous hydrocarbons.

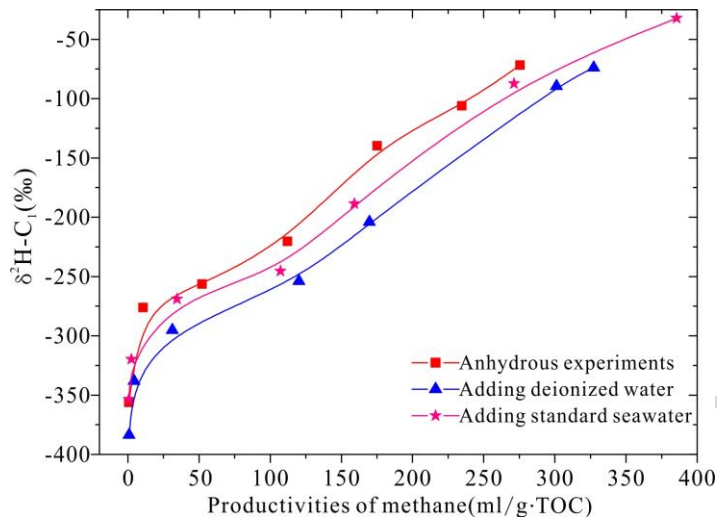


Fig. 10 Diagram of productivities of methane versus $\delta^2\text{H-C}_1$ in laboratory experiments under different water conditions. Data from Wang et al. (2011).

Previous experimental studies have suggested that the formation mechanism of oil and gas is through free radical reactions (Beltrame et al., 1989; Eisma and Jury, 1969; Kissin, 1987; Lewan, 1985). Methane is the product of methyl groups reacting with hydrogen atom that is formed during kerogen cracking, and hydrogen gas is the product of combination reactions between two hydrogen atoms. High energy is required for fracturing heavier isotope-containing functional groups (Sackett, 1978). As thermal maturity increases, carbon and hydrogen isotope compositions of methyl derived from kerogen cracking become heavier. Another important factor affecting methane hydrogen isotopes is the hydrogen atom bound to methyl groups. Since hydrogen molecules are the combination product of two hydrogen atoms, the isotopic composition of hydrogen atoms has a certain relationship with the isotope value of hydrogen gas. Because its contribution of hydrogen atom accounts for only 1/4 of hydrogens in methane molecules, hydrogen gas has less effect on hydrogen

isotope compositions of methane than methyl (-CH₃). The experimental results have shown a linear relationship between hydrogen isotope composition of methane and its yield. With the same methane yield, the hydrogen isotope composition of methane produced by the anhydrous experiment is the heaviest, followed by with seawater and deionized water (Wang et al., 2011).

Hydrogen in water can react reversibly with hydrogen atoms in kerogen with fast reaction rates. The hydrogens in kerogen are mainly bonded to heteroatoms, as in N-H, S-H, and O-H (Lewan, 1997; Mastalerz and Schimmelmann, 2002; Schimmelmann et al., 1999, 2001; Schoell, 1984; Seewald, 2003). Hydrogen atoms in alkyl groups of kerogen can retain their original hydrogen isotopic composition up to 150 °C (Lewan, 1997; Schimmelmann et al., 1999). Under natural conditions, hydrogen isotope exchange between hydrocarbons and water is very slow, and insignificant even at 200-240 °C for hundreds of millions of years (Li et al., 2001b; Mastalerz and Schimmelmann, 2002; Schoell, 1984; Yeh and Epstein, 1981). Therefore, the composition of hydrogen isotopes of oil and natural gas can still retain signatures from parent materials.

In summary, the hydrogen isotope composition of source rocks is the primary factor that influences hydrogen isotope composition of methane. The source rocks formed in marine environment display heavier hydrogen isotopes than those formed in terrigenous freshwater environment (Wang et al., 2015). With same maturation (R_o), methane derived from marine source rocks is heavier than that from terrigenous freshwater source rocks. On the other hand, methane yield in experiments is

positively related to the degree of thermal evolution of source rocks (i.e., the higher the degree of thermal evolution (R_o), the higher the yield of methane), while concentration and hydrogen isotope composition of hydrogen gas are related to the isotope compositions of both source rocks and aqueous medium during gas formation. Therefore, factors that affect hydrogen isotopes of methane in natural gas include: (1) Hydrogen isotope composition of organic matter in source rocks. (2) Degree of thermal evolution. The higher the thermal evolution degree, the heavier the hydrogen isotope composition of natural gas. (3) Ancient water medium during gas formation. Among them, hydrogen isotope compositions of organic matter in source rocks are further affected by two factors. One is the water body environment during the growth of biomatrix that forms organic matter of source rocks. The hydrogen isotope composition of organisms growing under terrigenous freshwater conditions is far lighter than that under marine and lagoon environments. The other factor is depositional environment of organisms. Changes in hydrogen isotopes can be achieved through isotope exchange reactions with aqueous media during diagenesis, including deposition of terrigenous freshwater organic matter in marine strata, and transformation of terrigenous organic matter by marine water during diagenesis.

4. Identification of Kerogen-Cracking Gas and Crude Oil-Cracking Gas

In sedimentary basins, humic organic matter mainly consists of aromatic and heterocyclic compounds. The products of thermal cracking are gases with less

amount of oil (Behar et al., 1995; Berner et al. 1995; Lorant et al., 1998; Stahl and Carey, 1975). However, sapropelic organic matter is mainly composed of long-chain aliphatic groups. A small amount of kerogen-cracking gas exist before liquid hydrocarbons are formed as the major product. Thermal cracking of both liquid hydrocarbons and kerogen occur at late stages, and the extent of thermal cracking of crude oil is far greater than that of kerogen (Tissot and Welte, 1984). Thus, there are two main pathways through which sapropelic organic matter can generate oil-type gas: kerogen-cracking gas generated by direct cracking of kerogen, and oil-cracking gas derived from thermal cracking of crude oil (Behar et al., 1995; James, 1990; Prinzhofe and Battani, 2003; Prinzhofe et al., 2000; Tang et al., 2000; Tian et al., 2012; Zhang et al., 2005).

4.1. Molecular compositions

The diagram, $\ln(C_1/C_2)$ vs. $\ln(C_2/C_3)$, has been established to distinguish kerogen-cracking gas from oil-cracking gas using thermal simulation in closed system (Behar et al., 1992). The kerogen-cracking gas displays higher formation rates of methane than heavy hydrocarbon gases (ethane and propane). The $\ln(C_1/C_2)$ value varies, whereas the $\ln(C_2/C_3)$ value remains constant with little variation. Crude oil-cracking gas shows a relatively rapid increase in production rate of heavy hydrocarbon gases. The $\ln(C_1/C_2)$ value of oil-cracking gas is constant with a small range of variation, while $\ln(C_2/C_3)$ value varies significantly (Prinzhofe and Battani, 2003; Prinzhofe and Huc, 1995).

In Turpan-Hami basin, $\ln(C_1/C_2)$ varies from 0.4 to 3.2, while $\ln(C_2/C_3)$ values are in the range of 0.23 to 2.3, showing a positive correlation for primitive kerogen-cracking gas (Fig. 11a). Natural gas shows low thermal maturity ($R_o = 0.4\text{-}0.9\%$) with type III kerogen that mainly generates alkane gases (Dai et al., 1985; Stahl and Carey, 1975) through cleavage of organic side chains and functional groups (Fu et al., 1990; Liu et al., 2007; Price, 1993). Due to low thermal maturity which is below the level of cracking crude oil, natural gas in Turpan-Hami basin has shown geochemical characteristics that correspond well to hydrocarbon generation processes (Li et al., 2001a).

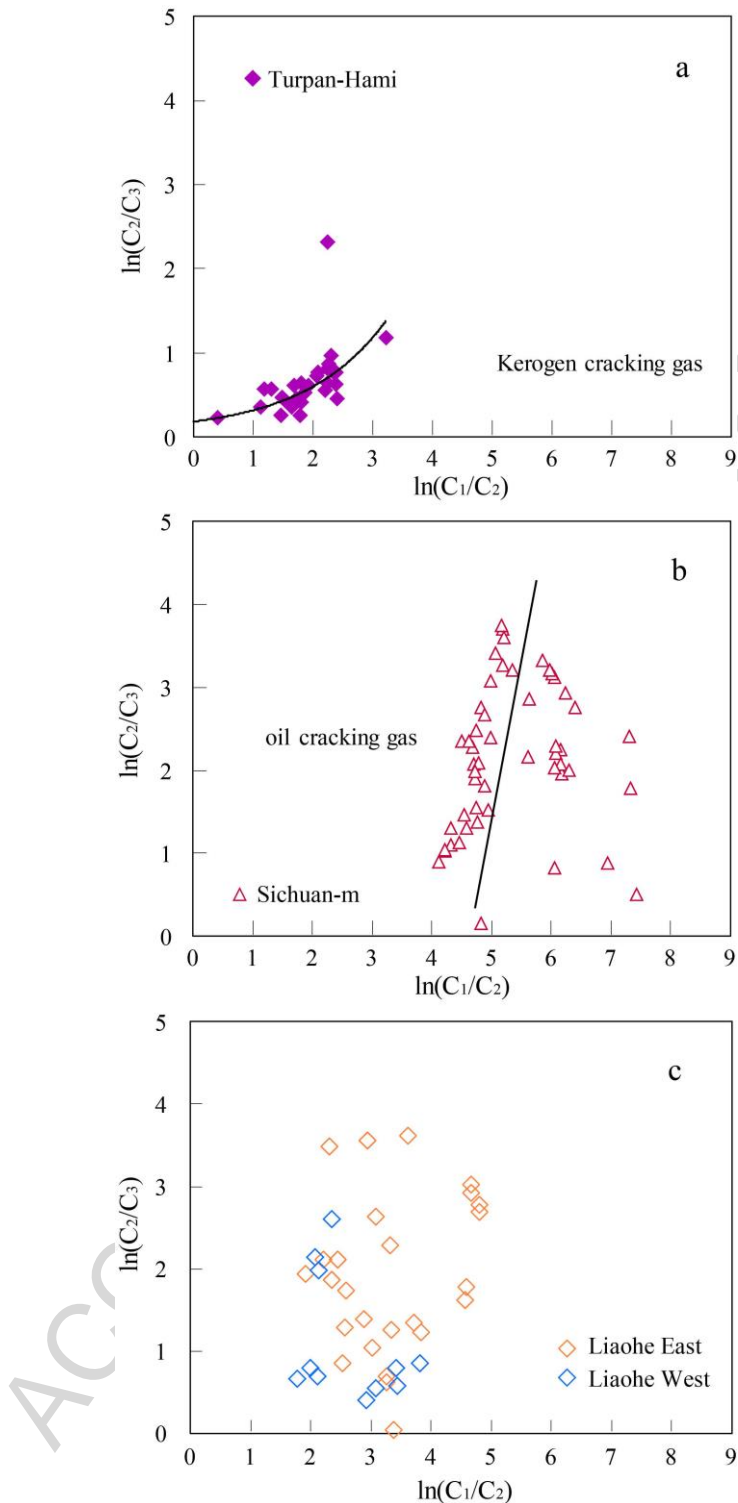


Fig. 11 The diagram of $\ln(C_1/C_2)$ versus $\ln(C_2/C_3)$ for source identification of natural gas: kerogen-cracking and oil-cracking. a. Kerogen-cracking gas, Turpan-Hami basin; b. Oil-cracking gas, from C₂h-P₂ch-T₁f marine reservoir in Sichuan Basin; c. Mixing of kerogen-cracking and oil-cracking gases, E₂s in Liaohe

Basin.

In Sichuan Basin, the $\ln(C_1/C_2)$ value of natural gas from C₂h-P₂ch-T₁f marine reservoirs varies from 4.2 to 6.4, whereas $\ln(C_2/C_3)$ value varies from 0.16 to 3.8 (Fig. 11b). Natural gas in this area comes from S₁l and P₂ dark mudstones. The organic matter contains Type II kerogen, and thermal maturity is at the stage of highly-over mature ($R_o = 2.5\text{--}3.5\%$) (Dai, 2014; Hao et al., 2008; Jin et al., 2012; Ma, 2007). The early generated sapropelic organic matter was completely decomposed into natural gas at higher stages. The wide distribution of solid bitumen also indicated that the reservoirs underwent early decomposition of crude oil to generate gases (Dai et al., 2007b; Jin et al., 2012).

When the source of natural gas in a gas reservoir is simple, either from kerogen cracking or oil cracking, the values of $\ln(C_1/C_2)$ and $\ln(C_2/C_3)$ are effective on source identification. However, owing to further cracking of crude oil during hydrocarbon generation and mixing with kerogen-cracking gas, uncertainty may exist for using both values to identify source materials (Xu, 1993). For example, the distribution of isotope values of natural gas from Liaohe Basin exhibits a wide band with no apparent relationship between $\ln(C_1/C_2)$ and $\ln(C_2/C_3)$ (Fig. 11c). The mixing between methane and gas that is from cracking of crude oil would preclude rational source identification by using this relationship only. Because of those limitations, the $\ln(C_1/C_2)$ vs. $\ln(C_2/C_3)$ diagram has been used for natural gas from same thermal maturity stages (Li et al., 2017; Liu et al., 2018a).

Discrepancies in $\ln(C_1/C_2)$ and $\ln(C_2/C_3)$ are present for both types of gas at

different thermal evolution stages (Liu et al., 2018b) (Fig. 12). With $R_o=0.5\%-0.8\%$, before thermal cracking of crude oil, the $\ln(C_1/C_2)$ and $\ln(C_2/C_3)$ values of kerogen-cracking gas increase with thermal maturity. Moreover, the $\ln(C_1/C_2)$ value changes faster than $\ln(C_2/C_3)$, suggesting the generation rate of methane is higher than that of ethane and propane at low-mature stage. At $R_o = 0.8\%-1.3\%$, the increase of $\ln(C_1/C_2)$ value for crude oil-cracking gas shows a higher slope than kerogen-cracking gas, though it is at the beginning stage of cracking oil. It suggests that compared to kerogen-cracking gas, methane from crude oil cracking has a much higher generation rate than ethane. Furthermore, the $\ln(C_2/C_3)$ curve of oil-cracking gas exhibits a lower slope, while $\ln(C_2/C_3)$ of kerogen-cracking gas has a higher slope. It indicates that compared to crude oil-cracking gas, the amount of C_2H_6 in kerogen-cracking gas increases faster than C_3H_8 . Within the range of $R_o = 1.3\%-1.8\%$, the curve of $\ln(C_1/C_2)$ shows a steep increase for both gases, suggesting that this maturation stage is characterized by fast generation of methane, with higher rates from crude oil cracking than kerogen cracking. In terms of ethane and propane, the higher slope of the $\ln(C_2/C_3)$ curve for kerogen-cracking gas than crude oil-cracking gas suggests that C_2H_6 and C_3H_8 share the same characteristics as in the previous stage. The C_2H_6 content in kerogen cracking gas increases faster than C_3H_8 , and the increasing trend for oil-cracking gas is relatively gentle. At $R_o = 1.8\%-2.5\%$, the $\ln(C_1/C_2)$ curve of kerogen-cracking gas is steeper than $\ln(C_2/C_3)$, suggesting that source rocks mainly generate methane at high maturity, and the abundance of CH_4 increases faster than C_2H_6 . Oil-cracking gas shows a steeper $\ln(C_2/C_3)$ curve than

$\ln(C_1/C_2)$, which suggests that the gas generation in a large amount occurs at this high-evolution stage with higher C_2H_6 generation rate than C_3H_8 . Compared to kerogen-cracking gas, the slope of the $\ln(C_1/C_2)$ curve for oil-cracking gas is low, while the $\ln(C_2/C_3)$ curve is high. The natural gas generation at this stage is mainly characterized by crude oil cracking. The $\ln(C_1/C_2)$ curve of oil-cracking gas is also steeper than $\ln(C_2/C_3)$ at $Ro \geq 2.5\%$, suggesting that the product of crude oil cracking at high temperatures is dominated by CH_4 .

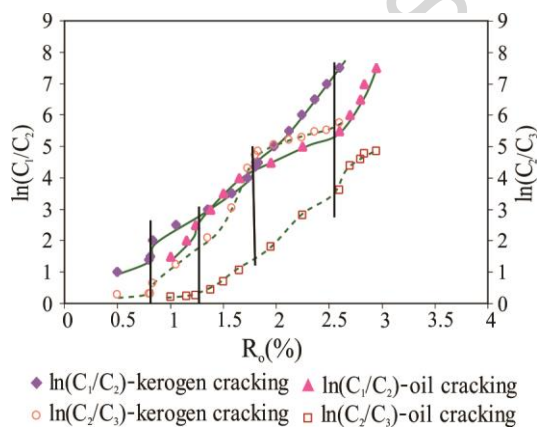


Fig. 12 The diagrams of R_o versus $\ln(C_1/C_2)$ and $\ln(C_2/C_3)$ for different types of natural gas. (Modified after Liu et al., 2018b)

Based on the relationship between $\ln(C_1/C_2)$ and $\ln(C_2/C_3)$ of kerogen-cracking gas and oil-cracking gas at different thermal stages, a modified diagram has been established to allow for effective source identification (Fig. 13). When R_o is less than 1.3%, natural gas is predominately from cracking of kerogen. The basins that contain this type of gas include Turpan-Hami, Santanghu, Huanghua, Liaohe and Pearl River Mouth basins. When R_o is higher than 1.3%, natural gas is mainly generated from oil

cracking. The gases in C₂h-P₂ch-T₁f marine reservoirs in Sichuan Basin, Ordovician marine reservoirs in Tarim Basin, O₁ in Ordos Basin, J-K in Songliao Basin and E₂s in Liaohe Basin, fall into this category. The gas generated from coal (coal-type gas) may show similar chemical characteristics to kerogen-cracking gas, for example, T₃x-J in Sichuan Basin, T-J in Tarim Basin, C-P in Ordos Basin, J in Turpan-Hami Basin, C in Santanghu Basin, and some areas in Huanghua Depression and Liaohe Basin. However, the genetic source of oil-type gas depends on thermal maturity. When R_o reaches 0.8-1.8%, natural gas is a mixture of products from both crude oil cracking and kerogen cracking processes. For example, source rocks in Northern Appalachian Basin are in the Ro range of 0.6 to 1.4% (Burruss and Laughrey, 2010). The hydrocarbon generation process includes cracking of kerogen in source rocks and further decomposition of crude oil that is generated earlier. The chemical abundances of natural gas in this area have explicitly shown the co-existence of kerogen-cracking and oil-cracking gases (Fig. 13).

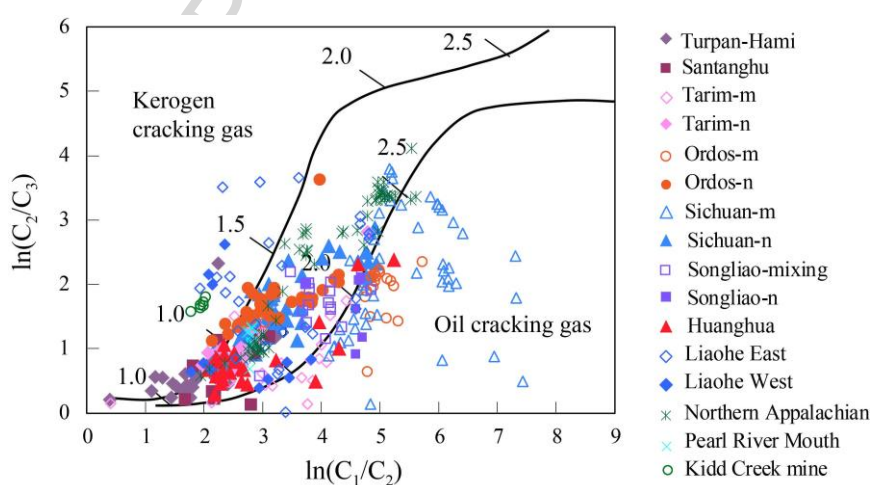


Fig. 13 The diagram of $\ln(C_1/C_2)$ versus $\ln(C_2/C_3)$ values of different types of natural gas. The maturation stage is incorporated for effective source identification.

¹-m, -n, and -mixing: see Fig. 1

4.2. Carbon isotopes of alkane gases

From the perspective of hydrocarbon generation kinetics, the gas generation process for large hydrocarbon molecules or crude oil can be divided into a series of stages, which coincidentally correspond to different thermal stages. At early stages, large molecules are decomposed into small hydrocarbons, which are similar to condensate hydrocarbons and gases. With thermal evolution, these condensate hydrocarbons are further cracked into light hydrocarbons and gases. When thermal evolution reaches a certain extent, these light hydrocarbons also undergo thermal cracking and become gases completely. In order to better distinguish kerogen-cracking gas from crude oil-cracking gas at different stages, detailed discussion is provided below using the C₂/C₃ vs δ¹³C₂-δ¹³C₃ diagram (Lorant et al., 1998; Prinzhofer and Battani, 2003; Prinzhofer and Huc, 1995), along with data collected from major petroliferous basins and experimental results of crude oil decomposition (Tang et al., 2000; Zhang et al., 2005) (Fig. 14).

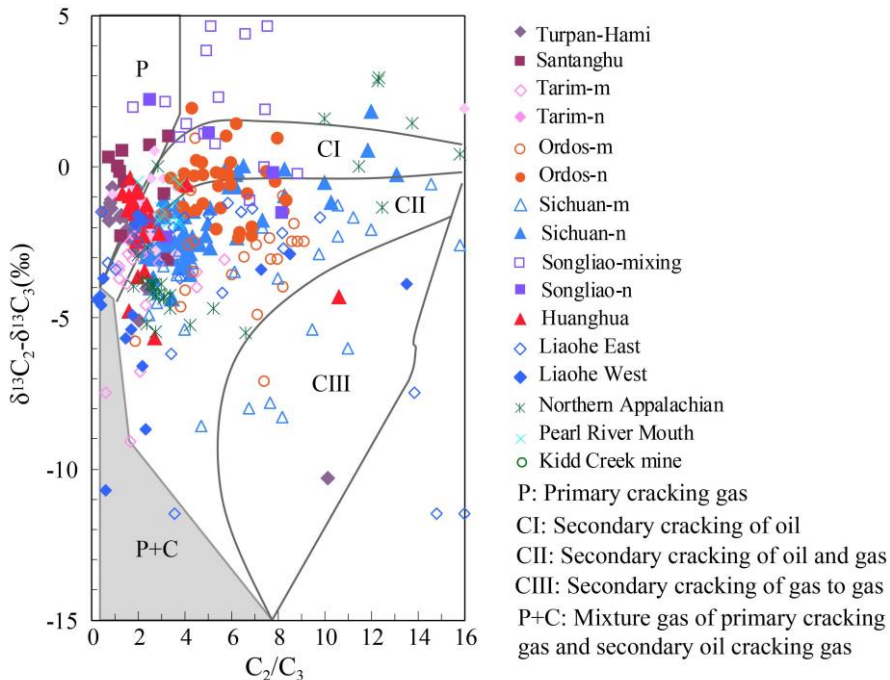


Fig. 14 Diagram showing C_2/C_3 versus $\delta^{13}C_2 - \delta^{13}C_3$ for identification of kerogen-cracking gas and oil-cracking gas at different thermal evolution stages (after Lorant et al., 1998).

¹ –m, –n, and –mixing; see Fig. 1

Natural gas in Turpan-Hami and Santanghu basins are generated by kerogen cracking, whereas natural gas in Huanghua, Liaohe, Pearl River Mouth and Songliao basins contains both kerogen-cracking gas (P) and oil-cracking gas. Depending on the extent of crude oil cracking, the gas is divided into three categories: oil-cracking gas (CI), oil-gas-cracking gas (CII), and gas-cracking gas (CIII). The natural gas in Ordovician of Tarim, C-P of Ordos, T₃-J of Sichuan, K of Songliao, Liaohe, Pearl River Mouth and Northern Appalachian basins are mainly composed of CI and CII, while natural gas in C₂h-P₂ch-T₁f of Sichuan basin and O₁ of Ordos basin belong to

CII and/or CIII (Fig. 14). The Ordovician gas in Tarim Basin and gas in Liaohe Basin show a wide range of content and carbon isotope values of C₂ and C₃, suggesting they may include P, CI, CII, and CIII, or mixture of P and CI (Liu et al., 2007).

The diversity of genetic types of gas in these gas fields is consistent with the wide range of thermal evolution degree of source rocks. For example, R_o of source rocks in Ordovician gas reservoir in Tarim Basin is 1.0-3.0%, equivalent to stages at which liquid hydrocarbons are generated and subsequently cracked under higher temperature conditions. The chemical and isotopic composition of natural gas are consistent with the genetic sources (predicted by R_o), including kerogen-cracking gas and oil-gas-cracking gas (Liu et al., 2018a). Some data of natural gas from Qingshen gas field in Songliao and Northern Appalachian are on the periphery of the diagram, which indicates the complexity of genetic types in these fields (Fig. 14). For example, methane in Qingshen gas field may be from deep mantle and FTT synthesis (Liu et al., 2016). The chemical reactions and isotopic exchange between methane and other hydrocarbons result in methane content and carbon isotope values differing from those of thermogenic gas. Natural gas in Northern Appalachian basin may have been subject to migration and diffusion, leading to preferential methane loss and heavier methane carbon isotopes (Burruss and Laughrey, 2010, Xiao, 2012). Therefore, for natural gas that has gone through secondary alteration or mixing with external components, the C₂/C₃ vs δ¹³C₂-δ¹³C₃ diagram can be used to distinguish kerogen-cracking gas from crude oil-cracking gas at different thermal stages.

However, the detailed chemical and carbon isotope compositions of methane, ethane and propane are required for identification. For highly or over-mature gas, for example, C₂h-P₂ch-T₁f in Sichuan Basin and O₁ in Ordos Basin, the propane content may be extremely low, and the genetic identification using this diagram is inconclusive.

5. Effect of secondary alteration on carbon and hydrogen isotope compositions

5.1. Thermochemical sulfate reduction (TSR)

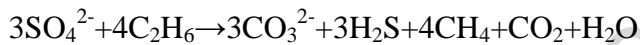
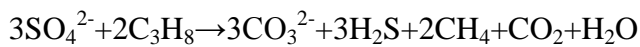
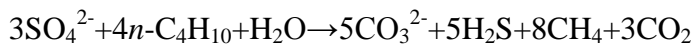
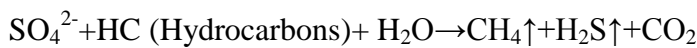
H₂S is acidic non-hydrocarbon gas. Its occurrence is in marine carbonates, dolomite gas reservoirs, and occasionally clastic rocks. Most H₂S is produced by reduction reactions between sulfate and hydrocarbons, under the influence of microorganisms (bacteria) or non-biological materials (inorganic minerals). With involvement of bacteria, the whole process is named as bacterial sulfate reduction (BSR), while when non-biological materials (inorganic minerals) are present, it is thermochemical sulfate reduction (TSR). Cohn (1867) first discovered that sulfur bacteria *Beggiatoa* could generate H₂S under certain conditions. Beijerinck (1895) officially named this process BSR, which occurs in sedimentary basins at low temperatures (60-80°C) (Machel, 2001; Orr, 1977). The geological environment where BSR would proceed includes subterranean aquifer layers, marine sediments, reef carbonate rocks, dispersed evaporites and clastic sediments. In BSR, H₂S is only a reduction product while nutrients are required for microbial consumption, resulting in a H₂S content lower than the level that may cause poisoning during microbial

metabolism. The content of H₂S formed by BSR is generally less than 5% (Worden and Smalley, 1996). Therefore, if there are BSRs in reservoirs and large amounts of H₂S are generated, an open system is needed to allow the generated H₂S escape and ensure no significant H₂S present (Krooss et al., 2008). Since BSR occurs at temperatures below 80 °C and the corresponding R_o of source rocks is about 0.2-0.3% (Machel and Foght, 2000), the contribution of BSR to the chemical and isotopic compositions of thermogenic alkane gases is trivial. The effect of BSR on natural gas generation is not discussed in this paper.

The TSR reaction was first reported in sulfate and hydrocarbon dissolution experiments by Toland (1960). It was subsequently found that TSR can occur at temperatures up to 175 °C in laboratory (Machel, 1998), and in geological environment its optimum temperature is between 100 and 140 °C (Chung et al., 1988). Although H₂S can also be produced directly by S-bearing kerogen, the content of H₂S generated through cracking barely exceeds 2 - 3% in crude oil with the total sulfur content of 3% (Orr, 1974). In TSR, H₂S content varies significantly. According to the statistics from 86 gas samples in C₂h-P₂ch-T₁f gas reservoirs in Sichuan Basin, the content of H₂S ranges from 0% to 62.17%. Among them, the H₂S contents between 5448.3-5469m and 5423.6-5443m in Well Puguang 3 are as high as 45.55% and 62.17%, respectively (Liu et al., 2013).

TSR is a redox reaction that consumes hydrocarbons and generates acidic gases (H₂S and CO₂) (Cai et al., 2001; Krouse et al., 1988; Machel et al., 1995; Worden et al., 1995). Laboratory experiments have shown that a large amount of CH₄ can also

be formed (Pan et al., 2006; Zhang et al., 2007, 2008a). The MgSO₄ solution is a key intermediate compound that triggers TSR (Zhang et al., 2008a; Zhang et al., 2008b). The reactions during TSR can be expressed as follows:



The generation rate of acid gases (H₂S + CO₂) is nearly equal to that of CH₄, resulting in a decrease of CH₄ proportion in natural gas, while the content of acid gases (H₂S + CO₂) increases. In marine carbonate reservoirs, CO₂ generated by TSR may become supersaturated and precipitate during burial to form calcite with more negative carbon isotopes (Zhu et al., 2005). During subsequent uplifting processes, at lower temperatures and pressures, reactions involving acidic fluids and carbonate reservoirs would generate CO₂ with less negative carbon isotopes (Liu et al., 2014a). In order to assess the effect of TSR on hydrocarbon transformation and carbon isotopic composition of alkanes, the gas souring index (GSI) (H₂S/(H₂S+ΣC₁₋₃)) was introduced to define the extent of TSR (Worden et al., 1996).

The results collected from the Upper Carboniferous, Upper Permian and Lower Triassic natural gas (C₂h-P₂ch-T₁f) in Sichuan Basin are discussed here to illustrate the relationship between GSI and carbon and hydrogen isotopic compositions of

alkane gases during TSR (Fig. 15). Overall, there is a positive correlation between GSI and the ratio of $(\text{H}_2\text{S} + \text{CO}_2) / (\text{H}_2\text{S} + \text{CO}_2 + \sum \text{C}_{1-3})$. When GSI is higher than 0.01, $(\text{H}_2\text{S} + \text{CO}_2) / (\text{H}_2\text{S} + \text{CO}_2 + \sum \text{C}_{1-3})$ increases significantly, and is in the range of 0.03–0.78. According to this change, the GSI value of 0.01 was proposed as the threshold of TSR (Liu et al., 2013). When GSI is less than 0.01, natural gas is mainly generated by cracking of kerogen and crude oil. When GSI is above 0.01, TSR starts to occur. The TSR intensity increases with GSI. The gas in P₂ and T₁ reservoirs has GSI values higher than 0.01, whereas the gas in C₂ reservoirs has values less than 0.01. Hence, natural gas in C₂ has not undergone TSR. Alternatively, the TSR alteration is relatively weak. According to Fig. 13, gas in C₂h-P₂ch-T₁f is generated by crude oil cracking. Therefore, natural gas in C₂ has mainly experienced thermal cracking of crude oil, with no apparent TSR alteration, while gas in P₂ and T₁ has been subject to TSR.

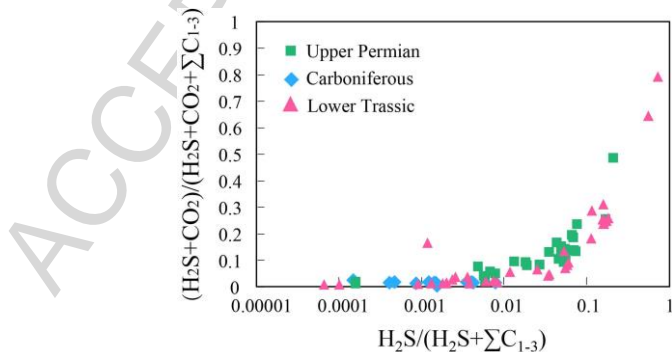


Fig. 15 The diagram of GSI [$\text{H}_2\text{S}/(\text{H}_2\text{S}+\sum \text{C}_{1-3})$] versus $(\text{H}_2\text{S}+\text{CO}_2)/(\text{H}_2\text{S}+\text{CO}_2+\sum \text{C}_{1-3})$ for natural gas from $\text{C}_2\text{h}-\text{P}_2\text{ch}-\text{T}_1\text{f}$ reservoirs in Sichuan Basin

The relationship between GSI and carbon isotope compositions of alkane gases

in Sichuan Basin is illustrated in Fig. 16. With increasing GSI, the variation of carbon isotope compositions of methane becomes limited (Fig. 16a), with similar average values. This carbon isotope feature with GSI is not observed for ethane and propane, and is also in stark contrast to the carbon isotope trend for thermogenic alkanes. For alkane gases generated in a single geological thermal event, with increasing carbon number, the carbon isotope becomes heavier with narrower variation. Due to involvement of sulfur in TSR, the activation energy required for the oxidative alteration of alkanes (other than methane) reduces significantly, and they are altered within a short period of time (Machel, 2001). That results in carbon isotopic compositions of methane generated from TSR much close to the value of original hydrocarbons, which is higher than methane formed by thermal cracking. Methane in gas reservoirs will be heavier if there is a mixing between methane from TSR and thermal cracking. The heavier hydrocarbon gases, ethane and propane, act as reactants in TSR. Their carbon isotopes are controlled by thermal cracking and oxidative alteration by TSR. When GSI is less than 0.01, there is no apparent correlation between GSI and isotopic compositions of ethane and propane (Fig. 16b, c). When GSI is higher than 0.01, it is positively correlated with the carbon isotopes of ethane and propane. Ethane is substantially consumed at the GSI value of 0.2 (Fig. 16b), while no propane is observed if GSI is above 0.1 (Fig. 16c). Therefore, with increasing GSI value, heavier hydrocarbon gases (ethane and propane) are also oxidatively altered by TSR. However, this process is prior to similar oxidation reactions of methane (Liu et al., 2013; Worden and Smalley, 1996).

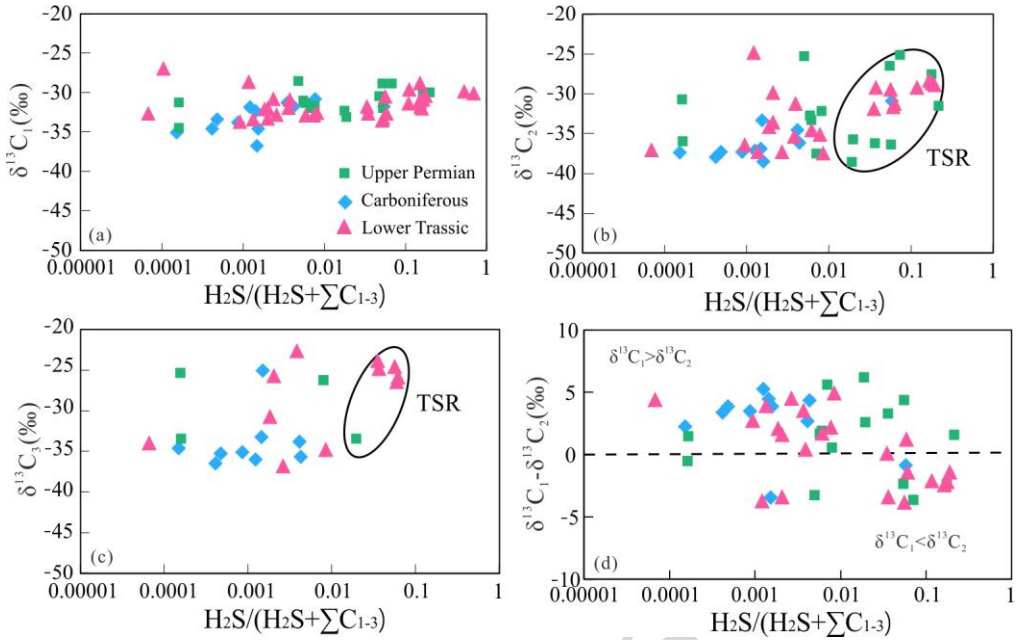


Fig. 16 Diagrams of GSI value [$\text{H}_2\text{S}/(\text{H}_2\text{S}+\sum \text{C}_{1-3})$] versus $\delta^{13}\text{C}_1$ (a), $\delta^{13}\text{C}_2$ (b), $\delta^{13}\text{C}_3$ (c), and $\delta^{13}\text{C}_1-\delta^{13}\text{C}_2$ (d) of natural gas in Sichuan Basin.

The difference in timing and/or reaction rate of TSR, controls the carbon isotope values of alkane gases. A model describing carbon isotope fractionation of methane and ethane has been summarized (Liu et al., 2013). When GSI is less than 0.01, methane is heavier than ethane ($\delta^{13}\text{C}_1 > \delta^{13}\text{C}_2$) (Fig. 16d). This carbon isotope reversal between methane and ethane may be associated with weak TSR reactions to produce heavier methane, or mixing of methane with different thermal maturities (for example, kerogen-cracking gas or oil-cracking gas). The temperature range of TSR is between 100 °C and 140 °C, and the corresponding R_o value is over 1.5% (Machel, 1998). The isotope reversal between methane and ethane in shale gas also happens in this range (Xia et al., 2013; Zumberge et al., 2012). The onset temperature of TSR varies in different reservoirs, due to a number of factors, including hydrocarbon

compositions in the reactions, catalysts, distribution and dissolution rates of anhydrite, humidity, and transport and diffusion coefficients of hydrocarbon gases (Machel, 2001). When the $\text{H}_2\text{S}/(\text{H}_2\text{S}+\sum \text{C}_{1-3})$ ratio is above 0.01, TSR plays a major role in alteration of oil and gas reservoirs. A large amount of hydrocarbons are oxidized and become heavier in carbon isotopes. The carbon isotope value of methane tends to be constant with limited variation. With heavier carbon isotopes of ethane, the trend between methane and ethane becomes normal ($\delta^{13}\text{C}_1 < \delta^{13}\text{C}_2$). At higher GSI values, the reaction continues for methane as a reactant. The finding of a large number of native sulfur in P₂ch and T₁f reservoirs of Sichuan Basin supports the oxidation and alteration of ethane at late stages of TSR. The formation of native sulfur can be expressed as:



The hydrogen isotope fractionation of alkanes in TSR follows the similar mass-dependent kinetic principles to carbon. It is related to the bonding energy between ¹H and D (Coleman et al., 1981; Dai, 1990; Tang et al., 2005). The hydrogen isotope composition of CH₄ is controlled by organic precursors, water as the external hydrogen source (Schimmelmann et al., 2001; Wang et al., 2011; Yoneyama et al., 2002), and exchange reactions between organic matter and water (Lewan, 1993; Schimmelmann et al., 2004). Hydrogen atoms in water participate in chemical reactions with organic matter, and are incorporated into hydrocarbon molecules. (Lewan, 1993; Schimmelmann et al., 2001, 2004, 2009; Yoneyama et al., 2002). Hydrogen isotope composition of methane, which is directly derived from

thermal degradation of kerogen, is mainly affected by water around source rocks.

Other than exchange reactions between hydrogens in water and kerogen (see Section 3.2), participation of TSR can also affect the hydrogen isotope composition of water, which subsequently changes the isotope composition of methane.

Similar to carbon isotopes, the hydrogen isotope composition of methane exhibits a narrow range with increasing GSI (Fig. 17a). Methane from TSR becomes heavier due to kinetic isotope effect (Liu et al., 2014). It becomes dominant in mixing with gases from thermal cracking, making the overall hydrogen isotope of methane within a limited range. The majority of ethane, however, is from thermal cracking, and acts as a reactant in TSR. When GSI is less than 0.01, there is no apparent correlation between GSI and hydrogen isotope composition of ethane (Fig. 17b). When GSI is higher than 0.01, the hydrogen isotope composition of methane ranges from -126‰ to -107‰, while ethane ranges from -165‰ to -89‰. There is a positive relationship between GSI and hydrogen isotope composition of ethane. As TSR intensity increases, ethane tends to become heavier in hydrogen isotope. This correlation suggests the existence of TSR alteration which is dominated by consumption of heavy alkanes rather than methane.

When GSI is less than 0.01, the hydrogen isotope composition of methane is heavier than ethane ($\delta^2\text{H-C}_1 > \delta^2\text{H-C}_2$), due to lack of TSR (Fig. 17c). The reason of this hydrogen isotope reversal may be similar to that of carbon isotopes, which is mainly associated with mixing of a small amount of methane produced by TSR, or mixing of methane with different thermal maturities. In areas that contain gases with

different H₂S contents, the possible reason for the variation of δ²H-C₁ values is that formation water is involved in TSR, and the exchange of hydrogen between methane and formation water causes hydrogen isotope fractionation. The hydrogen isotope composition of methane gradually approaches the value of the hydrogen source (Jiang et al., 2015), as observed in P₂ and T₁ gas reservoirs in Sichuan Basin. When H₂S content is low, the effect of TSR is trivial, and the hydrogen isotope composition of methane mainly reflects its parent material, such as C₂ gas reservoir in Sichuan Basin. Therefore, the large variation of hydrogen isotopes of methane in P₂ and T₁ in eastern Sichuan Basin is mainly related to water participation during TSR (Liu et al., 2014b).

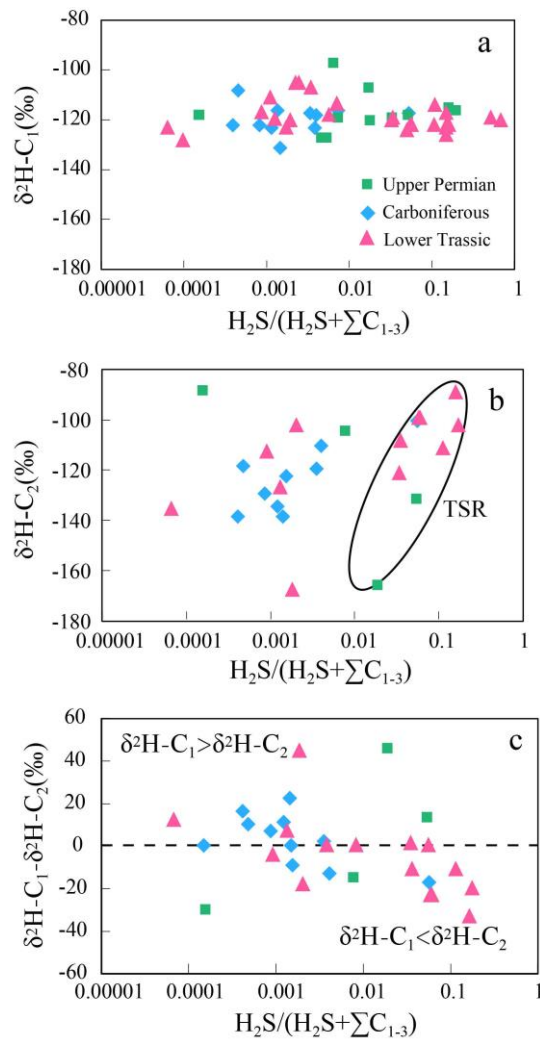


Fig. 17 Diagrams of GSI versus $\delta^{2\text{H}}\text{-C}_1$ (a), $\delta^{2\text{H}}\text{-C}_2$ (b), and $\delta^{2\text{H}}\text{-C}_1 - \delta^{2\text{H}}\text{-C}_2$ (c) of natural gas in Sichuan Basin.

5.2. Biodegradation and Secondary Oxidation

There are a large number of microorganisms in geosphere. When microorganisms have access to hydrocarbons, hydrocarbons can be degraded by electron acceptors with the carbon atoms on the secondary end of hydrocarbons (Kniemeyer et al., 2007). Hydrocarbons have different resistant abilities against microbial degradation, depending on molecular structures. Generally, n-alkanes are preferentially to be degraded, followed by branched alkanes (i-alkanes), and

non-hydrocarbons (Peters et al., 2005). Compared with macromolecules with carbon number higher than 5, gaseous alkanes are difficult to be degraded by microorganisms. The susceptibility of alkanes to degradation follows the order of $C_3 \approx nC_4 > nC_5 > iC_5 > iC_4 >> neOC_5$. It is difficult for ethane to be degraded due to lack of secondary end carbons in structure (Boreham and Edwards, 2008; Boreham et al., 2001; Head et al., 2003; James and Burns, 1984; Meng et al., 2017). It is generally accepted that methane is hard to be anaerobically oxidized by microorganisms and that the oxidation by bacteria causes natural gas components to be dry (Head et al., 2003). The distribution of microorganisms in geosphere is controlled by temperature. Bacteria can sustain temperatures of less than 80°C and burial depths of less than 2000 m or even 2400 m (Meng et al., 2017; Vandré et al., 2007). No H₂S or less than 5% H₂S is present in bacterial gas pools (Peters et al., 2005; Worden et al., 1995).

The influence of microorganisms on the carbon and hydrogen isotopic compositions of alkane gases (methane, ethane and propane) is summarized here, using natural gas reservoirs (less than 2500 m) in Turpan-Hami, Santanghu, Huanghua and Liaohe basins as examples. With increasing gas dryness (C_1/C_{1-3}), the carbon isotopes of methane, ethane and propane in Turpan-Hami gas field show a slight tendency of becoming heavier (Fig. 18). A similar change can be observed for carbon isotopes of ethane and propane in Santanghu gas field, while the opposite is true for methane. In Huanghua and Liaohe, the isotopic composition of methane tends to decrease, while ethane and propane become heavier with no apparent trend for ethane in Liaohe gas field. This isotopic signature is different than the one

observed during thermal evolution: the carbon isotope of alkane gases becomes heavier with increasing gas dryness. Therefore, microbial degradation may be lacking in Turpan-Hami, while natural gas in Santanghu, Huanghua and Liaohe is subject to different degrees of microbial degradation.

Microbial degradation leads to a decrease in content and heavier carbon isotope compositions of propane, as well as an increase in content and lighter carbon isotopes of methane. In Santanghu and Huanghua, ethane may not participate microbial degradation. The coexistence of ethane with both heavier and lighter carbon isotopes in natural gas reservoirs in Liaohe Basin may suggest that ethane with lighter carbon isotopes is produced by microorganisms. Its carbon isotope compositions become heavier due to late stage biodegradation. Due to preferential degradation of propane by microorganisms, the carbon isotope compositions of remaining hydrocarbons become heavier with components containing heavy isotopes barely oxidized by microorganisms (Boreham and Edwards, 2008; Huang et al., 2017; Kinnaman et al., 2007; Meng et al., 2017). The changes of hydrogen isotope composition of alkanes during biodegradation are similar to carbon isotopes. In summary, microbial degradation is a process that consumes propane and produces methane, resulting in a decrease in propane content, heavier carbon and hydrogen isotopes, and lower content of methane with lighter carbon and hydrogen isotope compositions.

In order to assess the effect of microbial degradation on the carbon and hydrogen isotope compositions of alkane, the C_3/C_{1-3} ratio was used to display compositional

changes of alkanes. With decreasing C_3/C_{1-3} , or increasing biodegradation intensity, the carbon isotope of methane becomes lighter (Fig. 19a). This feature is completely different than the one caused by thermal evolution or TSR alteration. As the C_3/C_{1-3} index decreases, the carbon isotope of propane tends to be heavier, due to the fact that ^{12}C is preferentially biodegraded (Fig. 19b) (Vandré et al., 2007). As a result, propane enriched in ^{12}C is preferentially degraded by microorganisms and ^{12}C -enriched methane is formed. The carbon isotope composition of residual propane in gas reservoirs becomes heavier. Other hydrocarbon gases (nC_4 , iC_4 , nC_5 and iC_5) may also be degraded by microorganisms to form ^{12}C -enriched methane.

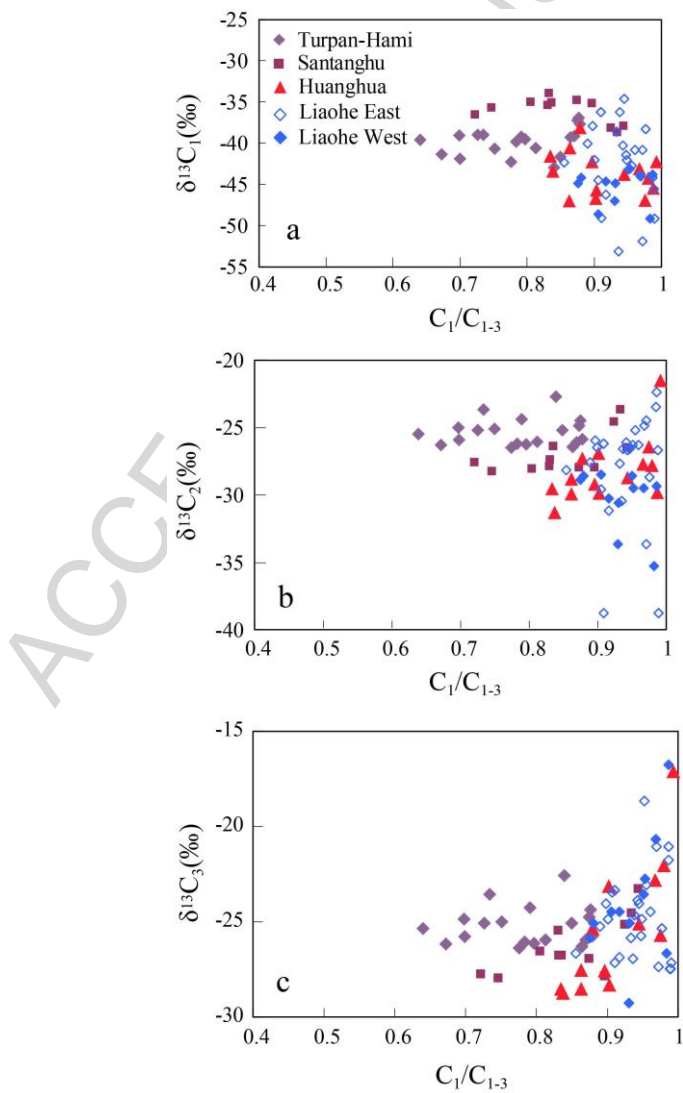


Fig. 18 Diagrams of gas dryness (C_1/C_{1-3}) versus $\delta^{13}C_1$ (a), $\delta^{13}C_2$ (b), and $\delta^{13}C_3$ (c) of alkane gases.

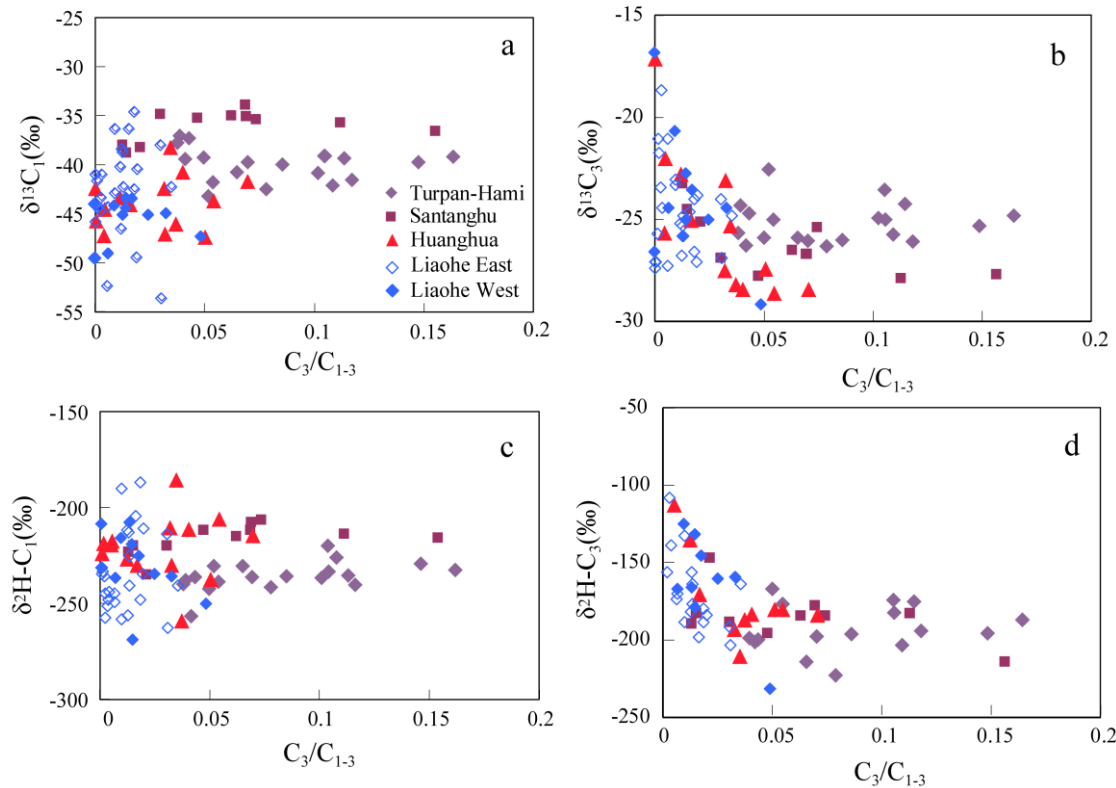


Fig. 19 Diagrams of C_3/C_{1-3} value versus $\delta^{13}C_1$ (a), $\delta^{13}C_3$ (b), δ^2H-C_1 (c), and δ^2H-C_3 (d) for natural gas from petroliferous basins in China.

With decreasing C_3/C_{1-3} value, the hydrogen isotope composition of methane shows tendency of becoming lighter (Fig. 19c), and propane becoming heavier (Fig. 19d). Methane becomes more enriched in 1H with higher intensity of microbial degradation, while propane becomes more depleted in 1H . Compared to carbon isotopes, there is little change in hydrogen isotope composition of methane with biodegradation. It may be related to the intervention of formation water which has a

constant hydrogen isotope value. However, the effect of microbial degradation on hydrogen isotope composition of propane is significant. Ethane acts as a product or reactant during microbial degradation. The effect of formation water on hydrogen isotope composition of alkanes remain to be studied. Recent studies have reported that methane can undergo microbial anaerobic oxidation in sediments, and this process is considered as an important pathway to consume methane within the global carbon cycle (Boetius et al., 2000; Knittel and Boetius, 2009; Valentine, 2011). However, the role of anaerobic oxidation of methane (AOM) in natural gas reservoirs is still uncertain.

5.3. Diffusion

In theory, the expulsion of natural gas from source rocks results in isotopic fractionation and changes in chemical composition. These changes, however, are often negligible for genetic identification and gas-source correlation (Lorant et al., 1998; Schoell, 1988). Due to small molecule sizes, light weights, and high diffusion coefficients, stable isotope fractionations of alkanes occur in gas reservoirs during diffusion (Krooss et al., 1992; Prinzhofner and Pernaton, 1997; Zhang and Krooss, 2001). As the molecular weight increases, the diffusion ability of alkane gas decreases, following the order of methane > ethane > propane (Krooss et al., 1986). Due to its mass-dependent feature, the diffusion of isotopes with less mass number is favored for each given element, for example, ^{12}C to ^{13}C , and ^1H to ^2H (Krooss et al., 1992; Zhang and Krooss, 2001).

Prinzhofer and Pernaton (1997) identified gas diffusion using the C₂/C₁ content ratio and methane isotopic values. As the carbon isotope of methane increases, the C₂/C₁ ratio in the gas reservoir that is subject to diffusion increases exponentially, whereas the C₂/C₁ ratio in reservoirs without diffusion shows a decreasing trend and is controlled by maturity. Xiao (2012) demonstrates that the carbon and hydrogen isotope reversal ($\delta^{13}\text{C}_1 > \delta^{13}\text{C}_2$ and $\delta^2\text{H-C}_1 > \delta^2\text{H-C}_2$) of the non-associated gases (NAG) in Northern Appalachian Basin is caused by diffusion using data from Burruss and Laughrey (2010). As the carbon isotope value of methane increases, the trend of C₂/C₁ ratio in NAG differs from that of oil associated gases (OAG) (Fig. 20a). The decreasing trend of C₂/C₁ ratio of OAG is most likely related to the increase of thermal maturity, which leads to the increase in content of methane and its carbon and hydrogen isotope values (Prinzhofer and Pernaton, 1997). In NAG, however, with increasing carbon isotope compositions of methane, the ratio of C₂/C₁ shows a dispersed pattern with a slight increasing trend. This pattern may be related to diffusion of methane that results in a decrease in methane content and an increase in its carbon isotope value (Prinzhofer and Pernaton, 1997; Zhang and Krooss, 2001). As the C₂/C₁ ratio decreases, the difference in carbon isotope values between methane and ethane ($\delta^{13}\text{C}_1 - \delta^{13}\text{C}_2$) in OAG show a decreasing trend, with partially reversed carbon isotopic sequence ($\delta^{13}\text{C}_1 > \delta^{13}\text{C}_2$) (Fig. 20b). In contrast, the $\delta^{13}\text{C}_1 - \delta^{13}\text{C}_2$ values in NAG show an increasing trend, with positive carbon isotope sequence between methane and ethane ($\delta^{13}\text{C}_1 < \delta^{13}\text{C}_2$). Laboratory experiments have shown that the diffusion of methane through mudstone leads to an increase of 4‰ in

carbon isotope compositions (Zhang and Krooss, 2001).

The effect of diffusion on hydrogen isotopes of methane is similar to carbon isotopes (Fig. 20c). With increasing hydrogen isotope composition of methane, the C₂/C₁ ratio of NAG decreases due to changes in thermal maturity, while variations of C₂/C₁ ratio exist for OAG with a decreasing trend that are controlled by both maturity and diffusion. In Fig. 20d, the difference of hydrogen isotope composition between methane and ethane ($\delta^2\text{H-C}_1 - \delta^2\text{H-C}_2$) in NAG shows a decreasing trend with increasing C₂/C₁ ratio, and the hydrogen isotope pattern between methane and ethane is positive (i.e., $\delta^2\text{H-C}_1 < \delta^2\text{H-C}_2$). However, there is a positive correlation between the $\delta^2\text{H-C}_1-\delta^2\text{H-C}_2$ value and C₂/C₁ ratio in OAG, and the hydrogen isotope pattern between methane and ethane are positive or negative. In summary, diffusion leads to a lower content of methane. The carbon and hydrogen isotope compositions of residual methane become heavier, causing the carbon and hydrogen isotope reversal between methane and ethane.

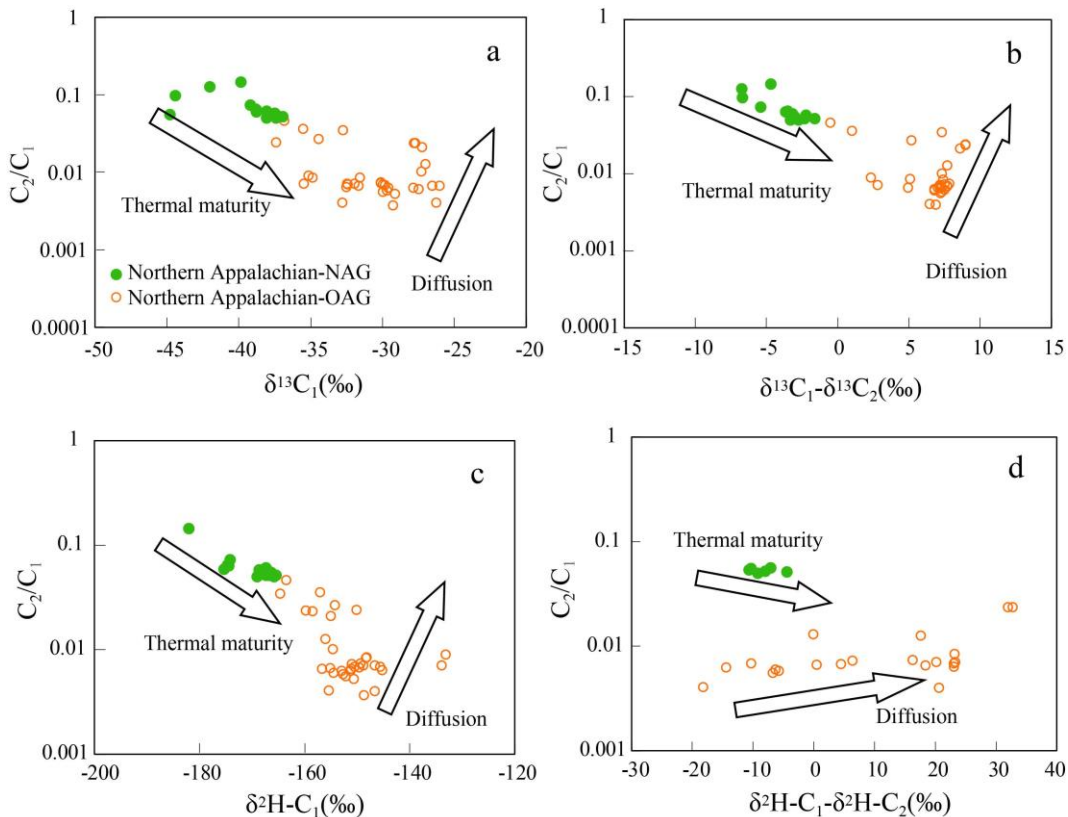
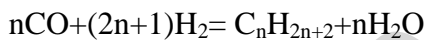
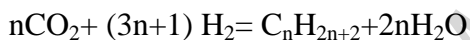


Fig. 20 Diagrams of C_2/C_1 ratio versus $\delta^{13}C_1$ (a), $\delta^{13}C_1 - \delta^{13}C_2$ (b), δ^2H-C_1 (c), and $\delta^2H-C_1 - \delta^2H-C_2$ (d) of alkanes in non-associated gases (NAG) and oil associated gases (OAG) in Northern Appalachian Basin. Data from Burruss and Laughrey (2010)

6. Abiogenic alkane gases (mantle-derived and Fischer-Tropsch type synthesis)

There are two types of abiogenic gases which have inorganic precursors: 1) small molecular gases, for example, methane from deep mantle; and 2) natural gas that is formed through processes involving water-rock interaction or Fischer-Tropsch type (FTT) synthesis. The analysis of fluid inclusions has shown that mantle-derived gases are dominated by CH_4 , CO or CO_2 , and noble gases (Giardini et al., 1982; Pineau and Javoy, 1983; Sugisaki and Mimura, 1994). Heavier hydrocarbon gas with

carbon number more than 2 has not been found. The Fischer-Tropsch synthesis was first developed by German chemists Franz Fischer and Hans Tropsch in 1923. The whole process includes heterogeneous catalytic hydrogenation of CO to generate hydrocarbons with different chain lengths and oxygenated organic compounds. The reactants in this synthesis are CO and H₂, and the products can be a number of organic compounds, depending on catalysts and temperature and pressure conditions (Anderson, 1984). Considering the lack of CO in geological environment, similar reactions that generate organic compounds from CO₂ are called Fischer-Tropsch type (FTT) synthesis. Combined together, reactions that contribute to formation of abiogenic alkane gases are listed as follows:



Compared to CO, the effectiveness of hydrocarbon formation in CO₂-involved FTT is much less. It may also be attributed to higher temperatures and pressures, and availability of transition metal catalysts under geological conditions. Lancet and Anders (1970) first reported the formation of CH₄ from CO₂ and H₂ using Co as a catalyst. Horita and Berndt (1999) used Ni-Fe alloy to observe the conversion of HCO₃⁻ to methane under subseafloor hydrothermal conditions. The formation of alkane gases through FTT has been demonstrated in laboratory experiments under different temperature, pressure, and constituent conditions (Fu et al., 2007; Fu et al., 2015; Horita and Berndt, 1999; McCollom and Seewald, 2001; Taran et al., 2007; Zhang et al., 2013).

In mid-ocean ridge hydrothermal systems, the carbon isotope composition of methane is in the range of $-18\text{\textperthousand}$ to $-15\text{\textperthousand}$ (Welhan, 1988). Due to the lack of sedimentary strata in reaction zones, methane from seafloor hydrothermal vents is considered to be abiogenic. The carbon isotope compositions of CH_4 in gas seeps from Zambales ophiolite in Philippines are between $-7.5\text{\textperthousand}$ and $-6.1\text{\textperthousand}$, similar to the values of mantle-derived or original atmospheric CO_2 (Abrajano et al., 1988). The gas from hot springs in eastern and southern China is dominated by CO_2 , and methane is major organic compound with trace amounts of heavier hydrocarbon gases (C_{2+}) (Dai et al., 2005b). The carbon isotope composition of methane varies from $-73.2\text{\textperthousand}$ to $-19.5\text{\textperthousand}$.

The carbon isotope compositions of CO_2 and methane from commercial gas wells in petroliferous basins in China and Permian Basin in U.S. are shown in Fig. 21. Among the reported carbon isotope values of CO_2 and methane, the lowest value of methane, $-54.4\text{\textperthousand}$, is obtained from Well Hua17 in Huagou gas field of Bohai Bay Basin (Dai et al., 2005b). The heaviest value, $-17.4\text{\textperthousand}$, is from Fangshen 2 well in Qingshen gas field of Songliao Basin, where the lowest carbon isotope value of CO_2 , $-16.5\text{\textperthousand}$, is also reported (Liu et al., 2016). The heaviest value of CO_2 is $-2.7\text{\textperthousand}$ from the Mitchell 103 No.3 well in Permian Basin (Ballentine et al., 2001). As the carbon isotope of CO_2 becomes heavier, there is a general trend showing that methane becomes lighter. The lightest hydrogen isotope value of methane is $-205\text{\textperthousand}$ in Fangshen 6 well from Qingshen gas field in Songliao Basin, while the heaviest is $-181\text{\textperthousand}$ from Zhuang 5-2 well in the same basin (Liu et al., 2016).

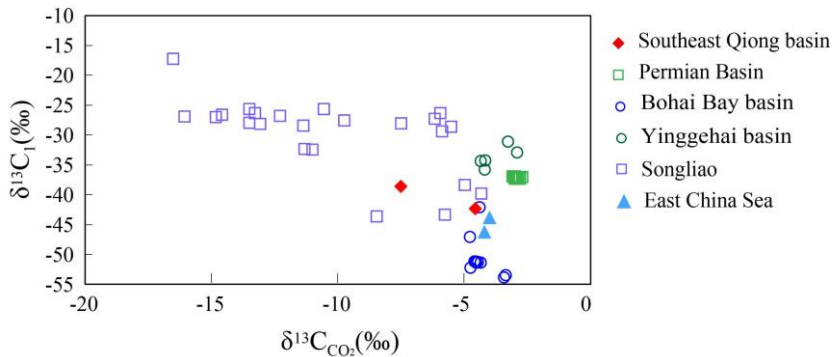


Fig. 21 The diagram of $\delta^{13}\text{C}_{\text{CO}_2}$ versus $\delta^{13}\text{C}_1$ for commercial gas reservoirs in some major petroliferous basins worldwide

The abundance and isotopic ratio of noble gases are controlled by physical processes (dissolution, adsorption and nuclear reactions), but not by chemical reactions during geological processes. They can be used effectively as signatures of deep sources. The presence of the mantle-derived gas can be identified by the $^3\text{He}/^4\text{He}$ ratio, with the value $>1.0\text{Ra}$ as an indicator of deep origin (Ballentine and O'Nions, 1992; Dai et al., 2005b; Poreda and Craig, 1989; Wakita and Sano, 1983; Xu et al., 1995, 1998). Ra represents the $^3\text{He}/^4\text{He}$ ratio of the air, and it is considered to be a constant ($^3\text{He}/^4\text{He}_{\text{air}} = 1.4 \times 10^{-6}$). Fig. 22 shows the relationship between R/Ra and carbon isotopes of methane and CO_2 in commercial gas reservoirs. As the R/Ra ratio increases, the carbon isotope value of CO_2 remains unchanged. For example, as R/Ra increases from 0.240 to 0.543 in the CO_2 -rich gas field in Permian Basin, the carbon isotope ratio of CO_2 is constant ranging from $-3.1\text{\textperthousand}$ to $-2.7\text{\textperthousand}$. The R/Ra ratio of natural gas from Songliao Basin increased from 0.218 to 5.543, and $\delta^{13}\text{C}_{\text{CO}_2}$ values varied from $-16.5\text{\textperthousand}$ to $-4.3\text{\textperthousand}$ (Fig. 22a). Therefore, as the R/Ra ratio increases, the contribution of mantle-derived gas increases. The carbon isotope

composition of CO₂ in different regions is not constant with the same R/Ra ratio, which may imply the heterogeneity of carbon isotopic composition of CO₂ in the mantle.

As the R/Ra ratio increases, the change in carbon isotope value of methane is complicated. The carbon isotope composition of methane from the CO₂-rich gas reservoir in Permian Basin shows a slightly lighter trend with increasing R/Ra (Fig. 22b). The variation of $\delta^{13}\text{C}_{\text{CO}_2}$ values in Songliao Basin (except Fangshen 2 well) and Bohai Bay Basin is more significant, and there is no apparent correlation with R/Ra ratio.

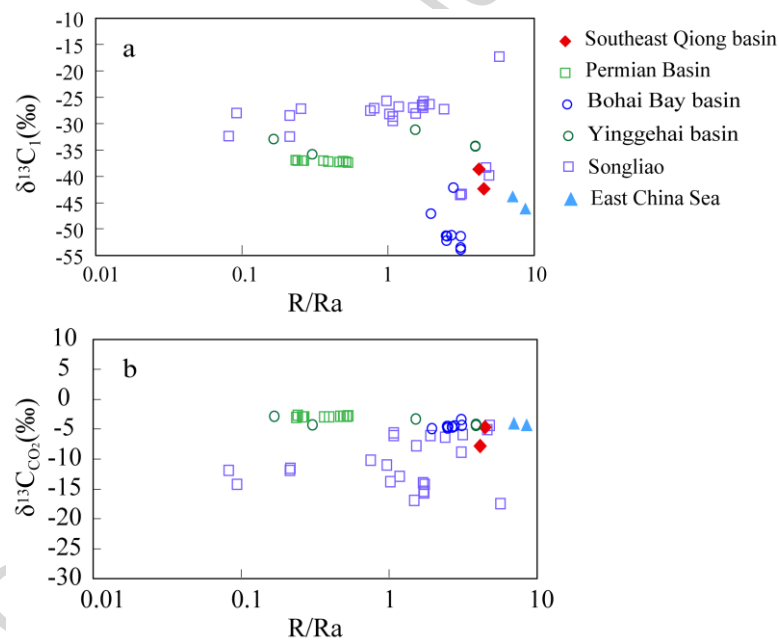


Fig. 22 The diagram showing R/Ra ratio versus $\delta^{13}\text{C}_1$ (a) and $\delta^{13}\text{C}_{\text{CO}_2}$ (b) for commercial gas reservoirs

The carbon isotope composition of methane becomes depleted in ¹³C with increasing carbon isotope value of CO₂, suggesting fractionations between CO₂ and

methane. Hu et al. (1998) reported that fractionation between CO₂ and CH₄ varies significantly, ranging from 5.6‰ to 69.9‰, while the equilibrium fractionation value (1000ln α) is between 28‰-24‰ at 270-300°C (Bottinga, 1969). This carbon isotope fractionation between CO₂ and CH₄ may be attributed to Fischer-Tropsch synthesis, because upwelling of magma carries large amounts of thermal energy with Fe-bearing minerals being effective catalysts for FTT reactions (McCollom et al., 2006). Methane in inclusions of alkaline volcanic rocks formed by FTT synthesis displays carbon isotope value of -11.8‰ to -3.2‰ and hydrogen isotope value of -167‰ to -132‰ (Potter et al., 2004). The carbon isotope value of methane from water-rock reactions in Hakuba Happo hot spring in Japan is from -38.1‰ to -33.2‰, and the hydrogen isotope value of methane is from -300‰ to -210‰, and the carbon isotope value of CO₂ is from -8.8‰ to -3.9‰ (Suda et al., 2014). The experimental results have also shown that as temperature increases, the discrepancy of $\delta^{13}\text{C}_{\text{CO}_2}$ - $\delta^{13}\text{C}_1$ gradually decreases (McCollom and Seewald, 2001; Taran et al., 2007).

The isotope fractionation during the abiotic generation process of alkane gases which is proposed as polymerization reactions from simple molecules (CO, CO₂, and CH₄), is constrained by kinetic isotopic effect. During polymerization, ¹²C is favored to form C-C chains. ¹²C tends to be enriched in products, which results in ¹³C depletion of ethane relative to methane. Since ¹²C-²H bonds are more stable than ¹²C-¹H bonds, ²H preferentially combines with ¹²C in polymerization, and ethane is enriched in ²H compared to methane. It causes that the formed alkane gas has a

lower $\delta^{13}\text{C}$ value, which generates the carbon isotope reversal of alkane gases ($\delta^{13}\text{C}_1 > \delta^{13}\text{C}_2 > \delta^{13}\text{C}_3 > \delta^{13}\text{C}_4$) (Dai et al., 2005b; Des Marais et al., 1981; Galimov, 2006; Hosgormez et al., 2005; Sherwood Lollar et al., 2002, 2008). The higher carbon isotope values of methane than ethane ($\delta^{13}\text{C}_1 > \delta^{13}\text{C}_2$) have been reported in geological samples (Dai et al., 2005; Liu et al., 2016), but not in laboratory experiments. Using data from spark discharge experiments in Des Marais (1981), Galimov (2006) suggested that C₁-C₃ hydrocarbons synthesized in spark discharge experiments share the same isotope distribution pattern as in volcanic rocks. The experiments with different reaction times have shown that the conversion rate of CO₂ increases with time. The carbon isotope trend of alkane gases gradually turns from completely reversal to partial reversal, and then to thermogenic trend. The spark discharge experiments take the shortest time, and the carbon isotopes of alkane gases are in a reversed order.

Sherwood Lollar et al. (1988, 1997) proposed that the C and H isotopes of abiogenic methane and ethane in Precambrian shields in Canada and South Africa are inversely correlated, i.e., $\delta^{13}\text{C}_1 > \delta^{13}\text{C}_2$, $\delta^2\text{H-C}_1 > \delta^2\text{H-C}_2$. However, the reversed trend of C and H isotopes of short alkanes has not been observed in laboratory experiments (Fu et al., 2007, 2015). In closed FTT synthesis, reaction time, temperature and product selectivity may control the isotope fractionation between hydrocarbons. The kinetic isotope fractionation during polymerization may be overshadowed by continuous buildup of hydrocarbons on mineral surfaces and reduced thermodynamic drive in closed systems. The isotope reversal may be

observed only at the very beginning stage of FTT (i.e., spark discharge experiments, short time with low conversion rates) or in open systems. The abiogenic gas collected in geological environment most likely is a mixture of gases from deep mantle and FTT synthesis, which involves complex reactions that cannot be observed in single laboratory experiments.

Overall, methane formed by FTT synthesis possesses a wide range of carbon and hydrogen isotopic compositions. It may be overlapped with thermogenic methane (Horita and Berndt, 1999). However, mantle-derived gas exists in the region with active deep fluids. Alkane gases, including methane, can be formed by CO₂/CO and H₂ through FTT synthesis with the catalysis of Fe-bearing minerals and tremendous energy carried by deep fluids.

7. Genetic identification of natural gas

Carbon and hydrogen isotope compositions of natural gas are controlled by source rocks (or organic matter). Secondary alteration following accumulation in reservoirs may also change the isotopic values. Those changes lead to ambiguities and uncertainties in genetic identification and gas-source correlation, which cannot be resolved using conventional methods. Here, a series of diagnostic tools are suggested to effectively pin down this complex cause-effect relationship.

7.1. Carbon and hydrogen isotopes of methane ($\delta^{13}\text{C}_1$ vs. $\delta^2\text{H-C}_1$)

To identify origins of CH₄, Whiticar (1999) established a diagram between carbon and hydrogen isotope compositions. Gases generated by microbial activities, thermocatalytical processes, and from hydrothermal, geothermal and crystalline rock

systems can be separated (Fig. 23). For example, natural gas from Qaidam and Luliang-Baoshan is typical microbial gas. The gas from Qaidam is derived from bacterial reduction of carbon dioxide, whereas the gas from Luliang-Baoshan area is from both bacterial reduction of carbon dioxide and methyl-type fermentation. The gases from Liaohe and Huanghua Depression in Bohai Bay Basin and Turpan-Hami are low-mature or immature that are formed at early thermal stages.

However, no clear separation can be observed between humic coal-type gas and sapropelic oil-type gas, for example, oil-type gas from Ordovician strata in Tarim Basin, O₁ in Ordos Basin, Pearl River Mouth Basin, and Northern Appalachian, and coal-type gas from the foreland of Tarim Basin, Upper Paleozoic strata in Ordos Basin, and T_{3x-J} in Sichuan Basin. Natural gas with TSR alteration from C₂h-P₂ch-T₁f strata in Sichuan Basin displays the characteristics of humic coal-type gas with high maturity (Fig. 23). In addition, diffusion has not been well represented in this classification. For example, oil-type gas from the Northern Appalachian Basin has migrated, resulting in heavier carbon and hydrogen isotopes of methane (Burruss and Laughrey, 2010; Xiao, 2012).

The characteristics of abiogenic gas can be obtained from Fig. 23. For example, methane in Qingshen gas field of Songliao Basin and Hakuba Happo hot spring are of hydrothermal origin, although it is uncertain whether methane in hydrothermal systems is from deep mantle or other sources (FTT synthesis, organic matter, etc.). Methane in Kidd Creek Mine is more likely synthesized or metamorphosed through FTT than directly from mantle. Therefore, the classification using carbon and

hydrogen isotopes of methane can identify natural gas from organic matter with different thermal maturities, but secondary alteration (TSR, microbial degradation, and diffusion) may cause uncertainties.

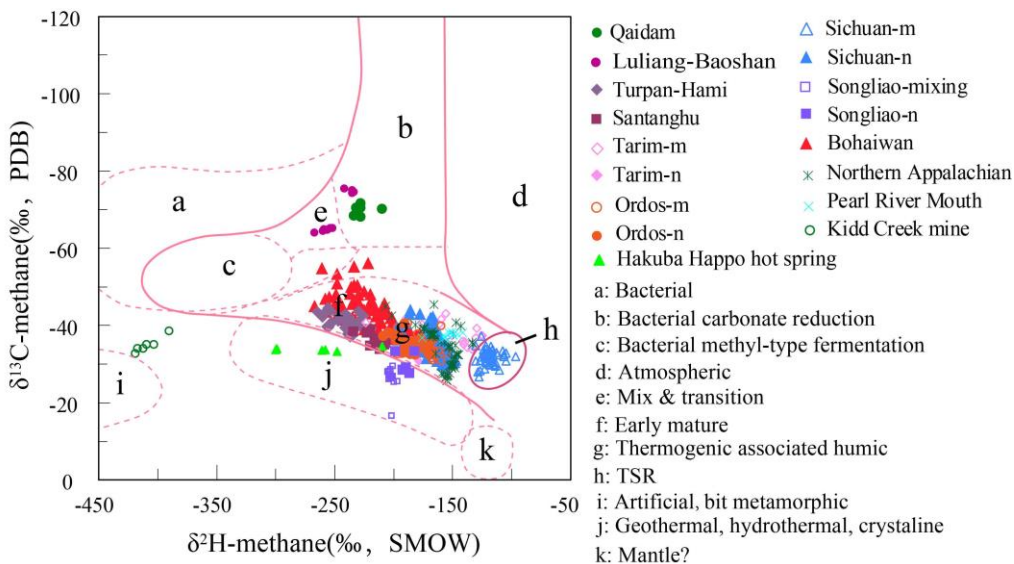


Fig. 23 The diagram of $\delta^2\text{H-C}_1$ versus $\delta^{13}\text{C}_1$ of methane with different origins (after Whiticar, 1999)

¹-m, -n, and -mixing: see Fig. 1

7.2. Carbon isotope of ethane and hydrogen isotope of methane ($\delta^{13}\text{C}_2$ vs. $\delta^2\text{H-C}_1$)

As discussed above, hydrogen isotopes of methane are more sensitive to the depositional environment of parent materials, while carbon isotopes of ethane and propane inherit signatures from parent materials very well. In Fig. 24, using hydrogen isotopes of methane and carbon isotopes of ethane, it shows that the carbon isotope composition of thermogenic ethane (coal-type and oil-type) tends to become heavier as the hydrogen isotope composition of methane increases. The

coal-type gas formed in fresh-brackish water depositional environments shows heavier ethane carbon isotopes and lighter methane hydrogen isotopes, including gas from the foreland of Tarim Basin, C-P of Ordos Basin, and the T₃x stratum in Sichuan Basin. The oil-type gas formed from marine saltwater depositional environment has higher methane hydrogen isotope values and relatively lower ethane carbon isotope values, including gas from Ordovician strata in Tarim Basin, C₂h-P₂ch-T₁f in Sichuan Basin and O₁ in Ordos Basin. However, natural gas formed in a brackish lacustrine depositional environment has lighter methane hydrogen isotopes and relatively low ethane carbon isotope values, which may also be referred to as oil-type gas, such as a portion of natural gas from the western and eastern Liaohe. The microbial gas formed in terrigenous freshwater environments has not only light methane hydrogen isotope compositions, but also light carbon isotope compositions, which is different than the gas from Luliang-Baoshan and Qaidam gas reservoirs.

The hydrogen isotopes of methane are strongly affected by both diffusion and TSR alteration. With increasing extents/intensities of diffusion and TSR alteration, methane becomes enriched in ²H. The carbon isotope value of ethane, however, exhibits a decreasing trend with increasing hydrogen isotope values of methane (Fig. 24), suggesting slightly stronger effects of diffusion and TSR alteration than thermal maturity. There is no correlation between hydrogen isotopes of methane and carbon isotopes of ethane formed by metamorphism. However, the hydrogen isotope composition of methane is obviously lighter than that of organic matter, but the

carbon isotope composition of ethane is overlapped with that of thermogenic ethane. Natural gas formed by mixing of thermogenic and abiogenic gas shows that hydrogen isotopes of methane remain constant while carbon isotopes of ethane vary significantly, as in the Qingshen gas field in Songliao Basin.

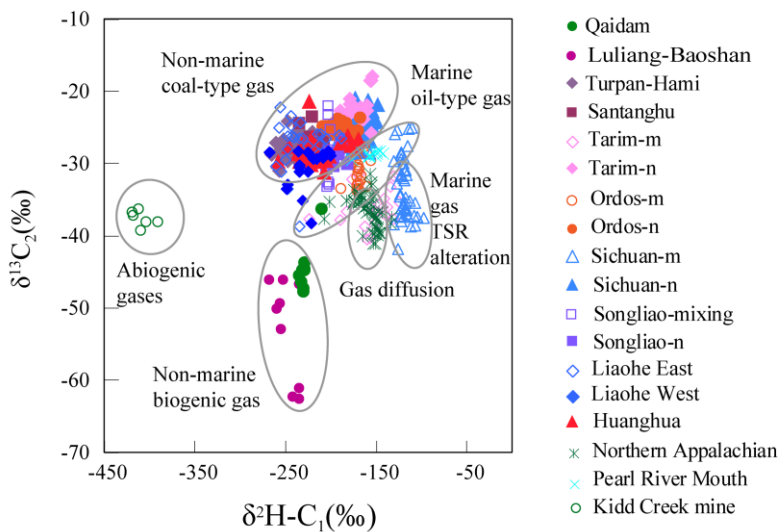


Fig. 24 The diagram of $\delta^2\text{H}-\text{C}_1$ versus $\delta^{13}\text{C}_2$ for different types of natural gas

¹-m, -n, and -mixing: see Fig. 1

7.3. Carbon and hydrogen isotopes of ethane and propane ($\delta^{13}\text{C}_2$ vs. $\delta^2\text{H}-\text{C}_2$ and $\delta^{13}\text{C}_3$ vs. $\delta^2\text{H}-\text{C}_3$)

Besides sources, depositional environments, and thermal evolution stages of organic matter, the isotope signature of methane is also affected by microbial degradation, TSR, and diffusion, while heavier hydrocarbon gases are mainly affected by organic sources and thermal evolution (with propane being altered mostly by microbial degradation). As can be seen in Fig. 25, the marine oil-type gas and terrigenous coal-type gas can be identified using carbon and hydrogen isotopes of ethane (Fig. 25a) and propane (Fig. 25b). The coal-type gas is distributed to the

lower right area of the oil-type gas, i.e., the carbon isotope of heavier hydrocarbons in coal-type gas is heavier than oil-type gas, and the hydrogen isotope follows the same trend as carbon. As the degree of thermal evolution increases, carbon and hydrogen isotope compositions of ethane and propane all show a tendency of becoming heavier. However, there is no apparent correlation between carbon and hydrogen isotopes of abiogenic hydrocarbon gas (metamorphic origin), most likely due to lack of data. For natural gas from the Qingshen gas field in Songliao Basin, the hydrogen isotope composition of propane has a wide range, while the carbon isotope is limited. Both of them show no relationship with thermal maturity. It is uncertain whether large amounts of heat from deep fluids lead to hydrogen isotope exchange between propane and formation water. Laboratory experiments have shown that hydrogen isotope fractionation between alkane gases and water favors molecules with higher weights as temperature increases (Reeves et al., 2012).

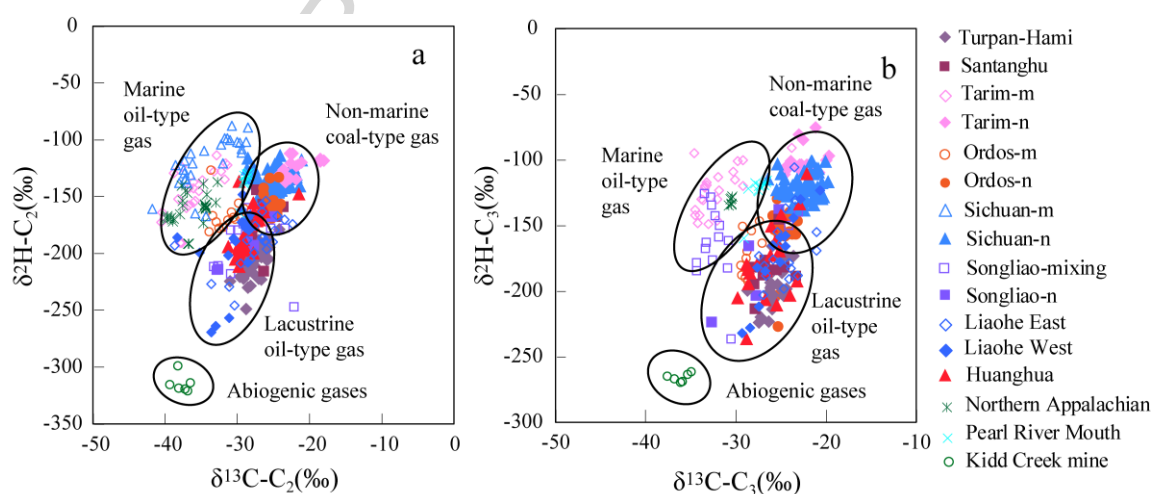


Fig. 25 The diagrams showing (a) $\delta^{13}\text{C}_2$ vs. $\delta^2\text{H-C}_2$ and (b) $\delta^{13}\text{C}_3$ vs. $\delta^2\text{H-C}_3$ for genetic identification of natural gas

¹-m, -n, and -mixing: see Fig. 1

Conclusions

In natural gas geochemistry, the carbon and hydrogen isotope compositions of gaseous alkanes contain ample information on organic source, along with geological and geochemical processes during hydrocarbon generation. In other words, the inheritance of isotope signatures is affected by physical and biochemical reactions in geological history. Alkane hydrocarbons (CH_4 , C_2H_6 , and C_3H_8) formed from saltwater sapropelic organic matter are oil-type gas and enriched in ^{12}C and ^2H , while gases from humic organic matter are called coal-type gas and enriched in ^{13}C and ^1H . As the degree of thermal evolution increases, the isotope compositions of oil-type and coal-type alkane gases gradually become heavier. The coal-type alkanes are heavier than oil-type under similar thermal evolution degree. As thermal maturity increases, the hydrogen isotope composition of alkanes also shows a tendency of becoming heavier. However, the hydrogen isotope composition of alkanes formed by saltwater deposition is heavier than that formed in the depositional environment of fresh-brackish water. The carbon isotope composition of alkanes is mainly controlled by organic sources, followed by thermal evolution, while the hydrogen isotope is mainly controlled by salinity of water body when organic matter is deposited, followed by the extent of thermal evolution. Thermal cracking of hydrocarbons under high temperatures does not change the increasing trend of carbon and hydrogen isotopes of alkane gases. However, the differences in generation rate and

chemical composition between hydrocarbons and kerogen during thermal cracking under high temperatures cause the variation of carbon and hydrogen isotope compositions of natural gas, in particular, the reversed trend between methane and ethane. The secondary TSR alteration and diffusion lead to heavier carbon and hydrogen isotope composition of methane, which may also cause the carbon and hydrogen isotope reversal between methane and ethane. Microbial degradation causes a decrease in propane content and heavier carbon isotopes. Abiogenic gas includes both deep mantle-derived methane and alkane gases derived from FTT reactions. Since mantle-derived fluids carry H₂, CO₂ and energy, gases from FTT may be accompanied by mantle-derived gases. The carbon and hydrogen isotope compositions of mantle-derived methane have a relatively small range, while alkane gases from FTT display a wide range of carbon and hydrogen isotopic compositions.

Due to the complexity of gas accumulation, there is no single pattern or parameter to effectively identify alkane gases from different origins. The carbon and hydrogen isotope reversal of alkanes is not unique to abiogenic gases. The geological background, combined with chemical and isotopic compositions, is important for assessing genetic types of natural gas.

Acknowledgments

We would like to thank Profs. Jinxing Dai and Wenhui Liu for constructive discussions.

Funding: This work was financially supported by the Strategic Priority Research Program of the Chinese Academy of Sciences [grant number XDA14010101] and National Natural Science Foundation of China [grant numbers 41625009, 41872122 & U1663201].

ACCEPTED MANUSCRIPT

References

- Abrajano, T.A., Sturchio, N.C., Bohlke, J.K., Lyon, G.L., Poreda, R.J., Stevens, C.M., 1988. Methane-hydrogen gas seeps, Zambales Ophiolite, Philippines: deep or shallow origin? *Chemical Geology* 71, 211-222.
- Anderson, R.B., 1984. The Fischer-Tropsch synthesis. *Acdemia Press*, Newyork.
- Ballentine, C.J., O'Nions, R.K., 1992. The nature of mantle neon contributions to Vienna Basin hydrocarbon reservoirs. *Earth and Planetary Science Letters* 113, 553-567.
- Ballentine, C.J., Schoell, M., Coleman, D., Cain, B.A., 2001. 300-Myr-old magmatic CO₂ in natural gas reservoirs of the west Texas Permian basin. *Nature* 409, 327-331.
- Behar, F., Kressmann, S., Rudkiewicz, J.L., Vandenbroucke, M., 1992. Experimental simulation in a confined system and kinetic modelling of kerogen and oil cracking. *Organic Geochemistry* 19, 173-189.
- Behar, F., Vandenbroucke, M., Teermann, S.C., Hatcher, P.G., Leblond, C., Lerat, O., 1995. Experimental simulation of gas generation from coals and a marine kerogen. *Chemical Geology* 126, 247-260.
- Beijerinck, M.W., 1895. Ueber Spirillum desulfuricans als Ursache von Sulfat-reduktion. *Centralblatt fur Bakteriologie, Parasitenkunde, Infektionskrankheiten und Hygiene Abteilung I*, 1-114.
- Beltrame, P.L., Carniti, P., Audisio, G., Bertini, F., 1989. Catalytic degradation of polymers:Degradation of polyethylene. *Polymer Degradatiuon & Stability* 26,

209-220.

Berner, U., Faber, E., Scheeder, G., Panten, D., 1995. Primary cracking of algal and landplant kerogen: kinetic models of isotope variations in methane, ethane and propane. *Chemical Geology* 126, 233-245.

Boetius, A., Ravenschlag, K., Schubert, C.J., Rickert, D., Widdel, F., Gieseke, A., Amann, R., Jorgensen, B.B., Witte, U., Pfannkuche, O., 2000. A marine microbial consortium apparently mediating anaerobic oxidation of methane. *Nature* 407, 623-626.

Boreham, C.J., Edwards, D.S., 2008. Abundance and carbon isotopic composition of neopentane in Australian natural gas. *Organic Geochemistry* 39, 550-556.

Boreham, C.J., Hope, J.M., Hartung-Kagi, B., 2001. Understanding source, distribution and preservation of Australian Natural gas: A geochemical perspective. *The APPES Journal* 41, 523-547.

Bottinga, Y., 1969. Calculated fractionation factors for carbon and hydrogen isotope exchange in the system calcite-carbon dioxide-graphite-methane-hydrogen-water vapor. *Geochimica et Cosmochimica Acta* 33, 49-64.

Burruss, R.C., Laughrey, C.D., 2010. Carbon and hydrogen isotopic reversals in deep basin gas: Evidence for limits to the stability of hydrocarbons. *Organic Geochemistry* 41, 1285-1296.

Cai, C., Hu, G., He, H., Li, J., Li, J., Wu, Y., 2005. Geochemical characteristics and origin of natural gas and thermochemical sulphate reduction in Ordovician

- carbonates in the Ordos Basin, China. *Journal of Petroleum Science and Engineering* 48, 209-226.
- Cai, C., Hu, W., Worden, R.H., 2001. Thermochemical sulphate reduction in Cambro-Ordovician carbonates in Central Tarim. *Marine and Petroleum Geology* 18, 729-741.
- Cai, C., Worden, R.H., Bottrell, S.H., Wang, L., Yang, C., 2003. Thermochemical sulphate reduction and the generation of hydrogen sulphide and thiols (mercaptans) in Triassic carbonate reservoirs from the Sichuan Basin, China. *Chemical Geology* 202, 39-57.
- Cai, C., Xie, Z., Worden, R.H., Hu, G., Wang, L., He, H., 2004. Methane-dominated thermochemical sulphate reduction in the Triassic Feixianguan Formation East Sichuan Basin, China: towards prediction of fatal H₂S concentrations. *Marine and Petroleum Geology* 21, 1265-1279.
- Cai, C., Zhang, C., He, H., Tang, Y., 2013. Carbon isotope fractionation during methane-dominated TSR in East Sichuan Basin gasfields, China: A review. *Marine and Petroleum Geology* 48, 100-110.
- Chung, H.M., Gormly, J.R., Squires, R.M., 1988. Origin of gaseous hydrocarbons in subsurface environments: theoretic considerations of carbon isotope distribution. *Chemical Geology* 71, 97-104.
- Clayton, C., 1991. Carbon isotope fractionation during natural gas generation from kerogen. *Marine and Petroleum Geology* 8, 232-240.
- Cohn, F., 1867. Beitrage zur Physiologie der Phycochromaceen and Florideen.

Archiv fuer Mikroskopische Anatomie, Band 3.

Coleman, D.D., Risatti, J.B., Schoell, M., 1981. Fractionation of carbon and hydrogen isotopes by methane-oxidizing bacteria. *Geochemica et Cosmochimica Acta* 45, 1033-1037.

Coveney, J.R.M., Goebel, E.D., Zeller, E.d.J., Dreschhoff, G.A.M., Angino, E.E., 1987. Serpentinization and the origin of hydrogen gas in Kansas. *AAPG Bulletin* 71, 39-49.

Dai, J., 1990. Characteristics of hydrogen isotopes of paraffinic gas in China. *Petroleum Exploration and Development* 17, 27-32 (In Chinese).

Dai, J., 2014. Giant coal-related gas field and gas source in China. Science Press, Beijing.

Dai, J., Li, J., Ding, W., Hu, G., Luo, X., Hou, L., Tao, S., Zhang, W., Zhu, G., 2007a. Geochemical characteristics of natural gas at giant accumulations in China. *Journal of Petroleum Geology* 30, 1-14.

Dai, J., Li, J., Luo, X., Zhang, W., Hu, G., Ma, C., Guo, J., Ge, S., 2005a. Stable carbon isotope compositions and source rock geochemistry of the giant gas accumulations in the Ordos Basin, China. *Organic Geochemistry* 36, 1617-1635.

Dai, J., Ni, Y., Zou, C., 2012. Stable carbon and hydrogen isotopes of natural gases sourced from the Xu{j}iahe Formation in the Sichuan Basin, China. *Organic Geochemistry* 43, 103-111.

Dai, J., Ni, Y., Zou, C., Tao, S., Hu, G., Hu, A., Yang, C., Tao, X., 2009. Stable

- carbon isotopes of alkane gases from the Xujiahe coal measures and implication for gas-source correlation in the Sichuan Basin, SW China. *Organic Geochemistry* 40, 638-646.
- Dai, J., Pei, X., Qi, H., 1992. Natural gas geology of China. Petroleum Industry Press, Beijing.
- Dai, J., Qi, H., Song, Y., 1985. Primary discussion of some parameters for identification of coal-and oil-type gases. *Acta Petrolei Sinica* 6, 31-38 (In Chinese).
- Dai, J., Yang, S., Chen, H., Shen, X., 2005b. Geochemistry and occurrence of inorganic gas accumulations in Chinese sedimentary basins. *Organic Geochemistry* 36, 1664-1688.
- Dai, J., Zou, C., Tao, S., Liu, Q., Zhou, Q., Hu, A., Yang, C., 2007b. Formation conditions and main controlling factors of large gas fields in china. *Natural Gas Geoscience* 18, 473-484.
- Des Marais, D.J., Donchin, J.H., Nehring, N.L., Truesdell, A.H., 1981. Molecular carbon isotopic evidence for the origin of geothermal hydrocarbons. *Nature* 292, 826-828.
- Eisma, E., Jury, J.W., 1969. Fundamental aspects of the generation of petroleum, in: Eglinton, G., Murphy, M.T.J. (Eds.), *Organic geochemistry: Methods and Results*. Springer, New York, pp. 676-698.
- Etiope, G., 2017. Abiotic methane in terrigenous serpentinization sites: an overview. *Peocedia Earth and Planetary Science* 17, 9-12.

- Fu, J.M., Liu, D.H., Sheng, G.Y., 1990. Geochemistry of coal-forming hydrocarbons. Science Press, Beijing.
- Fu, Q., Sherwood Lollar, B., Horita, J., Lacrampe-Couloume, G., Seyfried, J., William E., 2007. Abiotic formation of hydrocarbons under hydrothermal conditions: Constraints from chemical and isotope data. *Geochimica et Cosmochimica Acta* 71, 1982-1998.
- Fu, Q., Socki, R.A., Niles, P.B., 2015. Evaluating reaction pathways of hydrothermal abiotic organic synthesis at elevated temperatures and pressures using carbon isotopes. *Geochimica et Cosmochimica Acta* 154, 1-17.
- Galimov, E.M., 1988. Sources and mechanisms of formation of gaseous hydrocarbons in sedimentary rocks. *Chemical Geology* 71, 77-95.
- Galimov, E.M., 2006. Isotope organic geochemistry. *Organic Geochemistry* 37, 1200-1262.
- Giardini, A.A., Merlton, C.T., Mitchell, R.S., 1982. The nature of the upper 400km of the earth and its potential as the source for non-biogenic petroleum. *Journal of Petroleum Geology* 5, 173-190.
- Hao, F., Guo, T., Zhu, Y., Cai, X., Zou, H., Li, P., 2008. Evidence for multiple stages of oil cracking and thermochemical sulfate reduction in the Puguang gas field, Sichuan Basin, China. *AAPG Bulletin* 92, 611–637.
- Head, I.M., Jones, D.M., Larter, S.R., 2003. Biological activity in the deep subsurface and the origin of heavy oil. *Nature* 426, 344-352.
- Hoering, T.C., 1984. Thermal reactions of kerogen with added water, heavy water

- and pure organic substances. *Organic Geochemistry* 5, 267-278.
- Horita, J., Berndt, M.E., 1999. Abiogenic methane formation and isotopic fractionation under hydrothermal conditions. *Science* 285, 1055-1057.
- Hosgormez, H., Yalcin, M.N., Cramer, B., Gerling, P., Mann, U., 2005. Molecular and isotopic composition of gas occurrences in the Thrace basin (Turkey): origin of the gases and characteristics of possible source rocks. *Chemical Geology* 214, 179-191.
- Hu, W., Cai, C., Wu, Z., Li, J., 1998. Structural style and its relation to hydrocarbon exploration in the Songliao basin, northeast China. *Marine and Petroleum Geology* 15, 41-55.
- Huang, B., Tian, H., Huang, H., Yang, J., Xiao, X., Li, Li, 2015. Origin and accumulaiton of CO₂ and its natural displacement of oils in the terrigenous margin basins, northern South China Sea. *AAPG Bulletin* 99, 1349-1369.
- Huang, S., Feng, Z., Gu, T., Gong, D., Peng, W., Yuan, M., 2017. Multiple origins of the Paleogene natural gases and effects of secondary alteration in Liaohe Basin, Northeast China: Insights from the molecular and stable isotopic compositions. *International Journal of Coal Geology* 172, 134-148.
- James, A.T., 1990. Correlation of reservoird gases using the carbon isotopic compositions of wet gas components. *AAPG Bulletin* 74, 1441-1458.
- James, A.T., Burns, B.J., 1984. Microbial alteration of subsurface natural gas accumulations. *AAPG Bulletin* 68, 957-960.
- Jenden P D, Hilton D R, Kaplan I R, Craig, H., 1993. Abiogenic hydrocarbons and

- mantle helium in oil and gas fields. Howell D G (Ed.). The Future of Energy Gases. U.S. Geological Survey Professional Paper. 1570: 31-56.
- Jiang, L., Worden, R.H., Cai, C., 2015. Generation of isotopically and compositionally distinct water during thermochemical sulfate reduction (TSR) in carbonate reservoirs: Triassic Feixianguan Formation, Sichuan Basin, China. *Geochimica et Cosmochimica Acta* 165, 249-262.
- Jin, Z., Liu, Q., Qiu, N., Ding, F., Bai, G., 2012. Phase states of hydrocarbons in Chinese marine carbonate strata and controlling factors for their formation. *Energy Exploration & Exploitation* 30, 753-773.
- Jin, Z.J., Zhang, L.P., Yang, L., Hu, W.X., 2004. A preliminary study of mantle-derived fluids and their effects on oil/gas generation in sedimentary basins. *Journal of Petroleum Science and Engineering* 41, 45-55.
- Kinnaman, F.S., Valentine, D.L., Tyler, S.C., 2007. Carbon and hydrogen isotope fractionation associated with the aerobic microbial oxidation of methane, ethane, propane and butane. *Geochimic et Cosmochim Acta* 71, 271-283.
- Kissin, Y.V., 1987. Free-radical reactions of high molecular weight isoalkanes. *Industrial & Engineering Chemistry Research* 26, 1633-1638.
- Kniemeyer, O., Musat, F., Sievert, S.M., Knittel, K., Wilkes, H., Bulumenberg, M., Michaelis, W., Classen, A., Bolm, C., Joye, B., Widdel, F., 2007. Anaerobic oxidation of short-chain hydrocarbons by marine sulphate reducing bacteria. *Nature* 63, 898-901.
- Knittel, K., Boetius, A., 2009. The anaerobic oxidation of methane: progress with an

- unknown process. Annual Review of Microbiology 63, 311-334.
- Krooss, B.M., Leythaeuser, D., Schaefer, R.G., 1986. Experimental determination of diffusion parameters for light hydrocarbons in water-saturated rocks: some selected results. Organic Geochemistry 10, 291-297.
- Krooss, B.M., Leythaeuser, D., Schaefer, R.G., 1992. The quantification of diffusive hydrocarbon losses through cap rocks of natural gas reservoirs_ a reevaluation: reply. AAPG Bulletin 76, 1842-1846.
- Krooss, B.M., Plessen, B., Machel, H.G., Luders, V., Littke, R., 2008. Origin and distribution of non-hydrocarbon gases, in: Littke, R., Bayer, U., Gajewski, D. (Ed.), Dynamics of complex sedimentary basins -The example of the Central European Basin System. Springer, pp. 433-458.
- Krouse, H.R., Viau, C.A., Eliuk, L.S., Ueda, A., Halas, S., 1988. Chemical and isotopic evidence of thermochemical sulphate reduction by light hydrocarbon gases in deep carbonate reservoirs. Nature 333, 415-419.
- Lancet, M.S., Anders, E., 1970. Carbon isotope fractionation in the Fischer-Tropsch synthesis of methane. Science 170, 980-982.
- Lewan, M., 1993. Laboratory simulation of petroleum formation: Hydrous pyrolysis, in: Engel., M.H., Macko, S.A. (Eds.), Organic Geochemistry-Principle and applications. Plenum Press, New York, pp. 419-422.
- Lewan, M.D., 1985. Evaluation of petroleum generation by hydrous pyrolysis experimentation. Philosophical Transactions of the Royal Society 315, 123-134.
- Lewan, M.D., 1997. Experiments on the role of water in petroleum formation.

- Geochimica et Cosmochimica Acta 61, 3691-3723.
- Li, C.Q., Pang, Y.M., Chen, H.L., Chen, H.H., 2005a. Gas charging history of the Yingcheng Formation igneous reservoir in the Xujiaweizi Rift, Songliao Basin, China. Journal of Geochemical Exploration 89, 210-213.
- Li, J., Li, Z., Wang, X., Wang, D., Xie, Z., Li, J., Wang, Y., Han, Z., Ma, C., Wang, Z., Cui, H., Wang, R., Hao, A., 2017. New indexes and charts for genesis identification of multiple natural gases. Petroleum Exploration and Development 44, 536-543.
- Li, J., Xie, Z., Dai, J., Zhang, S., Zhu, G., Liu, Z., 2005b. Geochemistry and origin of sour gas accumulations in the northeastern Sichuan Basin, SW China. Organic Geochemistry 36, 1703-1716.
- Li, M., Bao, J., Lin, R., Stasiuk, L.D., Yuan, M., 2001a. Revised models for hydrocarbon generation, migration and accumulation in Jurassic coal measures of the Turpan Basin, NW China. Organic Geochemistry 32, 1127-1151.
- Li, M., Huang, Y., Obermajer, M., Jiang, C., Snowdon, L.R., Fowler, M.G., 2001b. Hydrogen isotopic compositions of individual alkanes as a new approach to petroleum correlation: case studies from the Western Canada Sedimentary Basin. Organic Geochemistry 32, 1387-1399.
- Li, P., Hao, F., Guo, X., Zou, H., Yu, X., Wang, G., 2015. Processes involved in the origin and accumulation of hydrocarbon gases in the Yuanba gas field, Sichuan Basin, southwest China. Marine and Petroleum Geology 59, 150-165.
- Liang, D., Zhang, S., Chen, J., Wang, F., Wang, P., 2003. Organic geochemistry of

- oil and gas in the Kuqa depression, Tarim Basin, NW China. *Organic Geochemistry* 34, 873-888.
- Liu, Q., Chen, M., Liu, W., Li, J., Han, P., Guo, Y., 2009. Origin of natural gas from the Ordovician paleo-weathering crust and gas-filling model in Jingbian gas field, Ordos Basin, China. *Journal of Asian Earth Sciences* 35, 74-88.
- Liu, Q., Dai, J., Jin, Z., Li, j., Wu, X., Meng, Q., Yang, C., Zhou, Q., Feng, Z., Zhu, D., 2016. Abnormal carbon and hydrogen isotopes of alkane gases from the Qingshen gas field, Songliao Basin, China, suggesting abiogenic alkanes? *Journal of Asian Earth Sciences* 115.
- Liu, Q., Dai, J., Li, J., Zhou, Q., 2008. Hydrogen isotope composition of natural gases from the Tarim Basin and its indication of depositional environments of the source rocks. *Science in China (Series D)* 51, 300-311.
- Liu, Q., Dai, J., Zhang, T., Li, J., Qin, S., Liu, W., 2007. Genetic types of natural gas and their distribution in Tarim Basin, NW China. *Journal of Nature Science and Sustainable Technology* 1, 603-620.
- Liu, Q., Jin, Z., Li, H., Wu, X., Tao, X., Zhu, D., Meng, Q., 2018a. Geochemistry characteristics and genetic types of natural gas in central part of the Tarim Basin, NW China. *Marine and Petroleum Geology* 89, 91-105.
- Liu, Q., Jin, Z., Wang, X., Yi, J., Meng, Q., Wu, X., Gao, B., Nie, H., Zhu, D., 2018b. Distinguishing kerogen and oil cracked shale gas using H, C-isotopic fractionation of alkane gases. *Marine and Petroleum Geology*, 91, 350-362.
- Liu, Q., Jin, Z., Meng, Q., WU, X., Jia, H., 2015. Genetic types of natural gas and

- filling patterns in Daniudi gas field, Ordos Basin, China. *Journal of Asian Earth Sciences* 107, 1-11.
- Liu, Q., Jin, Z., Wu, X., Liu, W., Gao, B., Zhang, D., Li, J., Hu, A., 2014a. Origin and carbon isotope fractionation of CO₂ in marine sour gas reservoirs in the Eastern Sichuan Basin. *Organic Geochemistry* 74, 22-32.
- Liu, Q., Zhang, T., Jin, Z., Qin, S., Tang, Y., Liu, W., 2011. Kinetic Model of Gaseous Alkanes Formed from Coal in a Confined System and Its Application to Gas Filling History in Kuqa Depression, Tarim Basin, Northwest China. *Acta Geologica Sinica* 85, 911-922.
- Liu, Q., Zhu, D., Jin, Z., Meng, Q., Wu, X., Yu, H., 2017. Effects of deep CO₂ on petroleum and thermal alteration: The case of the Huangqiao oil and gas field. *Chemical Geology* 469, 214-229.
- Liu, Q.Y., Worden, R.H., Jin, Z.J., Liu, W.H., Li, J., Gao, B., Zhang, D.W., Hu, A.P., Yang, C., 2013. TSR versus non-TSR processes and their impact on gas geochemistry and carbon stable isotopes in Carboniferous, Permian and Lower Triassic marine carbonate gas reservoirs in the Eastern Sichuan Basin, China. *Geochimica et Cosmochimica Acta* 100, 96-115.
- Liu, Q.Y., Worden, R.H., Jin, Z.J., Liu, W.H., Li, J., Gao, B., Zhang, D.W., Hu, A.P., Yang, C., 2014b. Thermochemical sulphate reduction (TSR) versus maturation and their effects on hydrogen stable isotopes of very dry alkane gases. *Geochimica et Cosmochimica Acta* 137, 208-220.
- Liu, W., Xu, Y., Shi, J., Lei, H., Zhang, B., 1997. Evolution model and formation

- mechanism of bio-thermocatalytic transitional zone gas. *Science China Earth Sciences (Science in China Series D)* 40, 43-53.
- Lorant, F., Prinzhofe, A., Behar, F., Huc, A.-Y., 1998. Carbon isotopic and molecular constraints on the formation and the expulsion of thermogenic hydrocarbon gases. *Chemical Geology* 147, 249-264.
- Ma, Y., 2007. Generation mechanism of Puguang Gas Field in Sichuan Basin. *Acta Petrolei Sinica* 28, 9-14.
- Machel, H.G., 1998. Gas souring by thermochemical sulfate reduction at 140 °C: Discussion. *AAPG Bulletin* 82, 1870-1873.
- Machel, H.G., 2001. Bacterial and thermochemical sulfate reduction in diagenetic settings -old and new insights. *Sedimentary Geology* 140, 143-175.
- Machel, H.G., Foght, J., 2000. Products and depth limits of microbial activity in petroliferous subsurface setting. Springer, Berlin.
- Machel, H.G., Krouse, H.R., Sassen, R., 1995. Products and distinguishing criteria of bacterial and thermochemical sulfate reduction. *Applied Geochemistry* 10, 373-389.
- Mastalerz, M., Schimmelmann, A., 2002. Isotopically exchangeable organic hydrogen in coal relates to thermal maturity and maceral composition. *Organic Geochemistry* 32, 921-931.
- McCollom, T.M., Seewald, J.S., 2001. A reassessment of the potential for reduction of dissolved CO₂ to hydrocarbons during serpentinization of olivine. *Geochimica et Cosmochimica Acta* 65, 3769-3778.

McCollom, T.M., Seewald, J.S., Sherwood Lollar, B., Lacrampe-Couloume, G., 2006.

Isotopic signatures of abiotic organic synthesis under geologic conditions.
Geochimica et Cosmochimica Acta 70, A0407.

Meng, Q., Wang, X., Wang, X., Shi, B., Luo, X., Zhang, L., Lei, Y., Jiang, C., Liu, P., 2017. Gas geochemical evidences for biodegradation of shale gases in the Upper Triassic Yanchang Formation, Ordos Basin, China. International Journal of Coal Geology 179, 139-152.

Ni, Y., Dai, J., Zou, C., Liao, F., Shuai, Y., Zhang, Y., 2013. Geochemical characteristics of biogenic gases in China. International Journal of Coal Geology 113, 76-87.

Orr, W.L., 1974. Changes in sulfue content and isotopic ratios of sulfur during petroleum maturation-study of Big Horn Basin Paleozoic oils. AAPG Bulletin 58, 2295-2318.

Orr, W.L., 1977. Geologic and geochemical controls on the distribution of hydrogen sulfide in natural gas, in: Campos R, G.J. (Ed.), Advances in Organic Geochemistry 1975. Pergamon Press, Oxford, pp. 571-597.

Pan, C., Yu, L., Liu, J., Fu, J., 2006. Chemical and carbon isotopic fractionations of gaseous hydrocarbons during abiogenic oxidation. Earth and Planetary Science Letters 246, 70-89.

Peters, K.E., Walters, C.C., Moldowan, J.M., 2005. The Biomarker Guide, Biomarkers and Isotopes in Petroleum Exploration and Earth History. Cambridge University Press.

- Pineau, F., Javoy, M., 1983. Carbon isotopes and concentrations in mid-oceanic ridge basalts. *Earth and Planetary Science Letters* 62, 239-257.
- Poreda, R., Craig, H., 1989. Helium isotope ratios in circum-Pacific volcanic arcs. *Nature* 338, 473-478.
- Potter, J., Siemann, M.G., Tsypukov, M., 2004. Large-scale carbon isotope fractionation in evaporites and the generation of extremely ^{13}C -enriched methane. *Geology* 32, 533-536.
- Price, L.C., 1993. Thermal stability of hydrocarbons in nature: Limits, evidence, characteristics, and possible controls. *Geochimica et Cosmochimica Acta* 57, 3261-3280.
- Prinzhofe, A., Battani, A., 2003. Gas isotopes tracing: an important tool for hydrocarbons exploration. *Oil & Gas Science and Technology Rev. IFP* 58, 299-311.
- Prinzhofe, A., Pernaton, E., 1997. Isotopically light methane in natural gas: bacterial imprint or diffusive fractionation? *Chemical Geology* 142, 193-200.
- Prinzhofe, A., Vega, M.A.G., Battani, A., Escudero, M., 2000. Gas geochemistry of the Macuspana Basin (Mexico): thermogenic accumulations in sediments impregnated by bacterial gas. *Marine and Petroleum Geology* 17, 1029-1040.
- Prinzhofe, A.A., Huc, A.Y., 1995. Genetic and post-genetic molecular and isotopic fractionations in natural gases. *Chemical Geology* 126, 281-290.
- Reeves, E.P., Seewald, J.S., Sylva, S.P., 2012. Hydrogen isotopic exchange between n-alkanes and water under hydrothermal conditions. *Geochimica et*

- Cosmochimica Acta 77, 582-599.
- Rice, D.D., Claypool, G.E., 1981. Generation accumulation and resource potential of biogenic gas. AAPG Bulletin 65, 5-25.
- Sackett, W.M., 1978. Carbon and hydrogen isotope effects during the thermocatalytic production of hydrocarbons in laboratory simulation experiments. Geochimica et Cosmochimica Acta 42, 571-580.
- Schimmelmann, A., Boudou, J.P., Lewan, M.D., Wintsch, R.P., 2001. Experimental controls on D/H and $^{13}\text{C}/^{12}\text{C}$ ratios of kerogen, bitumen and oil during hydrous pyrolysis. Organic Geochemistry 32, 1009-1018.
- Schimmelmann, A., Lewan, M.D., Wintsch, R.P., 1999. D/H isotope ratios of kerogen, bitumen, oil, and water in hydrous pyrolysis of source rocks containing kerogen types I, II, IIS, III. Geochimica et Cosmochimica Acta 63, 3751-3766.
- Schimmelmann, A., Mastalerz, M., Gao, L., Topalow, K., 2009. Dike intrusions into bituminous coal, Illinois Basin: H, C, N, O isotopic responses to rapid and brief heating. Geochimica et Cosmochimica Acta 73, 6264-6281.
- Schimmelmann, A., Sessions, A.L., Boreham, C.J., Edwards, D.S., Logan, G.A., Summons, R.E., 2004. D/H ratios in terrigenously sourced petroleum systems. Organic Geochemistry 35, 1169-1195.
- Schoell, M., 1980. The hydrogen and carbon isotopic composition of methane from natural gases of various origins. Geochimica et Cosmochimica Acta 44, 649-661.
- Schoell, M., 1983. Genetic characterization of natural gas. AAPG Bulletin 67,

2225-2238.

Schoell, M., 1984. Stable isotopes in petroleum research. Advance in Petroleum Geochemistry 1, 215-245.

Schoell, M., 1988. Multiple origins of methane in the Earth. Chemical Geology 71, 1-10.

Schoell, M., 2011. Carbon and hydrogen isotope systematics in thermogenic natural gases from the USA and China: West meets east, AAPG Hedberg Research Conference, Beijing, China, p. Abstract.

Seewald, J.S., 2003. Organic–inorganic interactions in petroleum-producing sedimentary basins. Nature 426, 327-333.

Seewald, J.S., Benitez-Nelson, B.C., Whelan, J.K., 1998. Laboratory and theoretical constraints on the generation and composition of natural gas. Geochimica et Cosmochimica Acta 62, 1599-1617.

Shen, P., Shen, Q., Wang, X., Xu, Y., 1988. Characteristics of the isotope composition of gas form hydrocarbon and identification of coal-type gas . Science in China(Series B) 31, 734-747.

Shen, P., Xu, Y., 1986. Characterization of the carbon and hydrogen isotopic composition in natural gases from terrigenous sediments in China. Academia Sinica, Beijing.

Sherwood Lollar, B., Ballentine, C.J., O'Nions, R.K., 1997. The fate of mantle-derived carbon in a terrigenous sedimentary basin: Integration of C/He relationships and stable isotope signatures. Geochimica et Cosmochimica Acta

62, 2295-2307.

Sherwood Lollar, B., Fritz, P., Frape, S.K., Macko, S.A., Weise, S.M., Welhan, J.A., 1988. Methane occurrences in the Canadian Shield. *Chemical Geology* 71, 223-236.

Sherwood Lollar, B., Lacrampe-Couloume, G., Slater, G.F., Ward, J., Moser, D.P., Gihring, T.M., Lin, L.H., Onstott, T.C., 2006. Unravelling abiogenic and biogenic sources of methane in the Earth's deep subsurface. *Chemical Geology* 226, 328-339.

Sherwood Lollar, B., Lacrampe-Couloume, G., Voglesonger, K., Onstott, T.C., Pratt, L.M., Slater, G.F., 2008. Isotopic signatures of CH₄ and higher hydrocarbon gases from Precambrian Shield sites: A model for abiogenic polymerization of hydrocarbons. *Geochimica et Cosmochimica Acta* 72, 4778-4795.

Sherwood Lollar, B., Westgate, T.D., Ward, J.A., Slater, G.F., Lacrampe-Couloume, G., 2002. Abiogenic formation of alkanes in the Earth's crust as a minor source for global hydrocarbon reservoirs. *Nature* 416, 522-524.

Stahl, J.W., 1973. Carbon isotope ratios of German natural gases in comparison with isotopic data of gaseous hydrocarbons from other parts of the world, in: Tissot, B., Biinner, F. (Eds.), *Advances in Organic Geochemistry*, pp. 453-462.

Stahl, W.J., Carey, J.B.D., 1975. Source-rock identification by isotope analyses of natural gases from fields in the Val Verde and the Delaware Basin, West Texas. *Chemical Geology* 16, 257-267.

Suda, K., Ueno, Y., Yoshizaki, M., Nakamura, H., Kurokawa, K., Nishiyama, E.,

- Yoshino, K., Hongoh, Y., Kawachi, K., Omori, S., Yamada, K., Yoshida, N., Maruyama, S., 2014. Origin of methane in serpentinite-hosted hydrothermal systems: The CH₄–H₂–H₂O hydrogen isotope systematics of the Hakuba Happo hot spring. *Earth and Planetary Science Letters* 386, 112-125.
- Sugisaki, R., Mimura, K., 1994. Mantle hydrocarbons: abiotic or biotic? *Geochimica et Cosmochimica Acta* 58, 2527-2542.
- Tang, Y., Huang, Y., Ellis, G.S., Wang, Y., Kralert, P.G., Gillaizeau, B., Ma, Q., Hwang, R., 2005. A kinetic model for thermally induced hydrogen and carbon isotope fractionation of individual n-alkanes in crude oil. *Geochimica et Cosmochimica Acta* 69, 4505–4520.
- Tang, Y., Perry, J.K., Jenden, P.D., Schoell, M., 2000. Mathematical modeling of stable carbon isotope ratios in natural gases. *Geochimica et Cosmochimica Acta* 64, 2673-2687.
- Taran, Y.A., Kliger, G.A., Sevastianov, V.S., 2007. Carbon isotope effects in the open-system Fischer-Tropsch synthesis. *Geochemica et Cosmochimica Acta* 71, 4474-4487.
- Tian, H., Xiao, X., Wilkins, R.W.T., Tang, Y., 2012. An experimental comparison of gas generation from three oil fractions:Implications for the chemical and stable carbon isotopic signatures of oil cracking gas. *Organic Geochemistry* 46, 96-112.
- Tissot, B.T., Welte, D.H., 1984. Petroleum formation and occurrences. Springer, Berlin.

- Toland, W.G., 1960. Oxidation of organic compounds with aqueous sulfate. *Journal of American Chemical Society* 82, 1911-1916.
- Valentine, D.L., 2011. Emerging topics in marine methane biogeochemistry. *Annual Review of Marine Science* 3, 147-171.
- Vandré, C., Cramer, B., Gerling, P., Winsemann, J., 2007. Natural gas formation in the western Nile delta (Eastern Mediterranean): Thermogenic versus microbial. *Organic Geochemistry* 38, 523-539.
- Wakita, H., Sano, Y., 1983. ${}^3\text{He}/{}^4\text{He}$ ratios in CH_4 -rich natural gases suggest magmatic origin. *Nature* 305, 792-794.
- Wang, W., 1996. Geochemical characteristics of hydrogen isotopic compositions of natural gas, oil and kerogen. *Acta Sedimentologica Sinica* 14, 131-135 (in Chinese).
- Wang, X., Liu, W., Shi, B., Zhang, Z., Xu, Y., Zheng, J., 2015. Hydrogen isotope characteristics of thermogenic methane in Chinese sedimentary basins. *Organic Geochemistry* 83-84, 178-189.
- Wang, X., Liu, W., Xu, Y., Zheng, J., 2011. Influences of water media on the hydrogen isotopic composition of natural gas/methane in the processes of gaseous hydrocarbon generation and evolution. *Science China Earth Sciences (Science in China Series D)* 54, 1318-1325.
- Welhan, J.A., 1988. Origins of methane in hydrothermal system. *Chemical Geology* 71, 183-198.
- Whiticar, M.J., 1999. Carbon and hydrogen isotope systematics of bacterial

- formation and oxidation of methane. *Chemical Geology* 161, 291-314.
- Worden, R.H., Smalley, P.C., 1996. H₂S-producing reactions in deep carbonate gas reservoirs: Khuff Formation, Abu Dhabi. *Chemical Geology* 133, 157-171.
- Worden, R.H., Smalley, P.C., Ox'roby, N.H., 1996. The effects of thermochemical sulfate reduction upon formation water salinity and oxygen isotopes in carbonate gas reservoirs. *Geochimica et Cosmochimica Acta* 60, 3925-3931.
- Worden, R.H., Smalley, P.C., Oxtoby, N.H., 1995. Gas Souring by Thermochemical Sulfate Reduction at 140°C. *AAPG Bulletin* 79, 854-863.
- Xia, X., Chen, J., Braun, R., Tang, Y., 2013. Isotopic reversals with respect to maturity trends due to mixing of primary and secondary products in source rocks. *Chemical Geology* 339, 205-212.
- Xiao, Q., 2012. Carbon and hydrogen isotopic reversals in deep basin gas: Evidence for limits to the stability of hydrocarbons by Burruss and Laughrey (Organic Geochemistry 41, 1285-1296) – Discussion. *Organic Geochemistry*, 44, 71-76.
- Xu, S., Nakai, S.I., Wakita, H., Wang, X., 1995. Mantle-derived noble gases in natural gases from Songliao Basin, China. *Geochimica et Cosmochimica Acta* 59, 4675-4683.
- Xu, Y., 1993. Genetic characteristics of natural gases-multi-source overlap and multi-stage continuity. *Chinese Science Bulletin* 38, 155-158(In Chinese).
- Xu, Y., 1994. Genetic theories of natural gases and their application. Science Press, Beijing.
- Xu, Y., Liu, W., Shen, P., Tao, M., 1998. Geochemistry of noble gases in natural

- gases. Science Press, Beijing.
- Xu, Y., Liu, W., Shen, P., Wang, W., Wang, X., Tenger, Yan, Y., Liu, R., 2006. Carbon and hydrogen isotopic characteristics of natural gases from the Luliang and Baoshan basins in Yunnan Province, China. *Science in China Series D: Earth Sciences* 49, 938-946.
- Yang, C., Luo, X., Li, J., Li, Z., Liu, Q., Wang, Y., 2008. Geochemical characteristics of pyrolysis gas from epimetamorphic rocks in the northern basement of Songliao Basin, Northeast China. *Science in China (Series D)* 51, 140-147.
- Yang, w., Li, Y., Gao, R., 1985. Formation and evolution of nonmarine petroleum in Songliao basin, China. *AAPG Bulletin* 69, 1112-1122.
- Yeh, H., Epstein, S., 1981. Hydrogen and carbon isotopes of petroleum and related organic matter. *Geochimica et Cosmochimica Acta* 45, 753-762.
- Yoneyama, Y., Okamura, M., Morinaga, K., Tsubaki, N., 2002. Role of water in hydrogenation of coal without catalyst. *Energy & Fuels* 16, 48-53.
- Yoshinaga, J., Morita, M., 1997. Determination of mercury in biological and environmental samples by inductively coupled plasma mass spectrometry with the isotope dilution technique. *Journal of Analytical Atomic Spectrometry* 12, 417-420.
- Zhang, H., Xiong, Y., Liu Jinzhong., Liao Yuhong., Geng, A., 2005. Pyrolysis kinetics of Pure n-C₁₈H₃₈(I): gaseous hydrocarbon and carbon isotope evolution. *Acta Geologica Sinica* 79, 569-574.
- Zhang, S., Mi, J., He, K., 2013. Synthesis of hydrocarbon gases from four different

- carbon sources and hydrogen gas using a gold-tube system by Fischer-Tropsch method. *Chemical Geology* 26, 349-350.
- Zhang, S.C., Hanson, A.D., Moldowan, J.M., Graham, S.A., Liang, D.G., Chang, E., Fago, F., 2000. Paleozoic oil-source rock correlations in the Tarim basin, NW China. *Organic Geochemistry* 31, 273-286.
- Zhang, T., Amrani, A., Ellis, G.S., Ma, Q., Tang, Y., 2008a. Experimental investigation on thermochemical sulfate reduction by H₂S initiation. *Geochimica et Cosmochimica Acta* 72, 3518-3530.
- Zhang, T., Ellis, G.S., Walters, C.C., Kelemen, S.R., Wang, K.-s., Tang, Y., 2008b. Geochemical signatures of thermochemical sulfate reduction in controlled hydrous pyrolysis experiments. *Organic Geochemistry* 39, 308-328.
- Zhang, T., Ellis, G.S., Wang, K.-S., Walters, C.C., Kelemen, S.R., Gillaizeau, B., Tang, Y., 2007. Effect of hydrocarbon type on thermochemical sulfate reduction. *Organic Geochemistry* 38, 897-910.
- Zhang, T., Krooss, B.M., 2001. Experimental investigation on the carbon isotope fractionation of methane during gas migration by diffusion through sedimentary rocks at elevated temperature and pressure. *Geochimica et Cosmochimica Acta* 65, 2723-2742.
- Zhu, G., Zhang, S., liang, Y., Dai, J., Li, J., 2005. Isotopic evidence of TSR origin for natural gas bearing high H₂S contents within the Feixianguan Formation of the northeastern Sichuan Basin, southwestern China. *Science in China Series D-Earth Sciences* 48, 1960-1971.

Zumberge, J., Ferworn, K., Brown, S., 2012. Isotopic reversal ('rollover') in shale gases produced from the Mississippian Barnett and Fayetteville formations. Marine and Petroleum Geology 31, 43-52.

ACCEPTED MANUSCRIPT

- Classification of natural gas and traditional geochemical methods for genetic identification of natural gas are reviewed.
- The effect of geological background and secondary alteration on carbon and hydrogen isotope compositions of light alkanes is assessed.
- New diagnostic tools for genetic classification of natural gas are suggested.

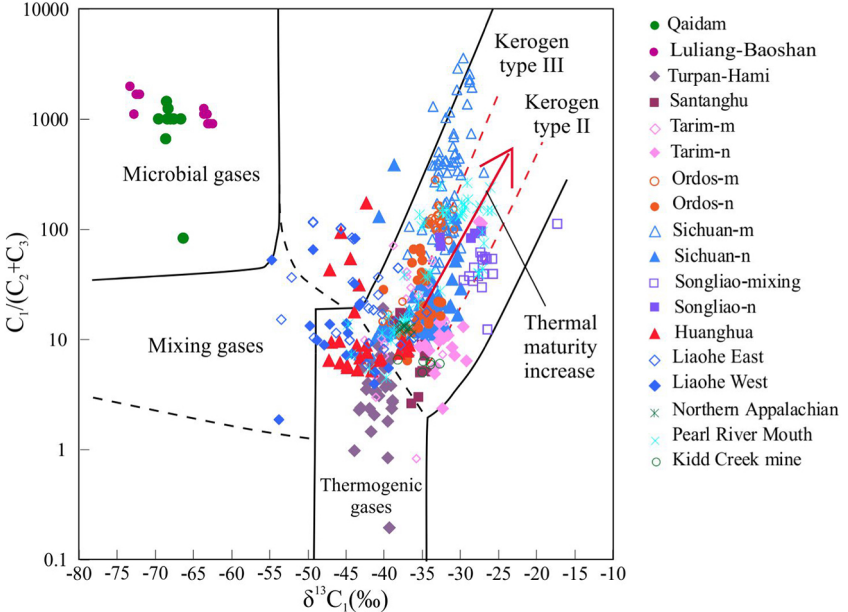


Figure 1

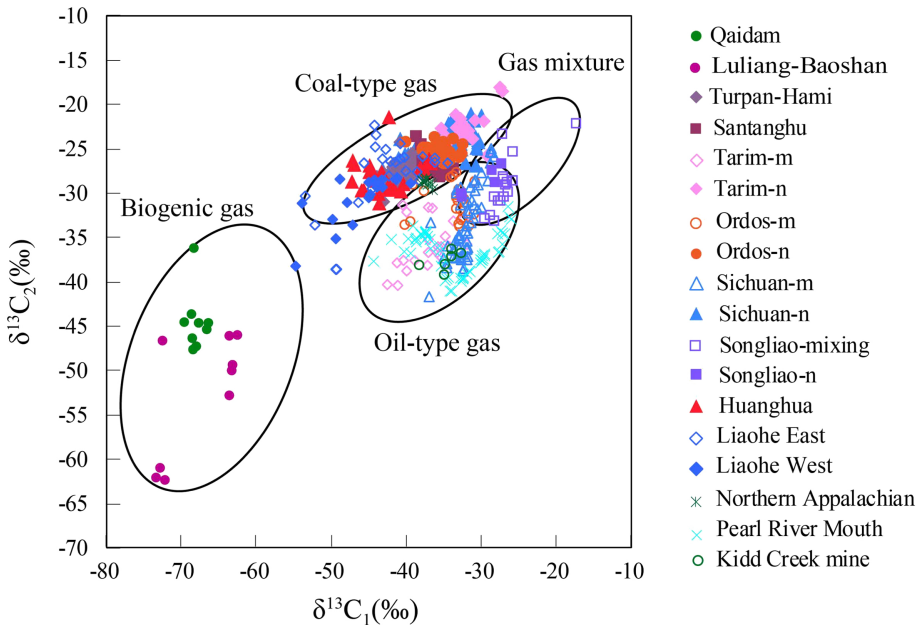


Figure 2

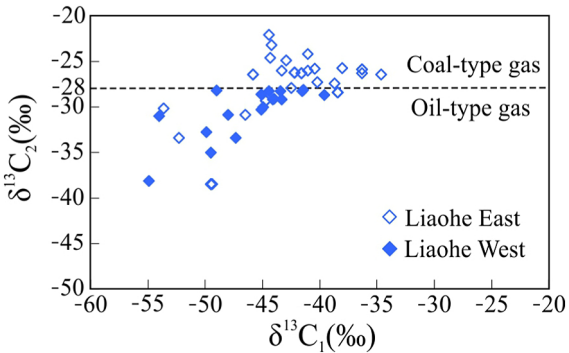


Figure 3

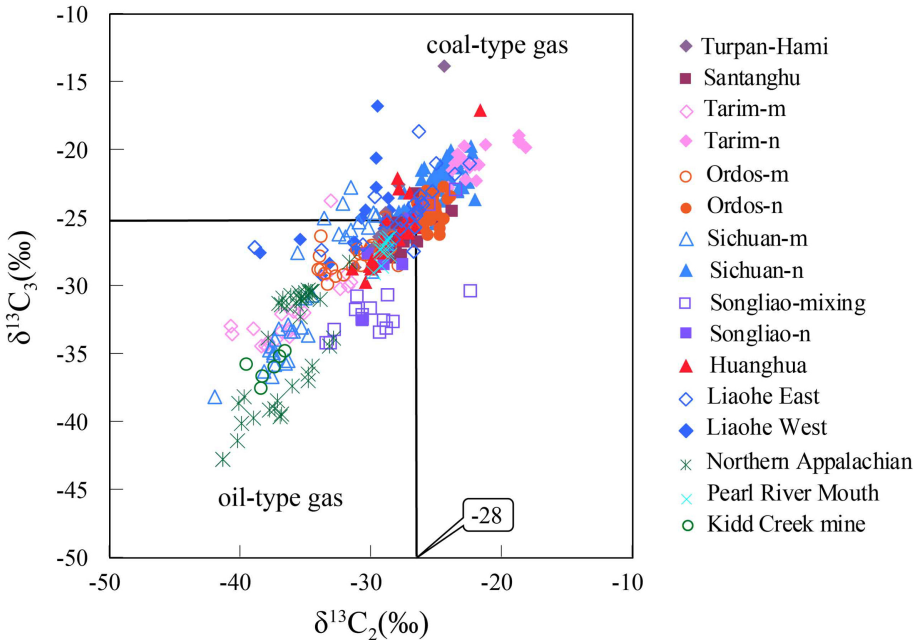


Figure 4

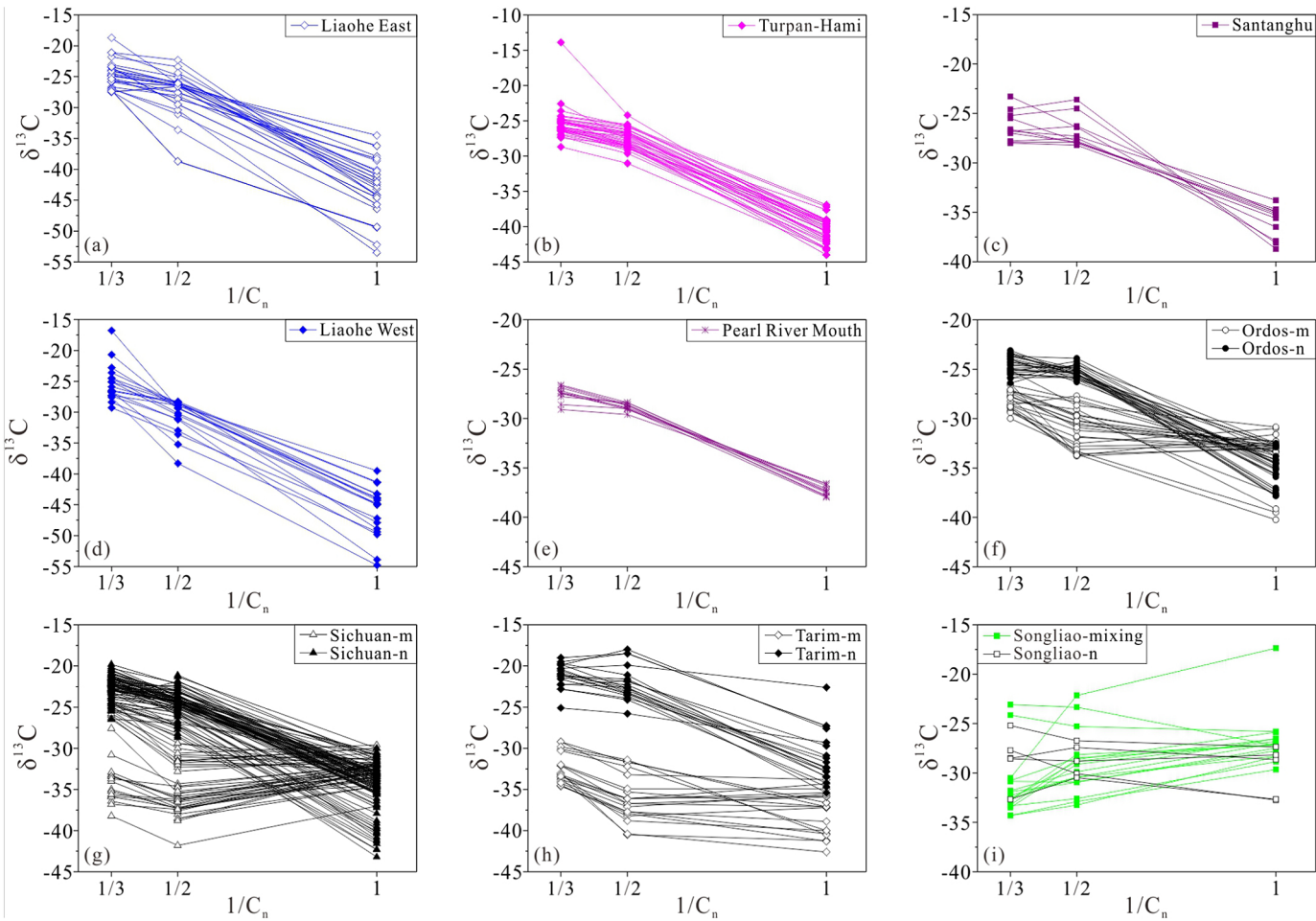


Figure 5

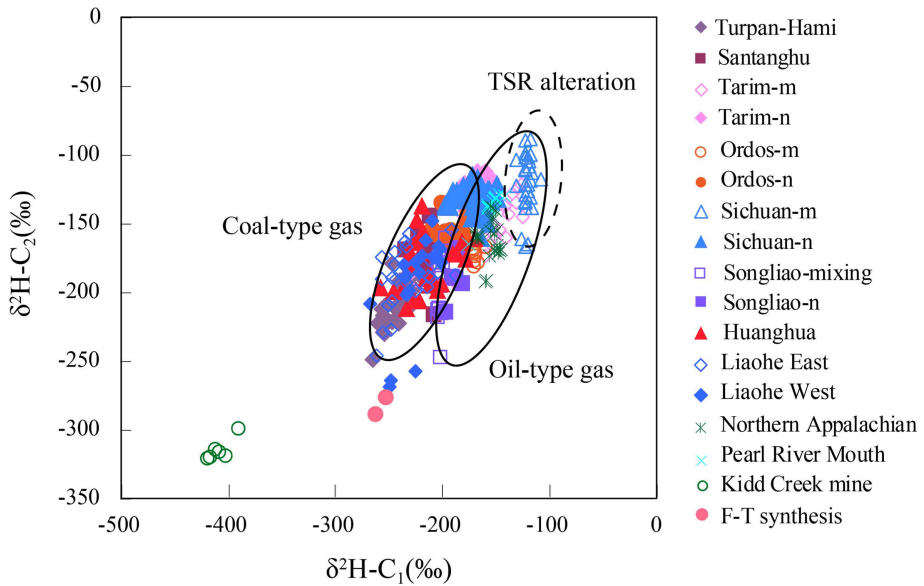


Figure 6

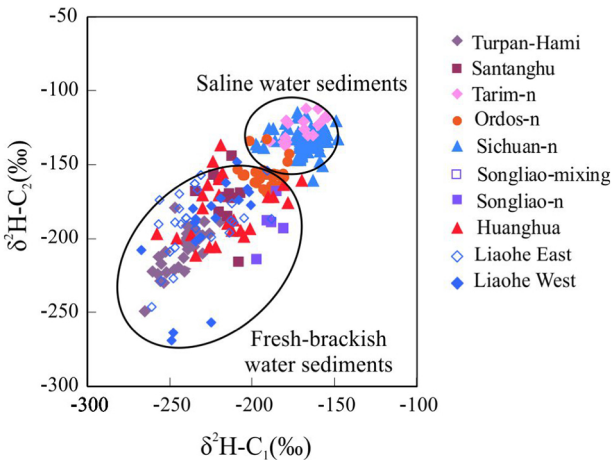


Figure 7

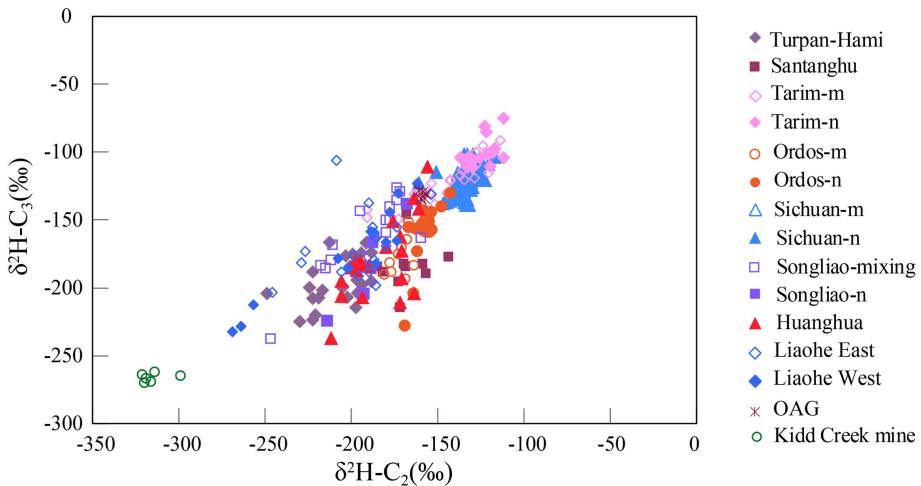


Figure 8

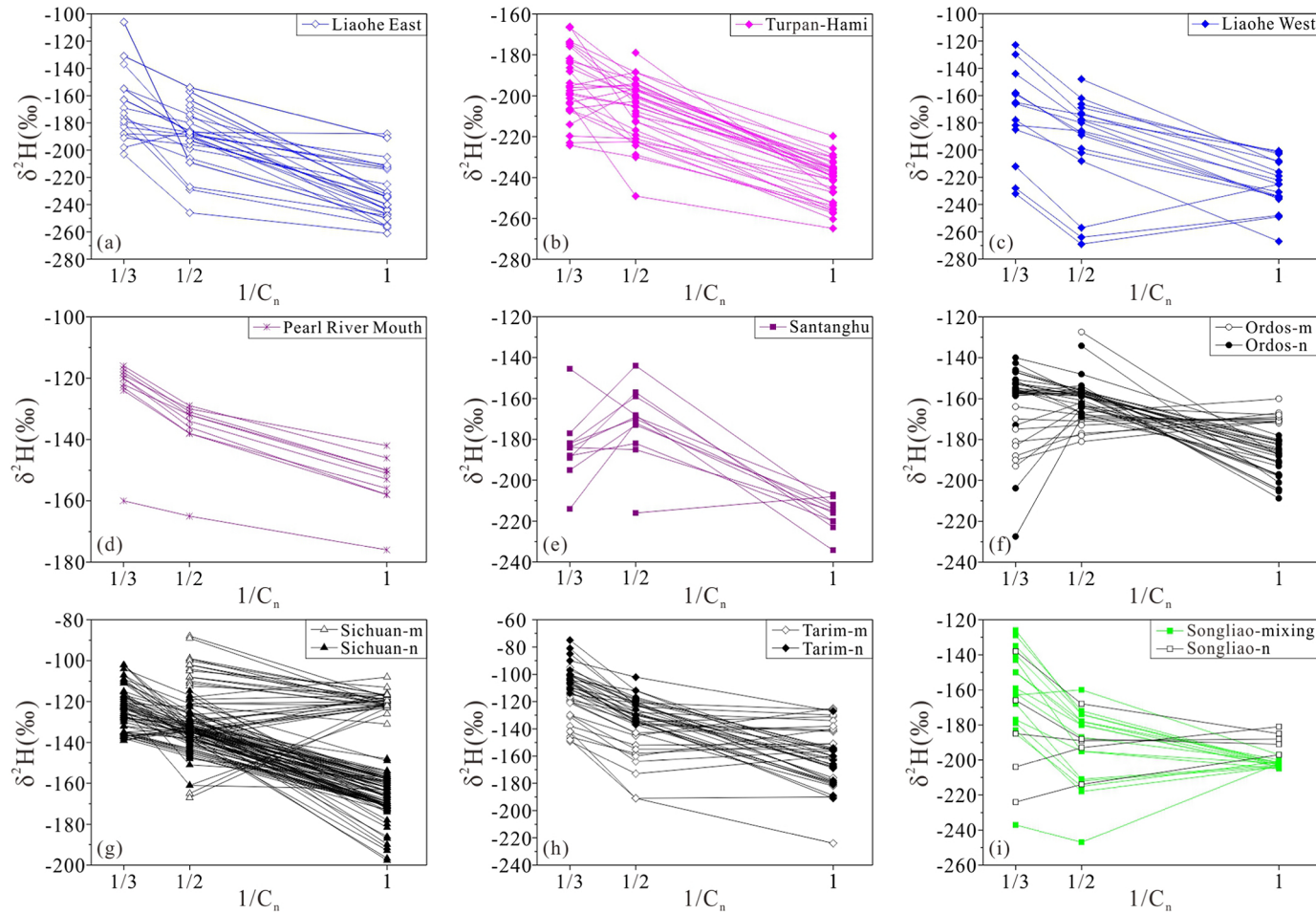


Figure 9

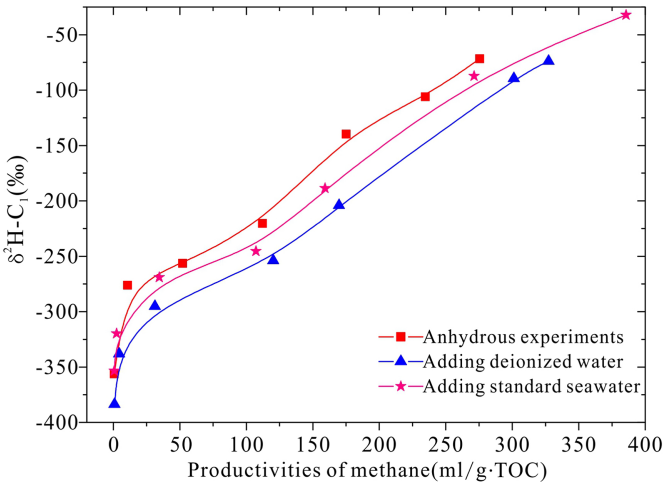


Figure 10

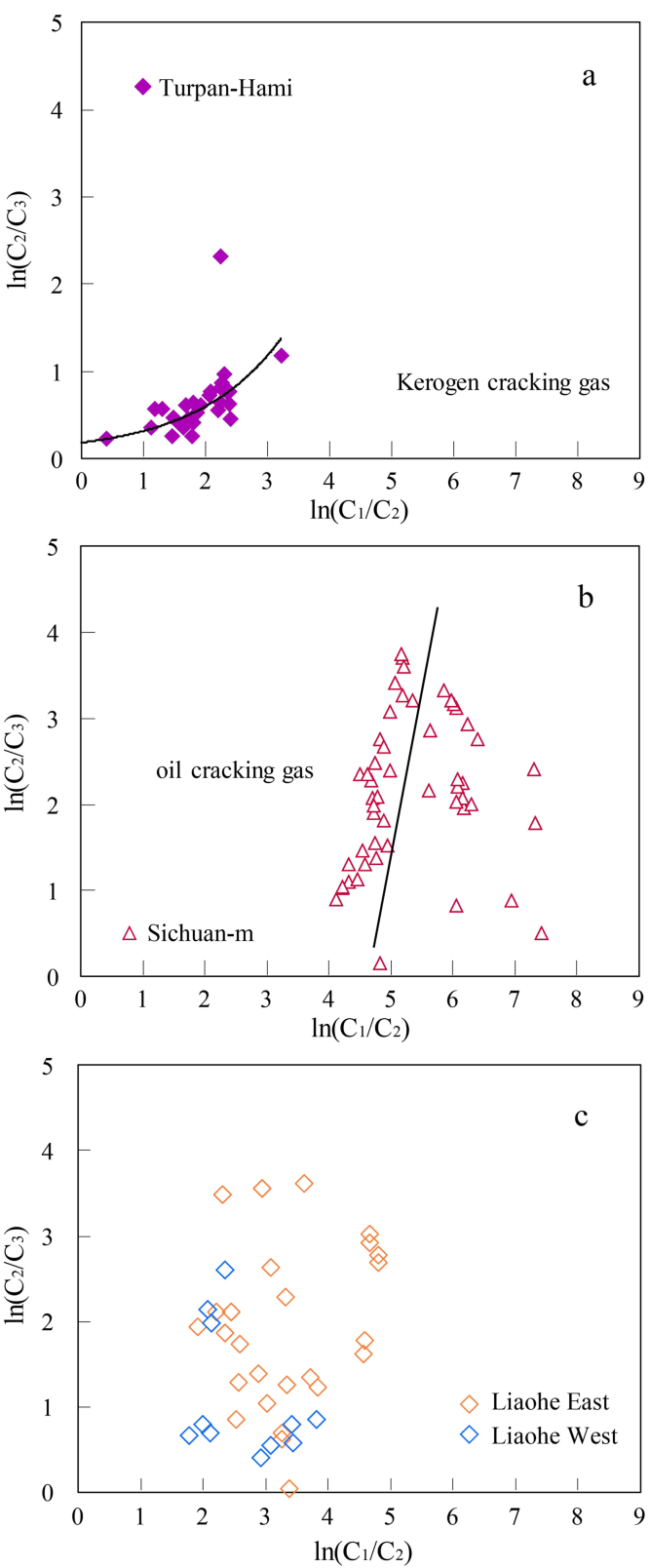
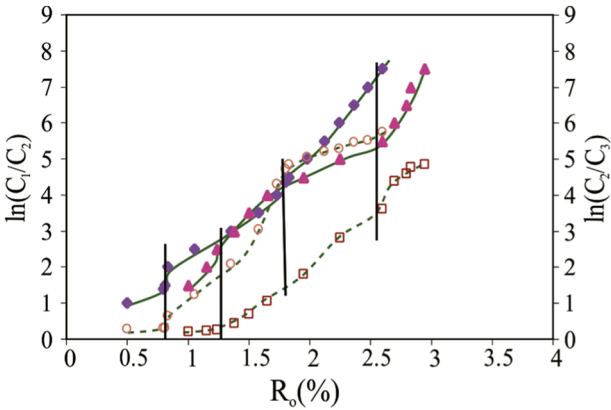


Figure 11



- ◆ $\ln(C_1/C_2)$ -kerogen cracking ▲ $\ln(C_1/C_2)$ -oil cracking
- $\ln(C_2/C_3)$ -kerogen cracking □ $\ln(C_2/C_3)$ -oil cracking

Figure 12

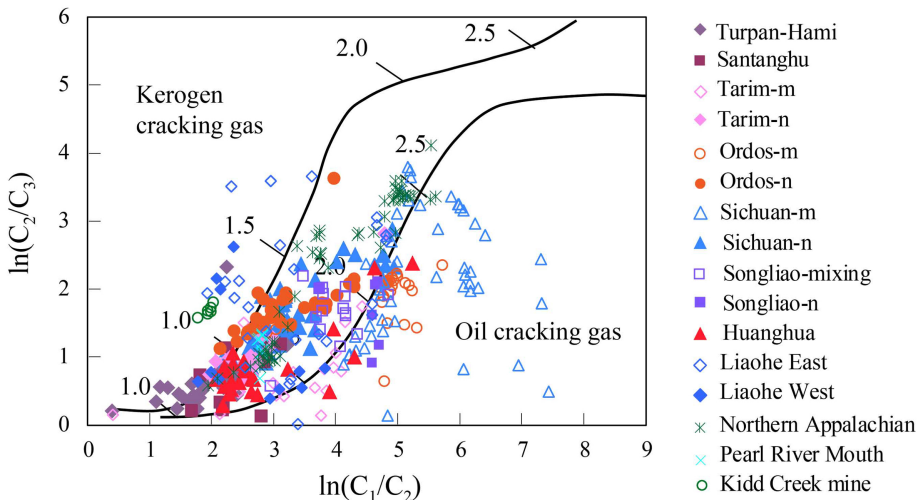


Figure 13

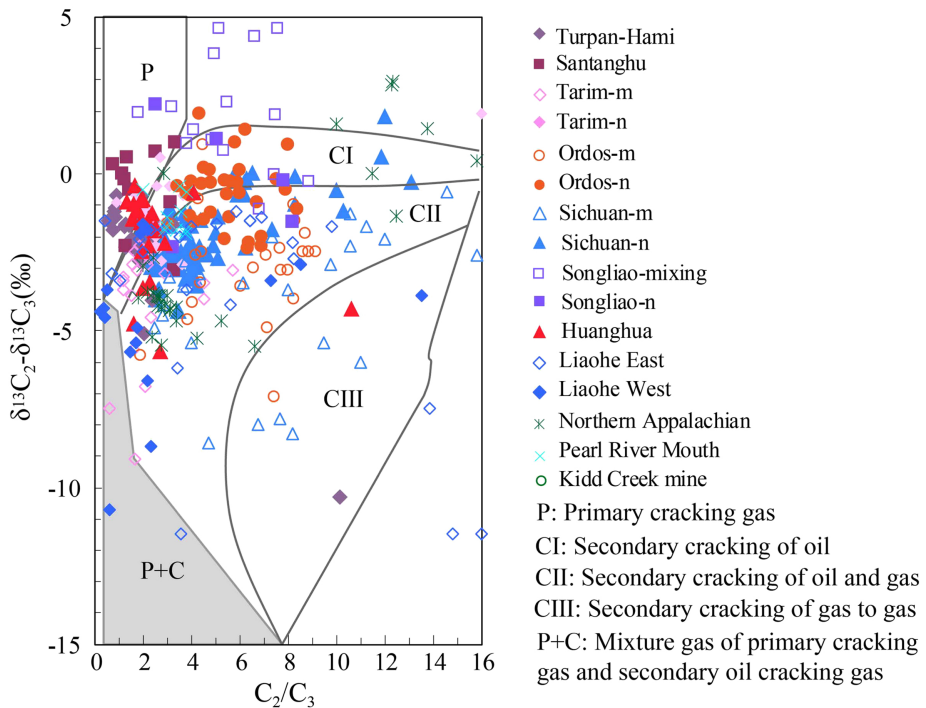


Figure 14

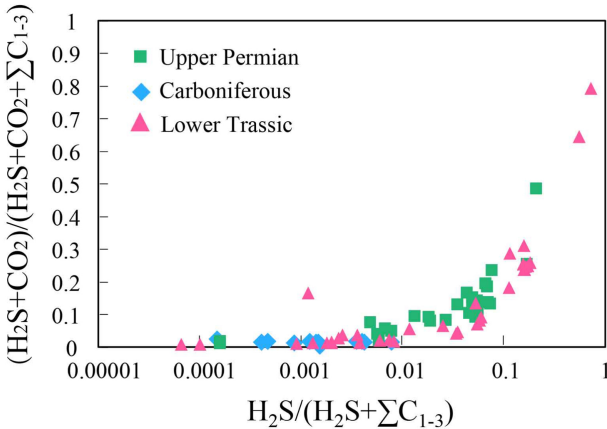


Figure 15

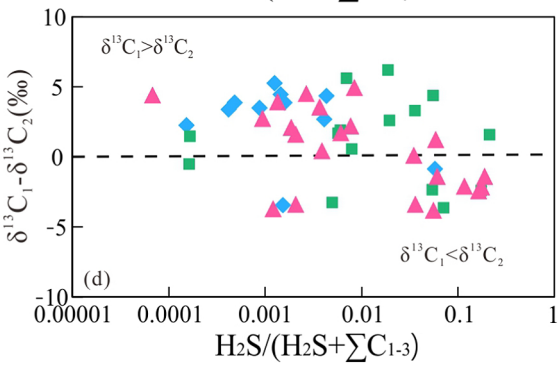
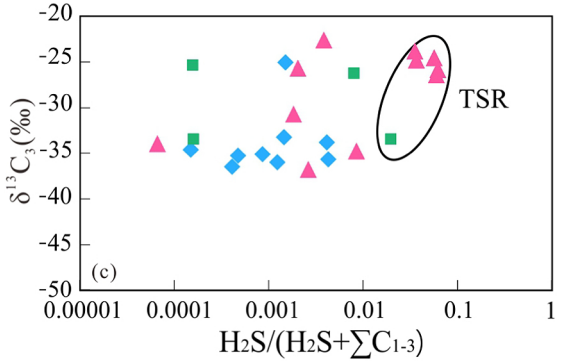
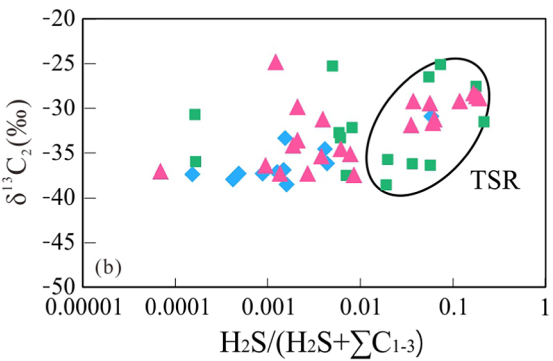
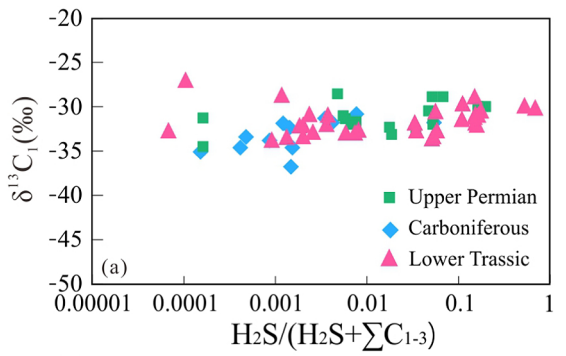


Figure 16

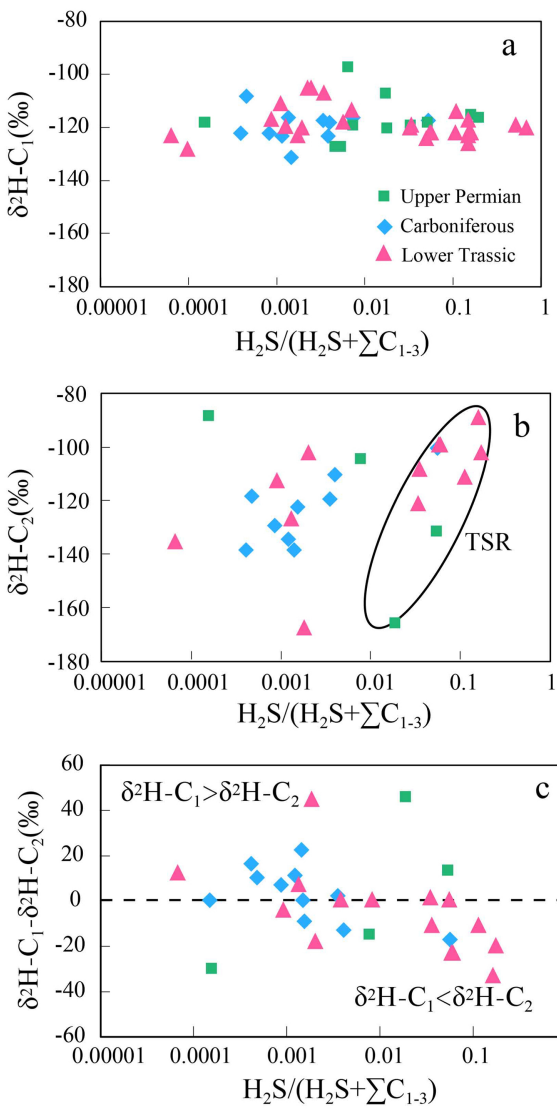


Figure 17

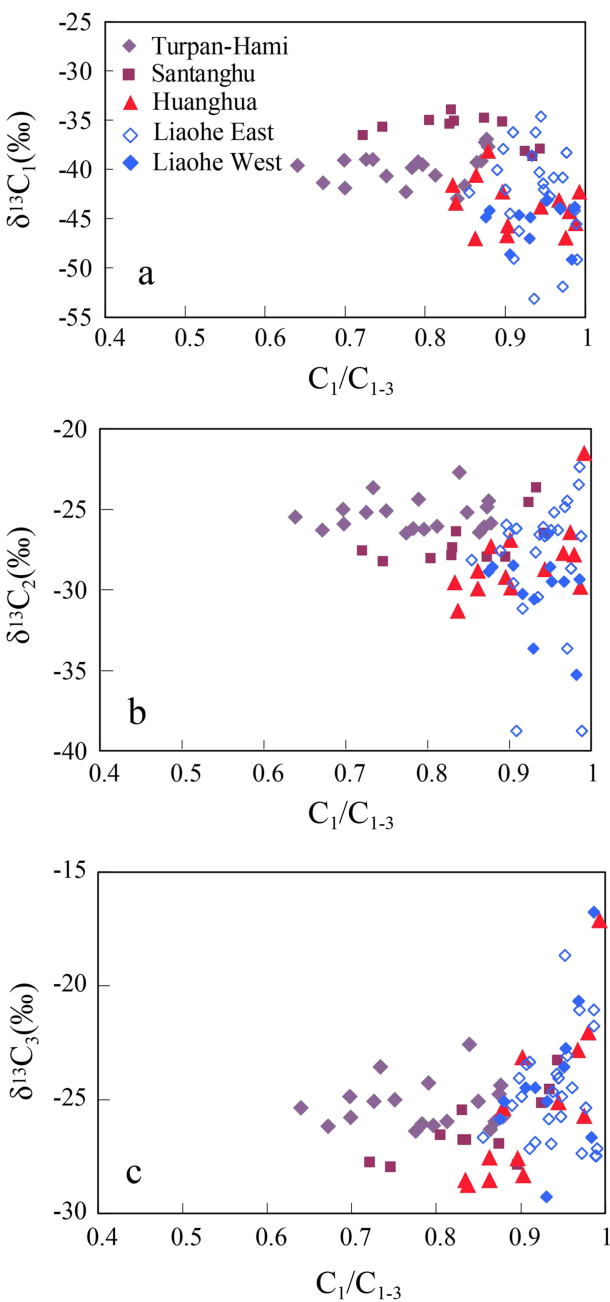


Figure 18

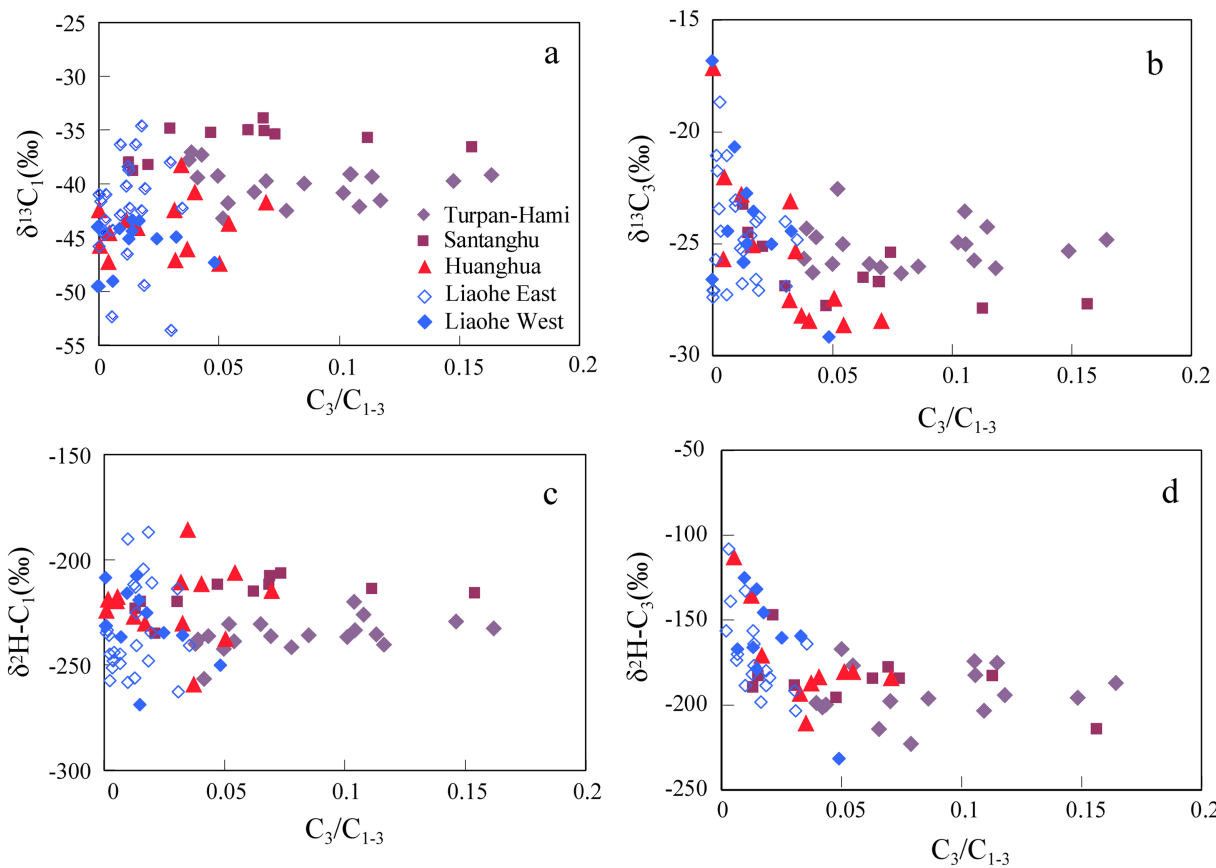


Figure 19

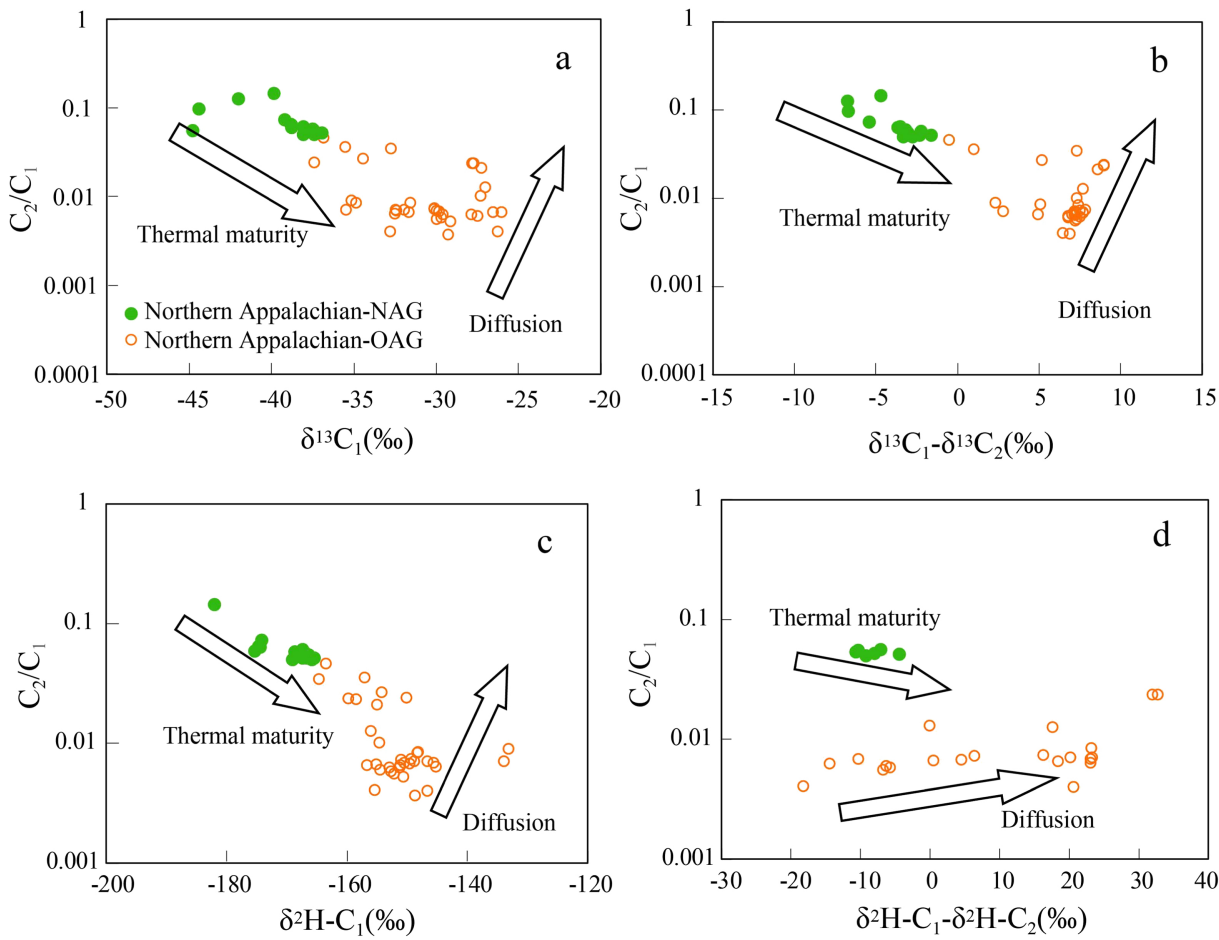


Figure 20

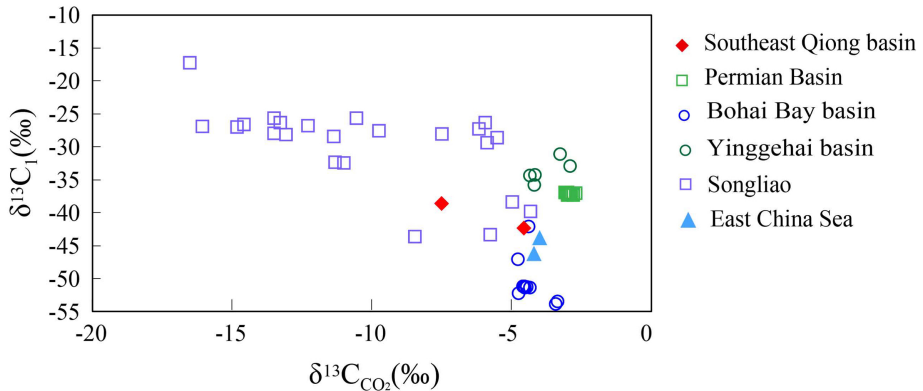


Figure 21

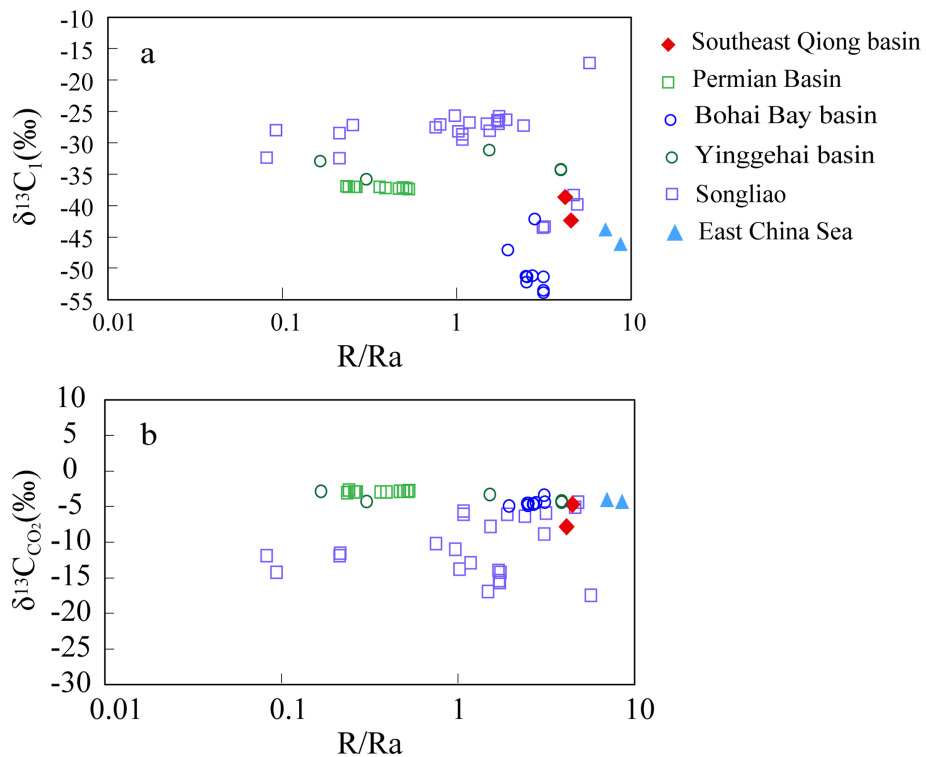


Figure 22

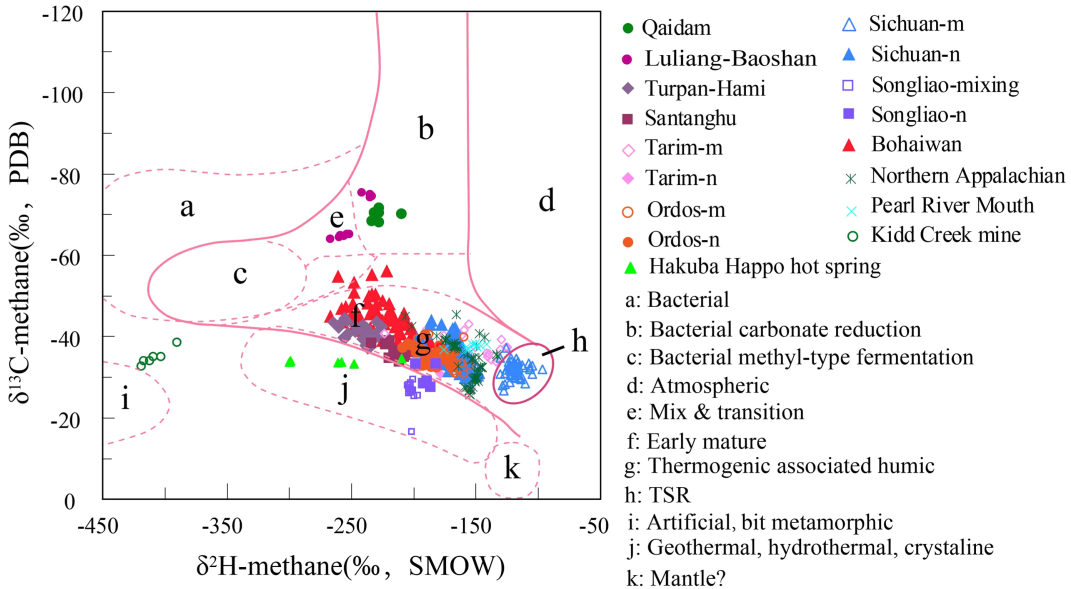


Figure 23

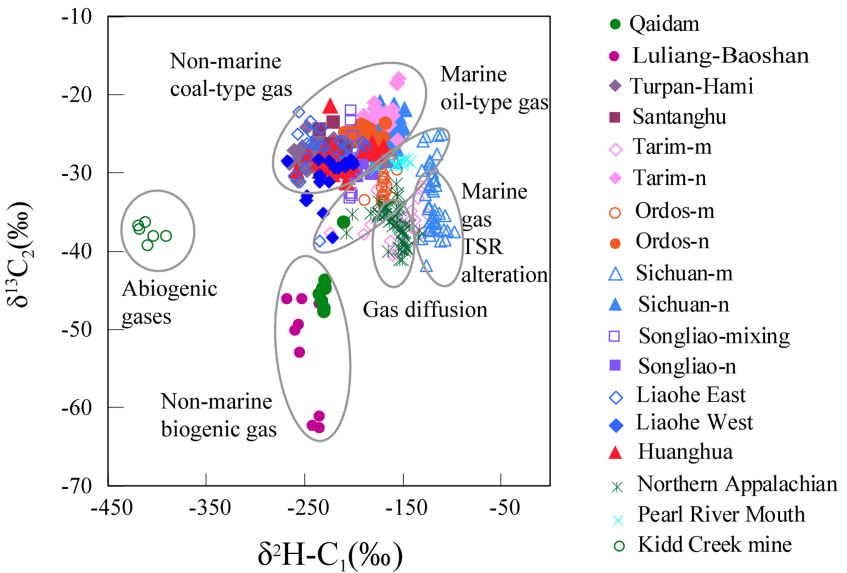


Figure 24

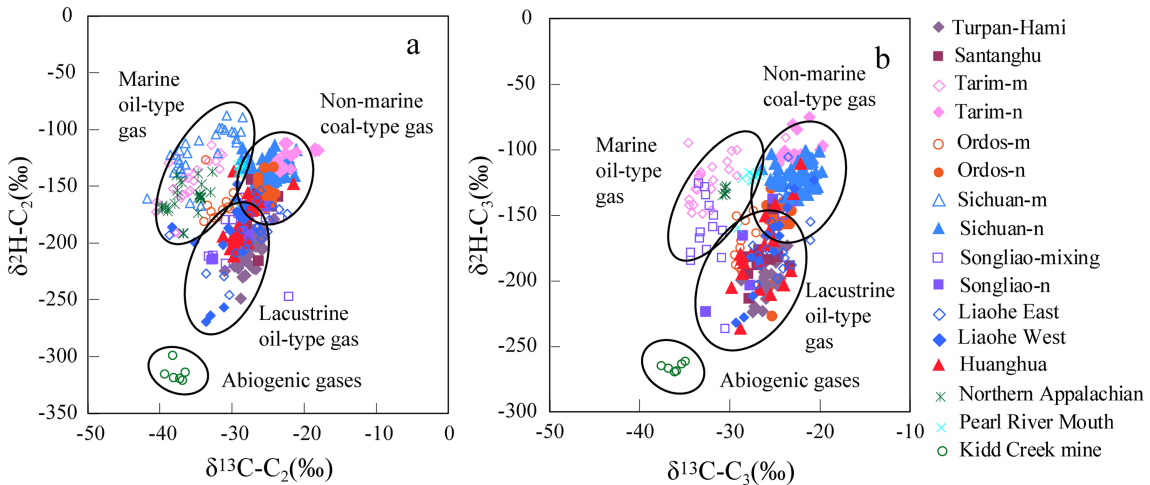


Figure 25